Metabolic and behavioral integration in social insect colonies

by

James S. Waters

A Dissertation Presented in Partial Fulfillment
of the Requirements for the Degree
Doctor of Philosophy

Approved November 2012 by the
Graduate Supervisory Committee:

Jon F. Harrison, Chair
Michael C. Quinlan
Stephen C. Pratt
Jennifer H. Fewell
Jürgen Gadau

ARIZONA STATE UNIVERSITY

December 2012

ABSTRACT

In social insect colonies, as with individual animals, the rates of biological processes scale with body size. The remarkable explanatory power of metabolic allometry in ecology and evolutionary biology derives from the great diversity of life exhibiting a nonlinear scaling pattern in which metabolic rates are not proportional to mass, but rather exhibit a hypometric relationship with body size. While one theory suggests that the supply of energy is a major physiological constraint, an alternative theory is that the demand for energy is regulated by behavior. The central hypothesis of this dissertation research is that increases in colony size reduce the proportion of individuals actively engaged in colony labor with consequences for energetic scaling at the whole-colony level of biological organization.

A combination of methods from comparative physiology and animal behavior were developed to investigate scaling relationships in laboratory-reared colonies of the seed-harvester ant*, Pogonomyrmex californicus*. To determine metabolic rates, flow-through respirometry made it possible to directly measure the carbon dioxide production and oxygen consumption of whole colonies. By recording video of colony behavior, for which ants were individually paint-marked for identification, it was possible to reconstruct the communication networks through which information is transmitted throughout the colony.

Whole colonies of *P. californicus* were found to exhibit a robust hypometric allometry in which mass-specific metabolic rates decrease with increasing colony size. The distribution of walking speeds also scaled with colony

size so that larger colonies were composed of relatively more inactive ants than smaller colonies. If colonies were broken into random collections of workers, metabolic rates scaled isometrically, but when entire colonies were reduced in size while retaining functionality (queens, juveniles, workers), they continued to exhibit a metabolic hypometry. The communication networks in *P. californicus* colonies contain a high frequency of feed-forward interaction patterns consistent with those of complex regulatory systems. Furthermore, the scaling of these communication pathways with size is a plausible mechanism for the regulation of whole-colony metabolic scaling. The continued development of a network theory approach to integrating behavior and metabolism will reveal insights into the evolution of collective animal behavior, ecological dynamics, and social cohesion.

DEDICATION

To my mother and father,

for dancing, falling in love, producing offspring, and

rearing three more clutches after their first brood had eclosed.

To my uncle, for his strength, and to the memory of my aunt,

whose love for all creatures knew no limits.

ACKNOWLEDGMENTS

"There is no such thing as a unique scientific vision, any more than there is a unique poetic vision." -- Freeman Dyson

The research presented here would not have been possible without the productive collaboration and generous feedback offered by my fellow graduate students in the Social Insect Research Group at Arizona State University. While this list is certainly incomplete, I thank Rebecca Clark, Adam Dolezal, Josh Gibson, Dani Moore, Rick Overson, Clint Pennick, Takao Sasaki, Zach Schaffer, and Adam Siegel for always being there to help answer my questions and offer their insight. Sydella Blatch, Arianne Cease, Colleen Ford, Erica Heinrich, Alex Kaiser, C. Jaco Klok, and John VandenBrooks, all members of our Harrison Lab family, have been a constant source of strength and encouragement.

For their help with collecting and rearing ant colonies, I would like to acknowledge the efforts of Phil Barden, Ioulia Bespalova, Elizabeth Cash, Rebecca Clark, Adam Dolezal, Tate Holbrook, Alyssa Holmes, Alison Ochs, Hemali Rajyaguru, Payal Rajyaguru and Zach Schaffer. For their technical, and occasionally emotional, support with respirometry training and troubleshooting, I am indebted to Barbara Joos, Robin Turner, and John Lighton of Sable Systems International.

Many funding agencies have contributed to this research, including: The American Physiological Society, The Graduate and Professional Students' Association at Arizona State University, The School of Life Sciences, Sigma Xi, and The Society for Integrative and Comparative Biology. The National Science Foundation has supported this research through both the Graduate Research Fellowship Program and a Doctoral Dissertation Improvement Grant (NSF IOS-1110796).

The direction for pursuing this research has been along a path I lead, but also one that has intersected the scientific vision of my committee members, colleagues, and many other scientists past and present who have focused on similar research objectives. For their contributions, specifically from committee members Jennifer Fewell, Jürgen Gadau, Devin Jindrich, Alex Kaiser, Stephen Pratt, and Michael Quinlan, I am sincerely grateful. One individual stands out though for his rather statistically significant contribution. I've estimated that over the last six years the two of us have exchanged at least 27,110 emails and over 15,825 pages of drafts, proposals, protocols, presentations, posters, and papers. If this dissertation has any merit, it is in the beauty of a poetic vision for science I hope to have developed from interacting with and learning from this tireless mentor and academic father, my graduate advisor, Jon F. Harrison.

TABLE OF CONTENTS

CHAPTER Page

LIST OF TABLES

LIST OF FIGURES

Figure Page

Chapter 1

INSECT METABOLIC RATES

INTRODUCTION

Insect physiological diversity

The insects are among the most species-rich, morphologically diverse, and physiologically complex groups of organisms on the planet. The number of documented insect species is between one and four million and some ecologists estimate that there are potentially as many as 7 million species alive today (Gaston, 1991; Wilson, 1985). Insects have evolved adaptations that allow them to occupy terrestrial, aquatic, and aerial ecosystems and environments that vary in temperature, humidity, salinity, oxygenation, and resource abundance.

Insects exhibit an impressive range of sizes over ontogenetic development, within and between species. One of the smallest adult insects is the 20 μg whitefly (Hemiptera: Aleyrodidae). Seven orders of magnitude larger, the Goliath beetle (Coleoptera: Scarabaeidae) is one of the most massive individual insects at ~50 g, larger than many birds and mammals. Among the shortest adult insects is a 0.1mm springtail collembolan (Minelli et al., 2010). The longest may be the stick insect (Phasmatodea: Phasmatidae), which stretches over 0.5 m. Fossil records from the Paleozoic include giants such as the griffenfly (Protodonata: Meganeuridae) that had wingspans as long as 0.71 m (Grimaldi and Engle, 2005). The sizes of eusocial insect superorganisms can be much larger. An average honeybee colony may weigh more than 10 kg and one single colony of ants may

stretch over many square kilometers (Giraud et al., 2002). In addition to exhibiting broad variation in size, insects are among the most ecologically dominant taxa, filling crucial roles in ecosystem functioning including pollination, seed dispersal, and nutrient cycling (Fittkau and Klinge, 1973; Janzen, 1987). Taking advantage of the ecological and physiological diversity among the insects presents a great opportunity to advance the development of a comprehensive and mechanistic theory of metabolic ecology.

Insect metabolism is primarily aerobic and is fueled by catabolic substrates transported by an open circulatory system, oxidized within cells by oxygen that is directly transported from the environment in the gas phase to metabolizing tissues by a system of branching and interconnected air-filled tracheal conduits (Figure 1.1). Although the transport capacity of the insect tracheal system was once thought to be limited by the passive mechanics of diffusive flux through stationary tubes, this is now known to be an antiquated paradigm (Chown and Nicolson, 2004; Socha et al., 2010). An impressive number of active mechanisms achieve convection through tracheal systems, including convective pumping of airsacs by ventilatory muscles of the abdomen (Miller, 1966; Socha et al., 2008), convection associated with thoracic volume changes during flight (Wasserthal, 2001; Weis-Fogh, 1967), ventilation associated with hemolymph transfer between compartments (Wasserthal, 1996), and "suction ventilation" associated with the reduced tracheal pressures that occur when spiracles are closed (Hetz and Bradley, 2005; Lighton et al., 1993b; Miller, 1981). Furthermore, the geometry of the tracheal system is sensitive to environmental

conditions and exhibits both phenotypic plasticity and evolutionary responses to compensate for changing oxygen availability (Harrison et al., 2006b; Klok and Harrison, 2009).

Measuring insect metabolic rates

Analyses of metabolic rate patterns in physiology and ecology rely on standardized conditions for measurement. In the field of mammalian biology, basal metabolic rate is relatively well-defined as the metabolic rate of resting, non-digesting, animals within their thermoneutral zone, the temperature range in which metabolic rate is constant (Hulbert and Else, 2004). The field of insect metabolic rate measurement does not have a thoroughly applied or well-defined set of criteria for standardizing metabolic rate measurements. To a large extent, this is not the result of researcher negligence but rather a consequence of the broad diversity of insect behaviors and physiology.

Defining criteria for standard metabolic rate is challenging in insects due to both behavioral and physiological issues. On the behavioral side, it can be difficult to get many insects to cease movement long enough to obtain metabolic measurements. For example, ants or bees removed from their colonies will often search ceaselessly for a way to rejoin their colonies. While it is possible to use movement sensors and chambers with short time constants to eliminate trials or time periods with locomotion, this approach can be challenging and is impossible for some species (Vogt and Appel, 1999). Decapitation eliminates most insect locomotory movements, and some insects will continue to metabolize and exhibit regular discontinuous gas exchange cycles following decapitation (Lighton et al.,

1993b); however, this terminal approach is not suitable for many studies and may cause other stresses that affect metabolic rate. A variety of studies have used respiratory patterns (exhibition of discontinuous gas exchange) as a way to determine when insects are in a "resting" state (Davis et al., 2000; Klok and Chown, 2005; Lachenicht et al., 2010). Lower metabolic rates do increase the likelihood of discontinuous gas exchange (Contreras and Bradley, 2009), but some insects can be quite active while exhibiting discontinuous gas exchange cycles and some simply never show such cycles, so this cannot be used as a uniform criteria for all insects. It is often challenging to determine whether insects are in a post-absorptive state, as is commonly done for vertebrates, again because of the great diversity among insects. Some insects tolerate starvation very well, while in other species (e.g. honey bees), high metabolic rates lead to rapid utilization of nutrient stores and death after only a few hours of starvation at a temperature such as 20°C. The lack of a uniform definition for conditions for measurement of insect metabolic rates has two important implications. First, meta-analyses that compile data from various studies need to carefully consider such problems. Second, investigators should monitor and report behavior and time since feeding during all metabolic measurements of insects. Although variability of this sort might be expected to only add noise to analyses of metabolic rate allometry, it may also contribute bias; for example, smaller animals might be more likely to more rapidly exhaust metabolic reserves during a set period of starvation, and respiratory patterns can be size-dependent (Davis et al., 1999; Lighton, 1991; Lighton and Berrigan, 1995).

Another source of confusion can be terminology. Here I define isometric scaling as following the standard predictions of Euclidian geometry, with volumes scaling with mass^{1}, surface areas with mass$^{0.67}$, and linear dimensions (e.g., leg length) with mass$^{0.33}$. Despite these scaling exponents ranging from 0.33-1.0, they all represent isometric scaling. Hypermetric scaling refers to allometric patterns in which the dependent parameter exhibits a significantly higher rate of change than predicted by isometry (e.g. leg length scaling with mass$^{0.5}$). Hypometric scaling refers to a significantly lower relationship than predicted by isometry (e.g., leg length scaling with mass$^{0.2}$). Since the vast majority of these patterns are non-linear, and since the sign (positive or negative) of the scaling relationship does not by itself indicate the nature of the allometry, I have chosen to use the hypometric/hypermetric language to consistently classify the deviation of allometric relationships from the predictions of isometry.

ENVIRONMENTAL AND BEHAVIORAL EFFECTS ON INSECT METABOLIC RATES

Temperature

One of the primary environmental influences on insect metabolic rates is temperature. The effect of temperature, however, is highly complex and depends on behavior, life-history stage, morphology, and size. Most insects are poikilothermic ectotherms, meaning that their body temperatures vary and that the source of that variation is environmental. Nonetheless, many insects utilize behavioral thermoregulation to achieve relatively constant body temperatures over

large parts of the day (Forsman, 2000; Ruf and Fiedler, 2002). A few insects are endothermic, often demonstrating considerable capacity for regulation of body temperatures using heat generated by the flight muscles (Heinrich, 1992). Some social bee colonies that generate their own heat and a stable core colony temperature exhibit features consistent with homeothermic endothermy (Heinrich, 1981b; Southwick, 1985). The ability of many insects to uncouple body from air temperature contributes to some of the variation in how insect metabolic rate responds to air temperature (Figure 1.2), an important factor to consider when extrapolating from climatic models to predicted insect energetics.

The temperature-dependence of metabolic rates has been analyzed with two main approaches. The MTE proposes an Arrhenius expression with a single activation energy that hypothesizes a broadly applicable, exponential effect of temperature on rate processes (Gillooly et al., 2001; Gillooly et al., 2006) in ectothermic poikilotherms. The classic physiological approach focuses on measuring an organism's Q_{10}, defined as the factorial change in metabolic rate for a 10-degree temperature difference (Lighton, 2008). In many cases, Q_{10} is not constant, but varies depending on the specific range of temperatures being modeled (Downs et al., 2008; Lighton, 1989; Nielsen et al., 1999). The intraspecific variation in Q_{10} and the interspecific variation in MTE-modeled activation energy may be due to potential behavioral, acclimatory, and evolutionary effects that cause deviations in thermal response patterns away from simple exponential models (Chown et al., 2003; Clarke, 2006; Nespolo et al., 2003; O'Connor et al., 2007).

In many cases, insect metabolic rates increase with temperature in a manner approximately consistent with the assumptions of MTE (Figure 1.2A; "inactive insects"). Typical fitted activation energy parameters for these cases are in the range of 0.5 to 0. 8, consistent with the findings of a recent meta-analysis using a much larger database of insect metabolic rates (Irlich et al., 2009) and with Q_{10} values in the range of 2-3.

These general patterns occur despite substantial variation in metabolic intensity. For example, similar thermal sensitivities of metabolic rate (i.e., slopes) are observed for scarab beetles and whiteflies, despite their very different metabolic rate at a given temperature (normalization constants, Figure 1.2A). In the scarab study, only data from insects exhibiting DGC are included, probably explaining their relatively low metabolic rate (Davis et al., 2000), while the whitefly data are for feeding groups (Salvucci and Crafts-Brandner, 2000).

Despite the modal trend for thermal effects on metabolic rates to be relatively well predicted by MTE (Figure 1.2B), there are some striking exceptions that illustrate potential dangers of not considering the physiological ecology of the species in question. While metabolic rates of social insect larvae or sleeping adults indicate fairly normal responses to temperature (Petz et al., 2004; Schmolz et al., 2002), endothermic flying insects or insect colonies can exhibit constant or even decreasing MR as temperature increases (Figure 1.2A). Because flight (foraging) costs can be a significant fraction of total metabolic rate for such insects (Harrison and Fewell, 2002), and metabolic rate during overwintering can affect survival of such colonies (Harrison et al., 2006a), it is important to consider

these mammal-like thermoregulatory responses of metabolic rate to temperature when considering the effect of climate on these species. Diurnal behavioral thermoregulation can result in higher than expected responses of metabolic rate to air temperature (Casey and Knapp, 1987), as can testing insects outside of their normal thermal ranges (Schultz et al., 1992). Exposure to naturally occurring fluctuating temperature regimes can also induce stress (e.g. oxidative damage) that increases metabolic rates even where the average temperature decreases (Lalouette et al., 2010). Furthermore, some insects exhibit seasonal and intra-seasonal variation in mass-specific and temperature-independent metabolic rate (McGaughran et al., 2009). In many of these cases, the biochemical/physiological mechanisms responsible for thermal responses that differ from MTE remain unknown.

Oxygen and supply limitation

Metabolism represents a balance between energy supply and demand integrated across the many tissues and systems within an organism. Energy is generated primarily by catabolism of fuels using oxygen transported by the tracheal system. One foundational concept of MTE is the proposition that allometric scaling of MR reflects a resource supply constraint (West et al., 2001). Alternatively, or additionally, the hypometric scaling of metabolic rate with body mass could relate to body-size related scaling of energy demand (Ricklefs, 2003; Seibel and Drazen, 2007). One way to consider the matching of oxygen supply and demand is to consider how metabolic rate is affected by ambient changes in

oxygen supply. To model this effect, it can be useful to consider the classic mass balance equation of respiratory physiology:

$$VO_2 = G \cdot \Delta P_{O_2}$$

in which VO_2 indicates an organism's oxygen consumption rate, G the conductance of the respiratory system, and ΔPO_2 the partial pressure gradient for oxygen from atmosphere to mitochondria. G is a measure of the capacity of the respiratory system to transport oxygen, and in this simplified case represents the combination of both diffusive and convective conductance (Buck, 1962). If ambient oxygen level is slowly lowered, and ΔPO_2 drops, animals will typically increase the conductance of their respiratory system (in the case of insects, by opening spiracles and increasing ventilation) to maintain a constant VO_2. Over this range, the organism is within its safety margin for oxygen transport and is not supply limited. The organism's critical PO_2 for that particular function is defined as the PO_2 when oxygen becomes limiting and below which VO_2 decreases (Figure 1.3). From work with isolated mitochondria (Gnaiger and Kuznetsov, 2002) it is known that mitochondria themselves need very little oxygen to perform maximally (less than 1 kPa) so at the critical PO_2, the average ΔPO_2 is likely approximately equivalent to the atmospheric PO_2. Under these circumstances, the maximal capacity of the respiratory system to conduct oxygen, G_{max}, can be estimated as VO_2/critical PO_2 (Harrison, 1997). Conductance varies with behavior, for example, it is much higher during insect flight than at rest due to recruitment of more active methods of ventilation (Harrison, 1997). Comparison of critical PO_2 values for a given behavior across insects of different sizes can

provide a direct way to test whether the ratio of oxygen supply to demand changes with body size. To our knowledge, insects are the only taxonomic group in which there have been systematic tests of the effect of body size on respiratory conductance and critical PO_2.

Most inactive insects exhibit very low critical PO_2 values (Figure 1.4), clearly indicating that resting metabolic rate is not oxygen-limited. However, critical PO_2 values do tend to be higher when metabolic rate is elevated as during flight (Figure 1.4). When comparisons are made controlling for behavior and developmental stage, there is no evidence that critical PO_2 values are higher in larger insects, and mass-specific tracheal conductances at least match the scaling of MR. Thus there is no evidence that oxygen demand out-strips supply as insects increase in size (Greenlee and Harrison, 2004a; Greenlee and Harrison, 2005; Greenlee et al., 2007; Greenlee et al., 2009; Harrison et al., 2005). However, there is a tendency for juvenile insects tested later within the development of a single instar (when mass increases without molting) to have much higher critical PO_2 values, suggesting that size increases without molting and resizing of the tracheal system might lead to oxygen supply limitation (Greenlee and Harrison, 2004b; Greenlee and Harrison, 2005).

While oxygen supply seems to meet demand as insects increase in size, this may occur because larger insects exhibit an increased investment in respiratory structure. Larger tenebrionid beetle species have a greater fraction of their body devoted to the tracheal system, and extrapolations of these trends suggest that this pattern could explain oxygen limitations on insect size (Kaiser et

al., 2007). Similar hypermetric patterns of tracheal investment have been observed in grasshoppers during ontogeny (Greenlee et al., 2009; Harrison et al., 2005). The increased investment in respiratory structure in larger insects suggests that body size influences metabolic rate via evolutionary trade-offs such as reduced proportions of active tissues per unit volume in larger insects (Harrison et al., 2010).

Locomotion

The metabolic rates of behaviorally active insects range from 3 to 30 times resting rates, and the maximal mass-specific metabolic rates of active insects can be more than double those of maximally active, similarly sized mammals or birds (Harrison and Roberts, 2000). Flying insects exhibit the highest metabolic scopes and flight metabolic rates are approximately 10 times greater than maximal metabolic rates for running insects of a similar size (Full, 1997). In some endothermic insects, transitions from rest to activity are associated with strong increases in body temperature, leading to very high metabolic scopes. For example, it has been reported that stridulating katydids (Stevens and Josephson, 1977) and running beetles (Bartholomew and Casey, 1977) exhibit metabolic scopes in the range of 50-100 fold during these behaviors as they endothermically warm their bodies by up to 20°C.

Metabolic rates increase linearly with running speed (Lipp et al., 2005; Weier et al., 1995) and peak metabolic rates among running and flying insects scale on average with $M^{0.86}$ (Full, 1997). Metabolic rates during flight have been reported to scale with $M^{0.9}$, but the degree of this allometry is likely influenced by

the tendency of larger endothermic insects to have higher body temperatures and flight metabolic rates than smaller insects (Niven and Scharlemann, 2005). Mechanical power output (usually estimated from the kinematics of limb or wing movements and dynamic models) scales isometrically with body size in running insects and either isometrically or hypermetrically in flying insects (Full, 1997). This pattern (increasing mechanical power output relative to metabolic power input) suggests that the relative efficiency (mechanical power output/metabolic power input) of locomotion increases with insect body size. If efficiency is defined as the ratio of locomotory power output to metabolic power input, isometric scaling of power output and input would predict that efficiency is invariant with mass ($\sim M^{0.0}$). For insects in general, efficiency scales hypermetrically (relative to the isometric prediction) with mass$^{0.12}$ and even more dramatically for honeybees, locomotory metabolic efficiency scales with $M^{0.45}$ (Harrison and Roberts, 2000).

Nutrition and feeding

The metabolic costs of insect foraging are usually tightly linked to the energetics of locomotion. In honey bee colonies, the energetic costs of foraging are approximately 30% of the estimated whole colony metabolic rate, but this fraction is likely much lower in terrestrial foraging species such as ants (Harrison and Fewell, 2002). However, the metabolic rates of stationary ants (*Atta sexdens rubropilosa*) during leaf-cutting may be more than 30 times their inactive metabolic rate, yielding a similar aerobic scope to flight (Roces and Lighton, 1995).

Metabolic rates typically increase in response to feeding and these increases may scale with both body size and meal type. The metabolic costs of post-feeding digestion can be quantified by the elevation of metabolic rate relative to baseline, the postprandial metabolic scope (~ 3.3 for insects) and also by the net energy expended for the duration of the specific dynamic action response (SDA), which ranges among the insect groups studied from 0.00025-0.102 kJ (Secor, 2009). Across a broad range of invertebrate taxa, SDA scales with $M^{0.31}$, meal-mass$^{0.72}$, and meal-energy$^{0.32}$; for comparison, among mammals, SDA scales with $M^{0.32}$, meal-mass$^{0.7}$, and meal-energy$^{1.21}$ and among reptiles SDA scales with $M^{0.08}$, meal-mass$^{1.13}$, and meal-energy$^{1.06}$ (Secor, 2009). Among insects, the kissing bug (*Rhodnius prolixus*) exhibits the highest postprandial metabolic scope (10-fold increase in whole-organism metabolic rate) as well as the greatest SDA (0.102 kJ) following feeding on a blood meal (Bradley et al., 2003). The specific dynamic action for migratory locust (*Locusta migratoria*) nymphs is in the 4-5-fold range (Gouveia et al., 2000). In addition to effects of being fed or not, the characteristics of the diet can also affect metabolic rate. A high-carbohydrate diet is linked to increased metabolic rates in honey bees (Blatt and Roces, 2001). In locusts, increased carbohydrate:protein intake can lead to strong elevation in metabolic rates, probably to dispose of excess energy in the diet and allow intake and assimilation of needed quantities of protein (Gouveia et al., 2000; Zanotto et al., 1997).

Restricted nutritional resource supply can have a range of effects on insect metabolic rates. Foraging honey bees given richer (higher carbohydrate) rewards

exhibit higher metabolic rates during periods of foraging that include both flight and non-flight (Balderrama et al., 1992), suggesting that in this species, metabolic rate is positively influenced by nutritional supply. Similarly, starvation may decrease metabolic rates or impair flight performance (Goldsworthy and Coupland, 1974; Matsura, 1981; Stoks et al., 2006), but this is not always the case. In the African fruit beetle (*Pachnoda sinuata*) voluntary flight performance and duration is not inhibited by 15-30 days of starvation (Auerswald and Gäde, 2000). Reduced water supply can elevate metabolic rate in growing insect larvae (Martin and Van't Hof, 1988) but does not affect the overall metabolic rate of adult locusts (Loveridge and Bursell, 1975). One of the reasons for the complex pattern of nutrient-supply effects on insect metabolic rates is the fact that there are often plastic physiological responses to resource deprivation including dramatic shifts in the metabolic pathways and nutrient substrates used to fuel metabolism, often without affecting overall metabolic rates (Auerswald and Gäde, 2000). However, both comparative and artificial selection studies suggest that an evolutionary response to starvation and water stress may involve reduced mass-specific metabolic rate (Harshman et al., 1999; Marron et al., 2003).

At the extreme of environmental nutrient restriction, insects may utilize torpor and diapause to survive long dearth periods, reducing metabolic rates for extended periods of time by more than 98% (Hahn and Denlinger, 2010; Schneiderman and Williams, 1953). A meta-analysis of the metabolic rate scaling for insect eggs, larvae, and pupae ($62.4M^{0.77}$) shows a similar hypometric exponent but a significantly reduced intercept (normalization constant) relative to

the allometry ($363M^{0.86}$) for the corresponding adult resting metabolic rates (Guppy and Withers, 1999).

Social insect colonies are particularly well adapted to maintaining physiological homeostasis in response to variation in environmental resource availability. For example, workers within the colony vary their foraging activity in response to the nutritional demands of the brood (Dussutour and Simpson, 2009; Sorensen et al., 1985) and many species harvest and store resources (Hölldobler and Wilson, 1990). Colonies may also catabolize somatic tissue to survive resource scarcity and environmental stress (Schmickl and Crailsheim, 2001; Sorensen et al., 1983; Wilson, 1971). In the acorn ant (*Temnothorax rugatulus*), decreases in activity levels and increases in trophallaxis (mouth-to-mouth food transfer) are hypothesized to facilitate this species' remarkable ability for colonies to survive greater than eight months of starvation (Rueppell and Kirkman, 2005). Kaspari and Vargo observed a hypermetric allometry for the duration of queen survival in the fire ant (*Solenopsis invicta*) which scaled with the size of the colony as $M^{0.21}$ (Kaspari and Vargo, 1995). This capacity for resilience has been hypothesized as one of the factors involved in the evolution of eusociality, caste ratios, and variation in colony size (Bouwma et al., 2006).

CORRELATIONS BETWEEN BODY SIZE AND METABOLIC RATE

Developmental allometries

Insect larvae represent excellent, albeit relatively unexplored, model systems for investigating the interface between physiology and ecology. As for

adults, larval insects are quite diverse. Many insect larvae live underground, in leaf litter, or in decaying fruits and likely experience a range of hypoxic environments, but others (e.g. many lepidopteran larvae) forage on leaves in normoxia. Many insect larvae are solitary, but other species rear brood cooperatively, such as the bessbug (*Odontotaenius disjuctus*) which raise larvae in communal galleries carved out of decaying wood. While most insect larvae are terrestrial, some are aquatic and of these some have open (e.g. mosquito) and others closed (e.g. caddisfly) tracheal systems. Some aquatic insect larvae, (e.g. the chironomids) have evolved the use of hemoglobin for oxygen transport (Oliver, 1971). The diversity of these environments and behaviors as well as the general paucity of literature data make it difficult to draw broad conclusions about the energetics of insect larvae.

Insect larvae metabolic rate allometries have been investigated on an intraspecific basis for a number of insect species that can be easily reared. While many of these studies report hypometric scaling exponents, there is weak support for a canonical 0.75 exponent. Growing honeybee larvae increase in mass by more than 400-fold in only four days and exhibit metabolic rates that scale with $mass^{0.9}$ (Petz et al., 2004). Larvae of the tobacco hornworm (*Manduca sexta*) span three orders of magnitude in body mass and exhibit CO_2 emission rate scaling with a mass exponent that ranges from 0.77 (Alleyne et al., 1997) to 0.98 across the entire larval stage (Greenlee and Harrison, 2005). However, individual instars show different patterns of metabolic rate scaling; as larvae grow within an instar, the mass-specific CO_2 emission decreases with age/size among early

instars, but it increases with size in final larval instar (Greenlee and Harrison 2005). Similarly in grasshoppers, the pattern of CO_2 emission rate scaling varies within different instars with exponents ranging between 0.45 and 0.91 (Greenlee and Harrison, 2004b), while across its entire development, metabolic rate scales with the exponent 0.73 (Greenlee and Harrison, 2004a). Larvae of the flour beetle (*Tribolium castaneum*) exhibit mass specific metabolic rates that decrease by over 90% during less than 12 days of development (Medrano and Gall, 1976) and the hemimetabolous milkweed bug exhibits a 38% decrease in mass-specific metabolic rate from the first instar to adult (Niswander, 1951).

Insect development from larvae to adults is associated with complex changes in body form and physiology in addition to alteration in body size. Metabolic rate scaling patterns may depend on the nature of these changes. Adult holometabolous insects are often substantially smaller than the terminal larval instar and the few studies available suggest that they have greater resting and maximal metabolic rates. Adults of vinegar flies (*D. melanogaster*) (Klok et al., 2010), fire ants (*S. invicta*) (Vogt and Appel, 1999), and honey bees (*A. mellifera*) (Lighton and Lovegrove, 1990; Petz et al., 2004) exhibit mass-specific metabolic rates approximately twice as high as their larvae. Are the higher mass-specific metabolic rates in adults due to their smaller size? If the adults and larvae are assumed to belong to a common mass-scaling allometry, then the ratio of their mass-specific metabolic rates can be calculated by:

$$\frac{B_2}{B_1} = \frac{b_0 M_2^{\alpha-1}}{b_0 M_1^{\alpha-1}} = \left(\frac{M_2}{M_1}\right)^{\alpha-1}$$

This equation can be re-arranged to solve for the mass ratio (ΔM) that would be necessary to generate an observed ratio in metabolic rate (ΔB):

$$\Delta M = \frac{M_2}{M_1} = (\Delta B)^{\frac{1}{\alpha-1}}$$

If the whole-animal scaling exponent (α) is 0.75, then we can predict what difference in masses would generate the observed ratio in mass-specific metabolic rates:

$$\Delta M = \Delta B^{-4}$$

In the case of a two-fold difference in mass-specific metabolic rates, the mass ratio would have to be 0.0625 for allometry to predict the observed difference in mass-specific metabolic rates. In other words, the adult stages of the ant, bee, and fly species mentioned above would have to be 94% smaller than their larval forms (or the larvae 16.67 times larger than the adults) for simple mass-scaling to explain the two-fold higher mass-specific metabolic rates in adults relative to larvae. Since adults are only approximately 10-30% less massive than larvae, the relatively high adult mass-specific metabolic rates are not simple allometric consequences of smaller body mass. An alternative ultimate explanation for the higher mass-specific metabolic rates of adults may be analogous to the higher metabolic rates of flying relative to non-flying adult insects (Reinhold, 1999). The complex changes (e.g., in body tissue composition and tracheal system

structure) that take place during metamorphosis in the holometabolous pupal stage apparently also enable fundamental changes in resting metabolic rate.

Intraspecific allometries

The relatively low range in masses among adults of a single species makes it difficult to accurately test for an intraspecific correlation between mass and adult insect metabolic rates in many species (Van Voorhies et al., 2004; Vogt and Appel, 1999). Ants are somewhat exceptional in this regard, with some species exhibiting substantial variation in worker size. For example, the dry masses of *Pheidologeton diversus* workers vary by more than 500-fold (Hölldobler and Wilson, 1990). In most cases, it appears that metabolic rates of such workers scale hypometrically with mass (with homogenous slopes ranging from 0.55-0.83 (Chown et al., 2007).

In some insects, intraspecific variation is associated with morphological allometries that produce surprising patterns in metabolic rate scaling and locomotory performance. Among female carpenter bees, flight metabolic rate scales hypometrically with $mass^{0.12}$ (Figure 1.5A), a very low scaling exponent. When these bees exhibit their maximal performance, flying in the lowest density air possible (to stay aloft in thin air requires more power), the scaling exponent is -0.22, meaning that both the mass-specific and absolute metabolic rates are lower in larger individuals than smaller individuals. The reduced mass-specific metabolic rate and flight performance of larger bees in this species is explained by variation in the relative amount of flight muscle, the primary site of oxygen

consumption in flying bees. In this species, larger females have proportionally larger abdomens (Figure 1.5B) and likely larger ovaries. As a consequence, larger individuals have significantly lower ratios of flight muscle to body bass, lower mass-specific metabolic rate and reduced scopes for flight performance and metabolic rate (Roberts et al., 2004).

Social insect colonies

Social insect colonies are intriguing organisms from the perspective of MTE because they span multiple levels of biological organization. Individuals within the colony may be expected to exhibit hypometric scaling of metabolic rate with mass, but whole colonies are made up of physically independent individuals at different developmental stages and engaged in a wide variety of different tasks and behaviors. Thus, whole colony metabolic rate should scale linearly with mass, depending proportionally on the number of individuals in the colony. Surprisingly, social insect colonies exhibit hypometric intraspecific scaling of metabolic rate with colony mass (Figure 1.6). Intriguingly, while the three social insect data sets illustrated in Figure 1.6 exhibit hypometric metabolic rate scaling consistent with the pattern for individual insects, they are each hypothesized to do so for different reasons. Honeybee clusters maintain a relatively constant core temperature when air temperature falls; mass-specific metabolic rates and mass-specific heat loss from the cluster falls in larger clusters due to a reduced surface area-to-volume ratio (Southwick et al., 1990). In the polymorphic ant *Pheidole dentata*, lower mass-specific colony metabolic rates arise from larger colonies

having a greater fraction of larger "major" workers (Shik, 2010). In a harvester ant species with monomorphic workers, *Pogonomyrmex californicus*, it is hypothesized that a lower mass-specific colonial metabolic rate in larger colonies may be due to larger colonies having a lower fraction of active workers (Waters et al., 2010). The similar hypometric scaling patterns with disparate mechanisms do suggest common underlying ecological/evolutionary forces that can be addressed by varied mechanisms in different species. Social insect colonies may be particularly useful for investigating mechanisms responsible for metabolic scaling patterns due to the capacity to more easily manipulate and measure specific components of the superorganism than is possible with individual organisms.

Interspecific allometries

On an interspecific basis, insect metabolic rates scale with $M^{3/4}$ (Chown et al., 2007) as in mammals. Analysis of the intercept (or normalization constant) of this relationship indicates that insects have low metabolic rates relative to mammals. After accounting for the effects of mass (the scaling exponent) and temperature (by adjusting insect rates from 25°C to 37°C following the activation energy method), insect metabolic rates are approximately half that reported for mammals (Figure 1.7A). This pattern fits with the ectothermic nature of most insects; ectothermic vertebrates also have lower MR than mammals at the same body temperature (Hulbert and Else, 2000).

Examination of the intercept of metabolic rate allometries (referred to as metabolic coefficient, intensity, elevation or normalization constant) has the

potential to reveal evolutionary differences in the metabolic physiology of different animal taxa. Among invertebrates, ticks and scorpions have been shown to exhibit significantly lower metabolic rates than other "typical" arthropods, possibly contributing to the high abundance of these species in some regions (Lighton et al., 2001). Similarly, predatory antlion larvae which build pits in which to capture prey exhibit common hypometric metabolic rate scaling exponents but with intercepts depressed lower than insects in general and even lower than similarly sized sit-and-wait predatory spiders (Lucas, 1985; Van Zyl et al., 1997). The normalization constant (y-intercept on log-log plots) of the scaling relationship for different insect orders varies by 18-fold (Figure 1.7B). While some of this variation may be related to methodology and behavioral variation among the taxa, it is likely that these order-level patterns at least partially reflect previously unrecognized evolutionary differences in physiology and life history.

DISCUSSION

The diversity of insect structure and function provides a powerful tool for testing physiological, ecological and evolutionary predictions of MTE. While the general equations of MTE seem to fit the modal responses of insects, and thus may be very useful for community and ecosystem ecology, behavioral and physiological divergences of individual species/taxa from the general theory of MTE are considerable. The temperature dependence of insect metabolic rates is highly variable, and as previously discussed, frequently depends on important ecological variables including behavior and thermal preferences. The temperature

dependence of insect metabolic rates can also be highly subject to thermal acclimation and adaptation (Chown and Nicolson, 2004). All of these factors are critical to developing predictive models for how insect populations will respond to global-scale changes in climate (Dillon et al., 2010). There is great potential for future developments of MTE to shed light on major unanswered questions in insect ecophysiology including understanding the evolution of endothermy, constraints on body size, and the physiological correlates of sociality. Future mechanistic developments of MTE may also help to explain sources of variation in mass and temperature independent metabolic intensity, both among distinct insect taxa and on a larger scale between insects, birds, and mammals. In addition, studying the energetics of insects is tremendously important for ecology and agriculture. As predators, scavengers, detritovores, and herbivores, insects play enormously important roles in ecosystem functioning, so that more energy flows through an ecosystem due to the activity of insects than the activity of vertebrates (Andersen and Lonsdale, 1990). Economic growth and stability may depend on understanding the thermal preferences, metabolic rates and behaviors of insect pollinators (Potts et al., 2010). By moving beyond broad assumptions and universal characterizations, MTE has the potential not only to integrate fields as diverse as insect ecophysiology and biofluid transport dynamics, but also to reveal questions of basic and fundamental importance to agriculture, biomechanics, ecology, and evolution.

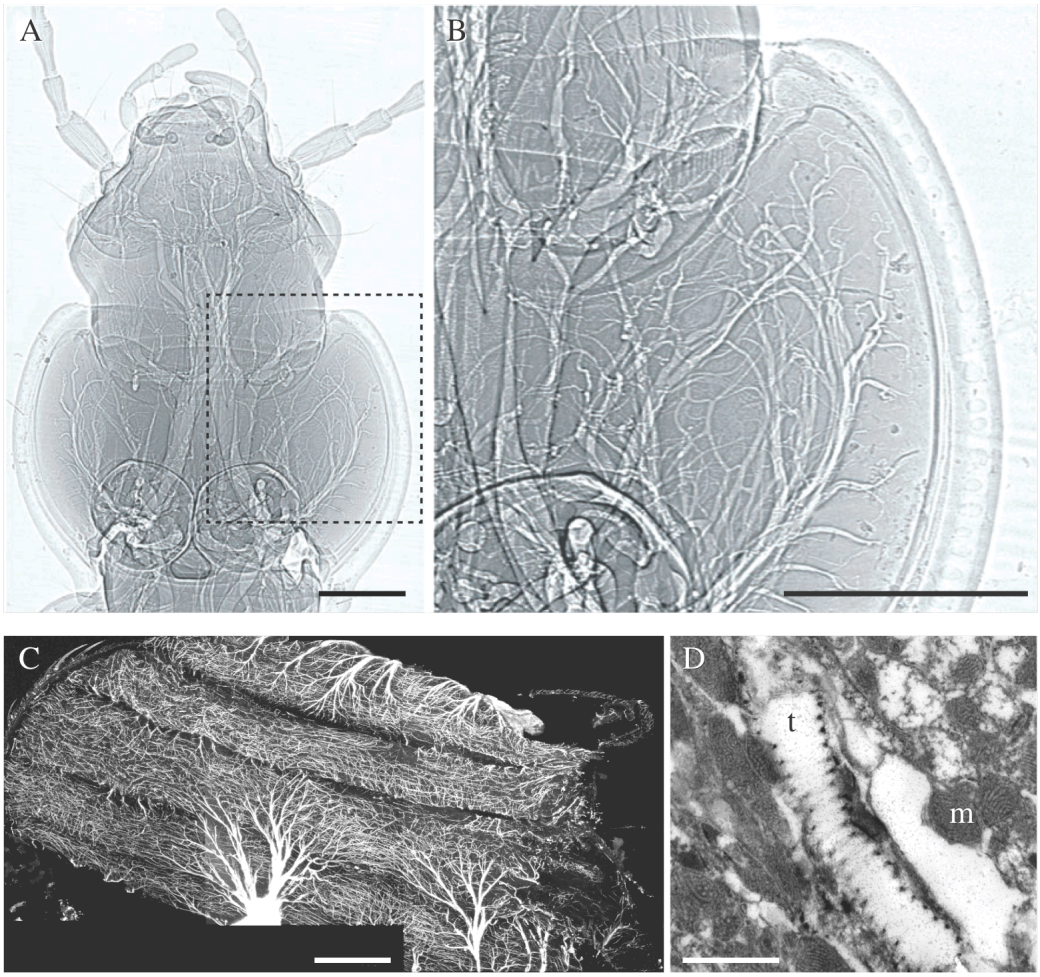

Figure 1.1. Insect tracheal systems provide the primary pathway for transporting oxygen from the environment to all of the metabolically active tissues within the body. **(A)** Synchrotron x-ray phase contrast image (Socha et al., 2007) of the head and thorax of the beetle, *Pterostichus stygicus*; scale bar: 1mm. (B) Magnified view of the thorax from the region enclosed by the dotted lines in (A); scale bar: 1mm (Socha et al., 2007). (C) Confocal microscopy image of the autofluorescent tracheae and tracheoles within the thoracic longitudinal flight

muscle of a *Drosophila melanogaster* male; scale bar: 200µm. (D) Transmission electron microscopy image of a single taenidia-reinforced tracheole (t) positioned near mitochondria (m) within the flight muscle of *Drosophila*; scale bar: 1µm. Data for figures 1C and 1D were collected by the authors at the Bioimaging Facility in the School of Life Sciences at Arizona State University.

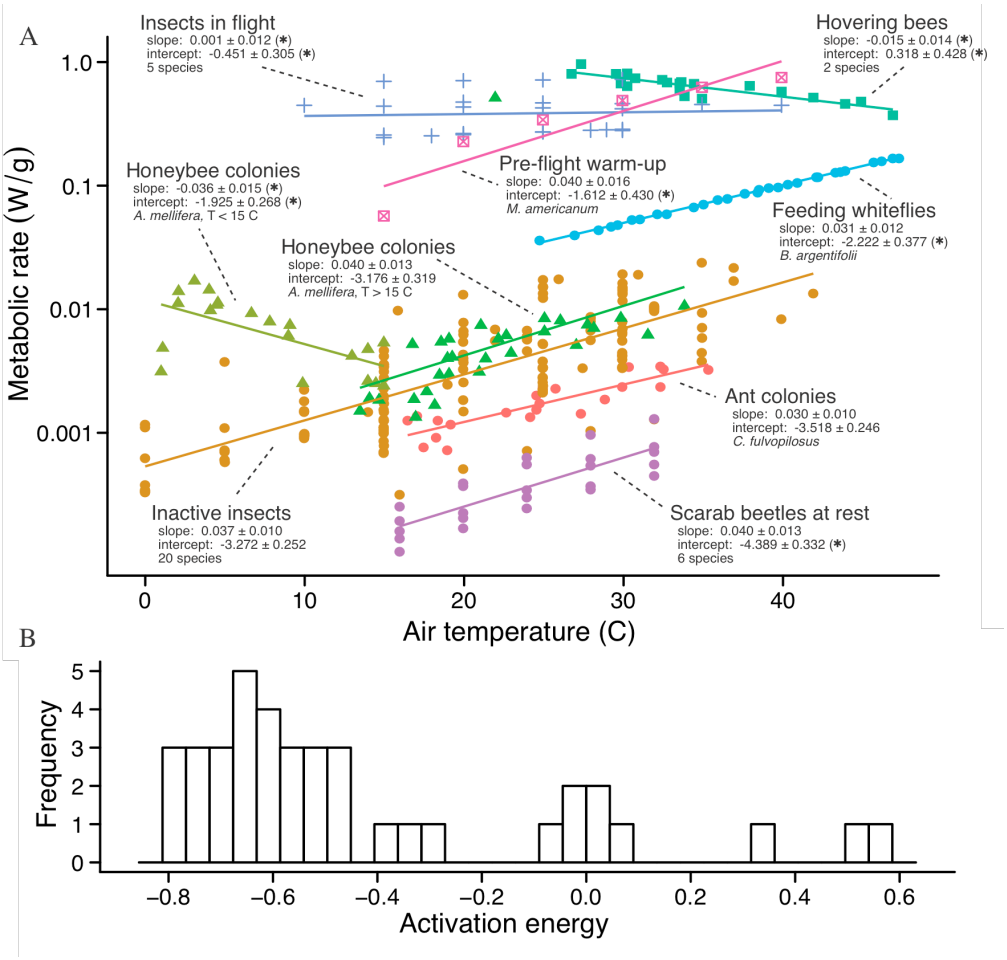

Figure 1.2. Insect metabolic rates are sensitive to air temperature and dependent on behavioral and environmental factors. In (A) the mass-specific metabolic rates for 31 insect species from eight taxonomic orders and also ranging across eight orders of magnitude in body size are plotted as a function of temperature. There is a common trend of insect metabolic rates increasing with temperature in the majority of sampled studies but there are also a number of exceptions. In particular, highly metabolically active, endothermic insects (e.g. endothermic flying insects, cold-exposed honey bee swarms) tend to show little effect of air

temperature on metabolic rate, or even an inverse relationship. The coefficients of the linear regressions describing the rate-temperature relationships are provided with asterisks (*) indicating whether the slope or intercept of the fitted data are significantly ($P<0.05$) different from the coefficients of the common regression parameters shared by the majority of inactive insects. (B) Frequency distribution of activation energies of insects. Activation energies were obtained as the slopes of OLS-regressions of the natural logarithm of mass-specific metabolic rate as a function of inverse absolute temperature for the 35 analyzed data sets. References for the data analyzed in (A) and (B) include: ant colonies (Lighton, 1989), flying insects (Casey and Ellington, 1989), hovering bees (Harrison and Fewell, 2002; Roberts et al., 1998), honeybee colonies (Heinrich, 1980b), inactive insects (Casey, 1977; Casey and Hegel-little, 1987; Chappell, 1983; Chappell, 1984; Fielden et al., 2004; Herreid et al., 1981; Klok and Chown, 2005; Morgan et al., 1985; Schultz et al., 1992; Terblanche and Chown, 2007; Vogt and Appel, 1999), pre-flight warm-up (Casey and Hegel-little, 1987), scarab beetles (Davis et al., 2000), and whiteflies (Salvucci and Crafts-Brandner, 2000).

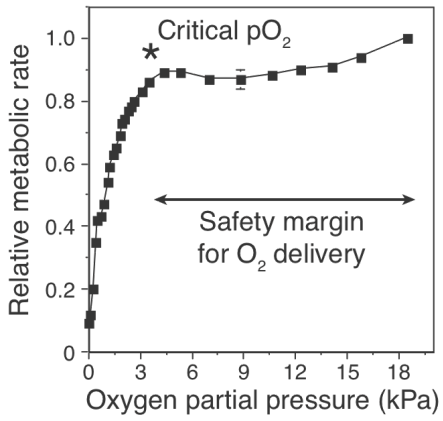

Figure 1.3. To quantify the safety margin for oxygen delivery, organism function can be measured over a range of oxygen partial pressures; the partial pressure (pO_2) at which the activity measure significantly decreases is referred to as that organism's critical oxygen partial pressure. The critical pO_2 for the metabolic rate of adult *D. melanogaster* is 3kPa or at about 85% less oxygen than normal, with a safety margin of 18 kPa O_2 (Van Voorhies, 2009).

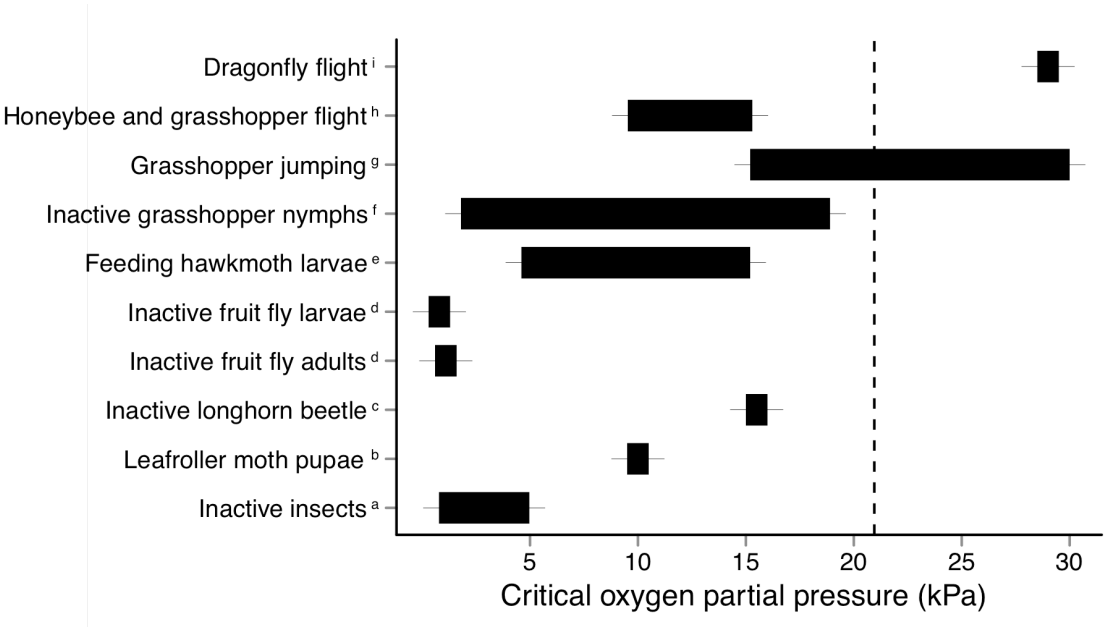

Figure 1.4. Insects often exhibit an impressively broad safety margin for maintaining measures of activity (e.g., O_2 consumption, CO_2 emission, performance) in spite of reduced partial pressures of oxygen in their environment. This figure plots the range of critical pO_2 in the literature for a diverse range of insects and their behaviors. Critical pO_2 tends to be higher in active insects. In cases where hyperoxic values are reported, this indicates that the measure of activity (i.e. dragonfly CO_2 emission and grasshopper jumping performance) increased in hyperoxia relative to normoxia. Normal pO_2 is 21 kPa, as indicated by the dotted line. The letter superscript associated with each row indicates the reference for that data set: a (Harrison et al., 2006b), b (Zhou et al., 2000), c (Chappell and Rogowitz, 2000), d (Klok et al., 2010), e (Greenlee and Harrison, 2005), f (Greenlee and Harrison, 2004a), g (Kirkton et al., 2005), h (Joos et al., 1997; Rascon and Harrison), and i (Harrison and Lighton, 1998).

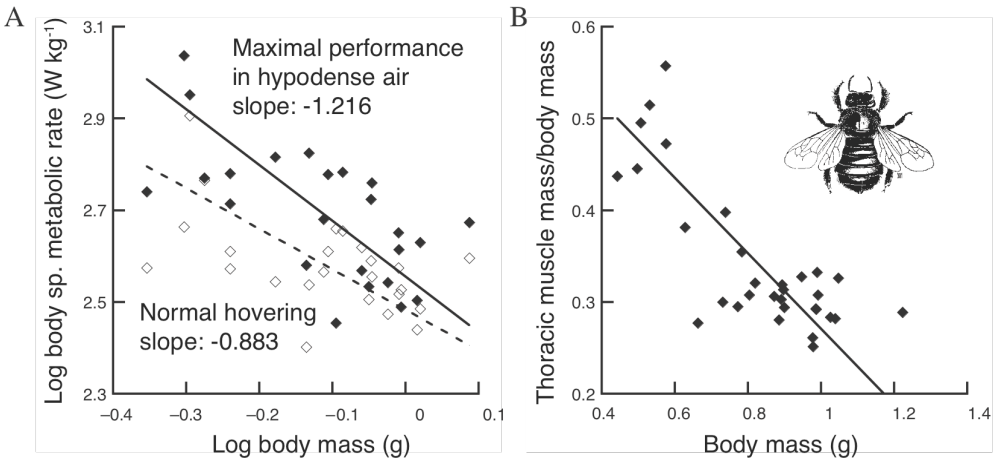

Figure 1.5. The allometry of body composition provides insight into the unusual intraspecific hypometric scaling of metabolic rate with body size in the carpenter bee, *Xylocopa varipuncta*. This figure, adapted from Roberts et al. (2004), shows in (A) that body mass-specific metabolic rates decrease very strongly with body mass (so whole-organism rates scale with $M^{0.22}$ for maximal performance in hypodense air and $M^{0.12}$ for normal hovering). This pattern occurs because the relative content of thorax muscle mass (the major site of oxygen consumption during flight) decreases with body size (B).

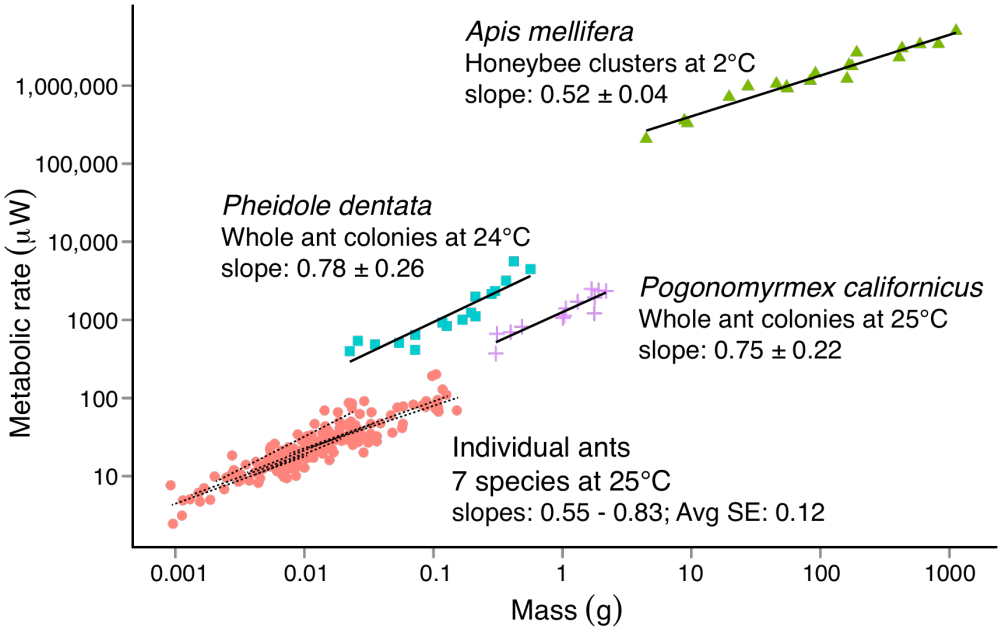

Figure 1.6. Allometry of colony metabolic rate in three colonial species compared with individual metabolic rate in seven solitary species. Social insect colonies, like individual insects, exhibit metabolic rates that scale hypometrically with mass. This figure combines intraspecific data for individual ants (Chown et al., 2007), two functioning whole ant colony species (Shik, 2010; Waters et al., 2010), and thermoregulating honeybee clusters (Southwick et al., 1990). The OLS-regression results for each group are displayed above (slopes are given with standard errors) and the overall model, which fits a separate slope and intercept for each species has an R^2=0.99. The average homogenous slope was 0.62 and the only species that show significantly higher than average scaling slopes are *Eciton hamatum* (slope=0.83, p<0.003) and *P. dentata* (slope: 0.78, p<0.002).

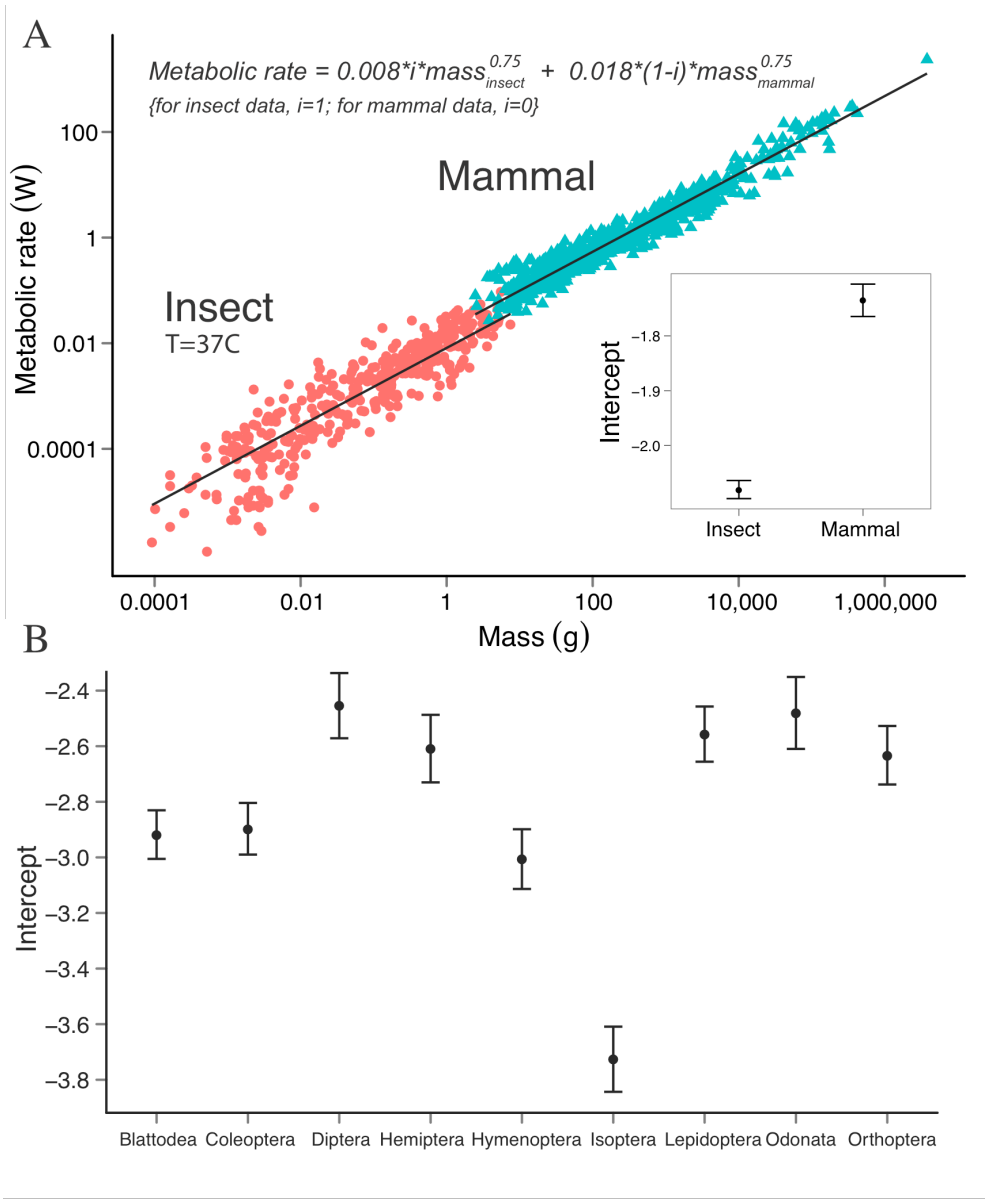

Figure 1.7. The hypometric scaling of inactive insect metabolic rates (Chown et al., 2007) is generally consistent with the pattern observed for mammals (Savage et al., 2004); both taxa exhibit similar ¾-power scaling slopes but insects have lower intercepts or normalization constants. In (A) the metabolic rates for 391 insect species have been adjusted using the Arrhenius equation to 37°C, a

standard mammalian body temperature. Independent of mass, inactive insects have metabolic rates about two times lower than inactive mammals with the same body temperature (figure inset displays the intercept values from the OLS regression on log-log data). (B) The interspecific data on insect metabolic rates at 25°C (Chown et al., 2007) can be analyzed by taxonomic order. A linear model that fits unique slopes and intercepts for each order was not a significantly better model than one that preserved a common slope (0.72 ±0.2 SE) but allowed for variation in intercepts by order. The maximum intercept (Diptera, 3.5mW) was more than 18 times greater than the minimal intercept (Isoptera, 0.19mW). Part of this variation may be due to behavioral variation among "inactive" insects, and methodological variation among researchers, but the data suggest substantial order-level variation in inactive metabolic rates among insects.

Chapter 2

ALLOMETRIC SCALING OF METABOLISM, GROWTH, AND ACTIVITY IN WHOLE COLONIES OF THE SEED-HARVESTER ANT *POGONOMYRMEX CALIFORNICUS*

INTRODUCTION

Colonies of social insects exhibit astonishing patterns of self-organization and emergent complexity (Bonabeau et al., 1997; Camazine et al., 2003; Hölldobler and Wilson, 2009). These patterns are generated by the collective action of individual behaviors in the absence of centralized control. Frequently, the emergence of a colony-level phenotype is dependent on colony size. Examples range from the ergonomic optimization of worker castes and task partitioning (Anderson et al., 1999; Porter and Tschinkel, 1985; Wilson, 1980) to the construction of physical nests that passively regulate colony environments (Korb, 2003; Noirot and Darlington, 2000). Size-dependent homeothermy at the colony-level has been observed in honeybee colonies in which individual clustering and thermogenesis regulate the core temperature of overwintering swarms and entire nests (Heinrich, 1980a; Southwick, 1985; Southwick, 1987). These patterns suggest that colonies may exhibit general patterns of integration similar to those that characterize the scaling of individual organisms.

Among individual organisms, size correlates strongly with rates of metabolism, growth, and locomotion, making it one of the single best predictors of the pace of life (Bonner, 2006). The regularity with which metabolic rates scale

with mass is a striking relationship that has fueled extensive research and substantial controversy (Glazier, 2005). While the null isometric hypothesis is that metabolic rate should scale with $mass^{1}$, generally, log-log plots of metabolic rate on mass have slopes significantly lower than predicted (negative allometry). Metabolic rate has been shown to scale with $mass^{0.86}$ for a diverse collection of terrestrial arthropods (Lighton et al., 2001) and with $mass^{0.75}$ among 391 insect species (Chown et al., 2007).

While the majority of studies of the scaling of metabolism have focused on interspecific analyses, intraspecific scaling is important due to the relevance of such patterns to species ecology, life history, and evolution. In general, the intraspecific scaling of metabolism with mass seems more variable than observed in interspecific comparisons (Glazier, 2005); however, this may partially be a consequence of the relatively limited body mass ranges available for intraspecific studies. Intraspecifically, metabolic rate frequently exhibits negative allometric scaling within insect species including *Oncopeltus fasciatus* (Niswander, 1951), *Tribolium castaneium* (Medrano and Gall, 1976), *Manduca sexta* (Alleyne et al., 1997; Greenlee and Harrison, 2005), *Schistocerca americana* (Greenlee and Harrison, 2004c), *Atta columbica* (Lighton et al., 1987) and *Pogonomyrmex rugosus* (Lighton and Bartholomew, 1988). A recent investigation into intraspecific allometries among individual ants demonstrated that in seven of eight species studied, metabolic rate scaled homogenously and with an average scaling exponent of 0.65 (Chown et al., 2007). Furthermore, it has recently been demonstrated that whole colonies of social insects may also exhibit negative

allometries on an interspecific basis (Hou et al., 2010), suggesting that a similar pattern may be present on an intraspecific basis between colonies of a single species that vary in size.

Social insect colonies are ideal model systems for investigating how the scaling of metabolic rate and associated parameters extends from individuals to societies. Colonies of social insects range widely in size and diversity of social organization. The nature of colonies as collections of physically independent individuals makes it possible to perform experimental manipulations on aspects such as size and composition that would not be feasible for individual organisms. Compared to other social insect species, nonreproductive ant colonies are particularly convenient model organisms for evaluating scaling relationships, due to the possibility of maintaining functioning colonies in the lab and the absence of flying individuals that would complicate models of whole-colony metabolic rate.

Several prior studies have examined the dependence of metabolic rate on group size in ants. In some of the first attempts at quantifying the metabolic effect of group size, mass-specific metabolic rates of workers did not scale with the number of ants being measured (Brian, 1973; Lighton and Bartholomew, 1988; Lighton, 1989). In other studies, it was shown that mass-specific metabolic rate depended on worker group size in a nonlinear fashion (Fonck and Jaffe, 1996; Galle, 1978). These investigations focused primarily on pseudo-colonies in which groups of individuals were removed from their more natural social milieu and placed into the artificial environment of a respirometry chamber. Such groups of ants likely were unable to engage in normal colony functions such as foraging,

allogrooming, or rearing brood, and consequently were without the potential for maintaining the kind of organizational networks that may be fundamental to regulating the metabolism of integrated social groups.

In this study, colonies of the seed-harvester ant *Pogonomyrmex californicus* were reared in laboratory nests from founding to 10-mo-old colonies that ranged in size from 95 to 659 ants, including queens, larvae, pupae, and adult workers. None of the colonies had begun to produce sexual castes. The nest design allowed for simple and non-invasive flow-through respirometric measures of the metabolic rate of whole colonies while they carried out normal colony functions, including foraging and brood-rearing. To control for the possibility that larger ant colonies are likely to also have larger workers (Tschinkel, 1999), I determined the caste, developmental stage, and mass compositions of each colony. To test for an effect of the colony social environment, metabolic rate measurements were also carried out with worker groups that had been removed from their colonies. To estimate the relative activity differences between colonies, I recorded and analyzed the patterns of locomotion among individual ants within colony nests.

METHODS

Collection and rearing

Queens of *Pogonomyrmex californicus* were collected 4-6 July 2007 following mating flights in Pine Valley, San Diego County, California (32°49’20”N, 116°31’43”W, 1136m elevation). Since this population is

pleometrotic (cooperative founding), laboratory colonies were initiated with three queens each. Colonies were maintained in an incubator at 28-32°C in plastic artificial nests with cotton plugged water tubes but no soil or other ground substrate. Each nest provided a total surface area of 242 cm^2 and was partitioned into a brood chamber and foraging arena (Figure 2.5). Kentucky bluegrass seeds and dead crickets were provided in excess of consumption to preclude resource limitation. Water tubes were replaced and debris removed as necessary. Metabolic rate measurements were conducted after 10 months of rearing. Colony mass data were collected following metabolic rate measurements; at which time colonies ranged in size from 95-659 ants and in mass from 311-2223 mg.

Modeling whole-colony metabolic rate

To quantitatively evaluate hypotheses on the scaling of metabolic rate among groups or colonies, it was necessary to develop a model to predict the metabolic rate of a group based on its composition. To a first approximation, the metabolic rate (MR) for each individual (with mass, m) within a colony can be predicted by $MR=a_0m^b$ where the allometric coefficient, a_0, and exponent, b, can be estimated by the analysis of standard respirometric measures of individuals. If colonies were simply collections of homogenous individuals, then summing their individually estimated metabolic rates would be predicted to generate an isometric scaling of colony metabolic rates. However, eusocial insect colonies are heterogeneous collections of individuals that vary in a number of factors that can influence their per-capita metabolic rates including mass, caste, and activity level.

I propose the following model for estimating whole-colony metabolic rate while taking into account individual-level variation (e.g., in mass, caste, or activity). In its most general form, the model is defined for a colony with numbers of individuals, N_i, in each of k distinct allometric subgroups by the following equation in which c is an activity coefficient, a_i is the allometric coefficient, m is individual mass, and b_i is the allometric exponent:

$$(1) \qquad MR_{net} = \sum_{i=1}^{k} \sum_{n_i=1}^{N_i} c_{n_i} a_i m_{n_i}^{b_i}$$

Applying this model to a social insect colony composed of queen, worker, larva, and pupa allometric subgroups (respectively identified by subscripts q, w, l, and p) and assuming homogenous activity across all individuals and colonies, colony metabolic rate is predicted by:

$$(2) \qquad MR_{colony} = \sum_{n=1}^{N_q} a_q m_n^{b_q} + \sum_{n=1}^{N_w} a_w m_n^{b_w} + \sum_{n=1}^{N_l} a_l m_n^{b_l} + \sum_{n=1}^{N_p} a_p m_n^{b_p}$$

This model may be simplified by assuming that a single allometric relationship predicts the metabolic rate of all individuals of a given species depending on their mass, and assuming average masses, $\overline{m}_i$, for each allometric subgroup within the colony. I refer to this as the additive model for colony metabolic rate:

$$(3) \qquad MR_{colony} = N_q a_0 \overline{m}_q^b + N_w a_0 \overline{m}_w^b + N_l a_0 \overline{m}_l^b + N_p a_0 \overline{m}_p^b$$

This model was computed a series of times using the census data for ants in our laboratory colonies and populated with scaling coefficients based on *P. rugosus* (Lighton and Bartholomew, 1988) and a general arthropod allometry (Lighton et al., 2001). Since data on brood metabolic rates were unavailable for this species,

following the results of a study of *Solenopsis invicta* (Vogt and Appel, 1999), I also computed the additive model with larvae and pupae estimated to have mass specific metabolic rates 72% and 56% that of individual *P. californicus* workers (Quinlan and Lighton, 1999). The additive model (3) predicts isometric colony metabolic rate scaling if average individual mass and subgroup composition are both invariant with respect to colony size. However, many factors could lead to either hypermetric or hypometric scaling of colonial metabolic rates, including changes in worker sizes, distribution of types of individuals in the colony (e.g. proportion of the colony that is brood), or variation in activity and metabolic rates among individuals within or across colonies.

Measuring whole-colony metabolic rate

Whole-colony metabolic rate was measured with flow-through respirometry. Entire colony enclosures (including brood chamber and foraging arena) were placed with minimal disturbance into a 1.0 L airtight plexiglass chamber. Dried, CO_2-free air from a compressed air tank flowed through the chamber (38 ml min^{-1}), regulated by Tylan mass flow valves and controller. In this way, the washout characteristics were such that 95% equilibration is estimated to take 79 min (Bartholomew et al., 1981). Using an infrared analyzer (LI-6252, LI-COR, Lincoln, NE, USA), the carbon dioxide concentration of dried, excurrent air was measured (Figure 2.6). Air temperature exiting the colony chamber was measured using thermocouples embedded in line with the excurrent airstream. Analog data were digitized [UI-2, Sable Systems International (SSI),

Las Vegas, NV, USA] and recorded on a PC (ExpeData v1.2.6, SSI) at 1 Hz sampling frequency and 10-20 Hz averaging.

Colonies were measured in the respirometry chamber for 24-48 hr at 28.4°C (±0.5°C SD). After this period, colonies were removed from their nest to count the number of individuals present and determine the average per-capita mass for each subgroup within the colony (queens, workers, pupae, larvae). Meanwhile, the colony nest was returned to the respirometry chamber to measure the background signal from the water tube, seeds, and debris. Metabolic rates were calculated from baseline- and debris-corrected excurrent carbon dioxide concentrations averaged over the most stable 12-hr recording, standardized to the average temperature of 28.4°C assuming a Q_{10} of 2.0, and converted to microwatts assuming an RQ of 0.80 (Lighton and Bartholomew, 1988).

Net colony growth rates were calculated by dividing wet-tissue biomass by colony age at the time of measurement. Net growth efficiency was calculated as power output divided by power input (calculated from whole colony metabolic rate, measured as described above). Power output was defined as the product of net rate of dry biomass production (converted from wet biomass data by direct calibration) and tissue caloric density. Caloric equivalents were estimated based on the published value found for *Crematogaster sp.*, 4.073 kcal/g (Cummins and Wuycheck, 1971).

Worker-group metabolic rate

To control for the effects of density and social environment, I measured the metabolic rates of groups of workers removed from their colonies. For three colonies of *P. californicus* (collected in 2007), workers in groups ranging in size from 1 to 225 ants were removed and a total of 20 worker groups were measured. Stop-flow respirometry was used to estimate metabolic rate. Worker groups placed in petri dishes with a small water tube were placed in an airtight aluminum-plexiglass chamber. Two respirometry chambers were used (30 mL and 600 mL volumes) with different surface areas (20 cm^2 and 314 cm^2) to accommodate the range of group sizes. Normoxic air from a compressed-gas cylinder was used to both baseline and purge the concentrations of oxygen and carbon dioxide within the chamber. A flow rate of 100 ml min^{-1} was used with the 30mL chamber and 500 ml min^{-1} was used with the 600 mL chamber. Following the purging of ambient air, the chambers were sealed for a period of time estimated to produce a decrease in oxygen concentration within the chamber of not greater than 0.5%. The amount of time chambers were sealed ranged from 0.5h to 15.3h and the average drop in oxygen concentration was 0.12% (±0.08 SD). Following the sealed phase, the airstream was redirected into the chamber and the excurrent air passed through, in order, a drierite column, a carbon dioxide analyzer, an ascarite column, and an oxygen analyzer (FC-2, SSI). Oxygen consumption (mLO_2 min^{-1}) was determined by integrating the baseline-corrected oxygen concentration recording (Lighton, 2008) and was converted to microwatts (20.1 J mLO_2^{-1}).

The data on worker-group metabolic rates were analyzed to determine if there was a correlation between worker group size and mass-specific metabolic rate. Additionally, since the density of ants between measurements varied in this experiment by up to 60-fold (0.05-3.06 ants/cm^2), I also tested for a correlation between density and mass-specific metabolic rate. Performing these analyses on a mass-specific basis is justified because the worker body size (2.76 mg ±0.28 SD) did not scale with experimental group size (linear regression: $F_{1,18}$=0.12, p=0.74) or vary significantly among the three originating colonies (one-way ANOVA: $F_{2,17}$=1.7, p=0.21).

Allometric analysis

Data were analyzed using a variety of regression techniques to validate that results obtained were statistically robust (Packard and Boardman, 2008). The allometric scaling coefficient and exponent for whole-colony metabolic rates were estimated using ordinary least squares and reduced major axis algorithms after log-transformation in GraphPad Prism version 5.0 (GraphPad Software, San Diego, CA, USA). Residuals were normally distributed (D'Agostino-Pearson p=0.3). The scaling coefficient and exponent were similarly estimated based on the predictions generated by the additive model (3). Additionally, scaling exponents were also estimated using non-linear regression on arithmetic-scaled data (Packard and Boardman 2008).

Activity analysis

Patterns of locomotory activity were assayed by digitizing the movements of ants in recorded video of colony behavior. Video recordings were made for 1h of the nest region of eight colonies. For each colony, a 60 s segment of video was sub-sampled at 1fps and exported as a TIFF image stack. The sub-sampling rate of 1fps was chosen to minimize the number of frames to be analyzed without excessive loss of spatial resolution due to ants moving more than one body length between frames. Image stacks were loaded into NIH Image and the coordinates of individual ants in each frame were manually digitized with QuickImage (Walker, 2001). These coordinate data (N=73,444) were analyzed to determine an average velocity for each ant in each of the colony nests. For each colony, I determined the frequency distribution of individual average velocities. Data on the relative speeds of individuals in each colony were also used to generate predictions for colony metabolic rate allometry using the compositional additive model (1) by incorporating an activity coefficient. Since metabolic rate increases linearly with the speed of a running ant (Lighton et al., 1987; Lipp et al., 2005), the activity coefficient was used to scale the predictions for individual metabolic rates proportional to their measured speed. Values are reported as means ± standard error (s.e.m.) throughout.

RESULTS

Whole colony metabolic rate allometry

Whole-colony metabolic rate scaled with colony mass with negative allometry, with a scaling exponent of 0.75 ± 0.09 (Figure 2.1, Tables 2.1-2.2). The empirically determined exponent was significantly less than the isometry predicted by equation (3), using the measured masses of individual queens, workers, larvae and pupae for each colony ($F_{1,22}$=7.20, p=0.01). All additive models generated isometric scaling (exponents not significantly different from 1) regardless of whether I used coefficients based on the general arthropod (Lighton et al., 2001) or *P. rugosus* (Lighton and Bartholomew, 1988) allometries, or included the data estimated for *P. californicus* workers and brood (table 1, $F_{1,33}$=0.86, p=0.43). The scaling exponent estimated through ordinary least squares regression of log-transformed data did not significantly differ from the estimate generated by reduced major axis linear regression (t_{24}=1.25, p=0.2) or the estimate generated by nonlinear regression using the arithmetic scaled data (t_{24}=0.11, p=0.9). Additionally, the scaling exponent did not depend on whether the minimum, average, or maximum colony metabolic rates were used in the analysis ($F_{2,33}$=0.12, p=0.9). The negative allometric scaling of whole colony metabolic rate is consistent with the general intraspecific scaling pattern observed for individual ants (Figure 2.1B; metabolic rate data adapted from Chown et al. 2007). Colonies of *P. californicus* exhibited an intraspecific scaling exponent not significantly different (one way ANOVA, $F_{7,200}$=1.2, p=0.3) than seven of the eight species for which intraspecific individual ant metabolic rate scaling data

were available (Figure 2.7).

Colony composition

Negative allometric scaling in *P. californicus* could not be explained by trends in the scaling of individual ant size across colonies or by changes in colony composition (Table 2.3). Average worker mass (mean 3.2 mg ±0.1) did not show a significant regression with colony size ($F_{1,11}$=0.96, p=0.35). There was also no significant scaling of average queen mass (12.0 mg ±0.2; $F_{1,11}$=2.77, p=0.12) or average larva mass (1.9mg ±0.3; $F_{1,11}$=4.39, p=0.06). The fractions of colony mass composed of workers (0.83 ±0.03), larvae (0.09 ±0.01) and pupae (0.05 ±0.02) all exhibited non-significant regression with colony size ($F_{1,11}$=0.07-1.29, p=0.28-0.78). Fractional composition of the colonies by queens did scale with colony size ($F_{1,11}$=28.03, p=0.0003), from 11.5% in the smallest colony to 0.6% in one of the largest, but overall, queen mass was a small proportion of colony size (0.04 ±0.01).

Since all colonies were the same age, the seven-fold range in colony mass means that net growth rate increased linearly with colony size, and was seven-fold greater in the largest compared to smallest colonies. Net growth efficiency increased more than 3X with colony size ($F_{1,11}$=5.96, p=0.03, r^2=0.35) due to larger colonies exhibiting 7-fold higher net growth rates and 30% lower mass-specific metabolic rates.

Isometric scaling of worker groups

Worker groups, removed from the social environment of the colony, exhibited isometric metabolic rate scaling (Figure 2.2A, Table 2.1, and Table 2.4), consistent with some of the results of previous studies on the effects of group size on the mass-specific metabolic rate of groups of ants placed in a respirometer outside of their colony. Metabolic rate scaled with group mass raised to the exponent 1.01 ±0.03 (linear regression on log-transformed data, $F_{1,18}$=913.7, p<0.0001, r^2=0.98). There was no effect of source colony on the estimated scaling exponent (one way ANOVA: $F_{2,17}$=0.98, p=0.39). Furthermore, despite a 60-fold range in the density of worker groups within the respirometry chambers in this study, there was no significant linear regression correlating mass-specific metabolic rate with worker density (Figure 2.2B; $F_{1,18}$=0.55, p=0.47). Due to the use of two different-sized respirometry chambers in the worker-group experiment, experimental group size did not correlate with worker density (Pearson r=0.08, p=0.73).

Velocity distributions

I recorded the trajectories and determined the average locomotor velocities for more than 1200 ants across eight colonies (Figure 2.8). Average ant velocity did not show a significant regression with colony mass (Figure 2.3A; $F_{1,6}$=2.75, p=0.09, r^2=0.41), though there was a trend toward slower speeds in larger colonies. Ant speed was positively correlated with colony mass-specific metabolic rate ($F_{1,5}$=6.40, p=0.05, r^2=0.56).

Velocity distributions within colonies were strikingly non-normal (Figure 2.3B) and more accurately represented by a power law of the form, $y=ax^b$, where a frequency, y, of individuals moving at a certain speed, x, scales with the exponent b. The exponent of this scaling equation was estimated following the method of log-transformation and linear regression. The linear regressions (Figure 2.3C) on double log-transformed axes were highly significant (for all eight colonies, $p<0.0001$ and mean $r^2=0.75$). The slopes of the regressions, equivalent to the exponents of the power laws describing the velocity distributions, decreased with colony size, from -0.39 in the smallest colony to -1.32 in the largest colony. The degree (or exponent) of the velocity distributions correlated significantly with colony size (Figure 2.3D; Pearson r=-0.93, p=0.0009). Larger colonies exhibit a greater disparity between fractions of active and inactive ants, with a few key individuals moving the most and the majority moving far less.

DISCUSSION

Colonies of *P. californicus* exhibited striking patterns of metabolic rate, growth, and activity scaling. Unlike the isometric scaling predicted for and empirically measured among groups of individual ants, functioning whole colonies exhibited ¾-power metabolic rate scaling. Since net growth rate exhibited isometric scaling, net growth efficiency was much higher in larger colonies than smaller colonies. The patterns of individual speeds within each colony were well represented by power-law distributions in which the majority of

ants were relatively inactive compared to the relatively few highly active individuals. Furthermore, the extent of this disparity among individual speeds within colonies increased with colony size.

As predicted given that these colonies were actively foraging and rearing brood, colonial metabolic rates were higher than measured for individual ants measured under standard conditions (Figure 2.1B), which usually mean that ants are alone, without food, in the dark, and often not moving (Chown et al., 2007). While the scaling slopes are homogenous, the difference in the metabolic elevation, or intercept, of our whole colony lines and the average intercept for intraspecific scaling of ant individuals in the Chown et al. study was 845μW, representing about a 3x-fold elevation of metabolic rate over that predicted for an average inactive "standard" ant. The data I collected are more analogous to the scaling of field metabolic rates for individuals, and the scaling of such field metabolic rates have the potential to differ for many reasons from that occurring for resting animals. However, the data that do exist suggest that field metabolic rates of individual vertebrates tends to scale with negative allometry (Nagy, 2005).

I investigated a number of possible explanations for the observed negative allometry of metabolic rate. Larger colonies of *P. californicus* consumed up to one-third less oxygen on a mass-specific basis than smaller colonies, and this result could not be explained by changes in colony demography, scaling of the size of individual ants or by changes in density. Two recent studies have demonstrated that density can influence population-level metabolic rates (Cao and

Dornhaus, 2008; DeLong and Hanson, 2009), however I did not see such an effect. Density manipulations on colonies of *Temnothorax rugatulus* showed a positive relationship between crowding and mass-specific metabolic rate (Cao and Dornhaus, 2008); in our case, the opposite trend was seen since larger colonies in the same size boxes had lower mass-specific metabolic rates. When groups of individuals were removed from their colonies in our study, density did not correlate with mass-specific metabolic rate. Although this pattern of increasing density correlating with reduced mass-specific metabolic rates was also observed among aquatic unicells (DeLong and Hanson, 2009), it is not immediately clear how a similar mechanism relating to resource constraint, as proposed in that study, could function among our colonies which all were fed with excess food always available.

Changes in the patterns of locomotory activity may contribute to the observed negative allometry of metabolic rate. The velocity distributions of ants within our colonies scaled with colony size so that larger colonies exhibited a greater disparity of active and inactive ants than smaller colonies. A general way to estimate the contribution of locomotory patterns to estimates of whole colony metabolic rate data is to modify the additive model so that individual metabolic rates are predicted as a function of their velocity. The average increase in metabolic rate for ants running at peak speeds relative to "resting ants" is about 6-fold (Fewell, 1988; Lighton et al., 1993a; Lighton et al., 1987; Weier et al., 1995). Thus, the activity coefficient in the additive model (1) can be used to scale each ant's metabolic rate to be linearly proportional to its speed and with the fastest

ants being modeled with 6x-greater metabolic rates than the least active ants. In this way, I estimated that the fraction of whole colony metabolic rate attributable to locomotory movement decreases with colony size (Figure 2.4A). I also used the additive model to predict how much of an effect velocity would have to have on individual metabolic rates to fully account for the observed ¾-power metabolic rate scaling. Based on the measured velocity distributions, the additive model predicts ¾-power metabolic allometry among our colonies if instead of a 6-fold elevation, running at peak velocity elevates metabolic rate above those of inactive ants by 25-fold (Figure 2.4B). This magnitude of an effect seems unlikely given that the scope of metabolic rate associated with running is about 6x in ants, suggesting that variation in locomotory performance is only part of the explanation for the observed negative allometry of metabolic rate.

A number of other hypotheses can be proposed to explain the negative allometry of metabolic rates observed for the whole ant colonies in this study. One possibility is that certain colonies grew faster due to relatively higher growth efficiency and relatively lower metabolic rates. In this way, colony size per-se is not hypothesized to be the factor that determines metabolic rate so much as the reverse; i.e., variation in colony-size independent metabolic physiology is hypothesized to result in different growth rates and effective colony sizes. A second possibility is that maintenance costs associated with colony growth and function scale with negative allometry (Jeanson et al., 2007). This hypothesis predicts that as colony size increases, the number of ants necessarily engaging in particular activities decreases so that a surplus of individuals with low metabolic

rates may accumulate and thus produce negative metabolic allometry. However, our evidence for higher efficiency in larger colonies should be considered preliminary, as I have not shown that these colonies have similar egg production rates or worker survival, or that metabolic rates are consistent during ontogeny.

Another non-alternative type of explanation for negative metabolic allometry in *P. californicus* colonies is that eusocial insect colonies may be metabolically and behaviorally integrated in ways that are more commonly thought of as restricted to the physiology of physically connected individual organisms. Marine colonial ascidians, for example, have been shown to exhibit near ¾-power metabolic scaling, but only when individuals are physically connected by a vascular network (Nakaya et al., 2003). In the same way that the geometry of vascular networks is proposed to be the emergent result of shear forces and material properties on the local scale (LaBarbera, 1990), conceivably the behavioral interactions in a networked social group may lead to emergent patterns of nutrient or information transfer that similarly influence the scaling of metabolism. Studies of the network interactions of food and behavior within ant colonies will help assess whether this is possible. The ability to perform direct manipulations on colony size and composition while observing patterns of activity make social insect colonies particularly useful models for evaluating general hypotheses of metabolic integration. It should be possible to directly observe the scaling properties of distribution networks between foragers and inside-nest ants, individual activity rates, and to directly manipulate superorganism size, an experimental approach not easily performed with individual organisms. In this

way, data can be collected to empirically test the predictions of hypotheses that aim to explain the mechanistic basis of negative metabolic allometry.

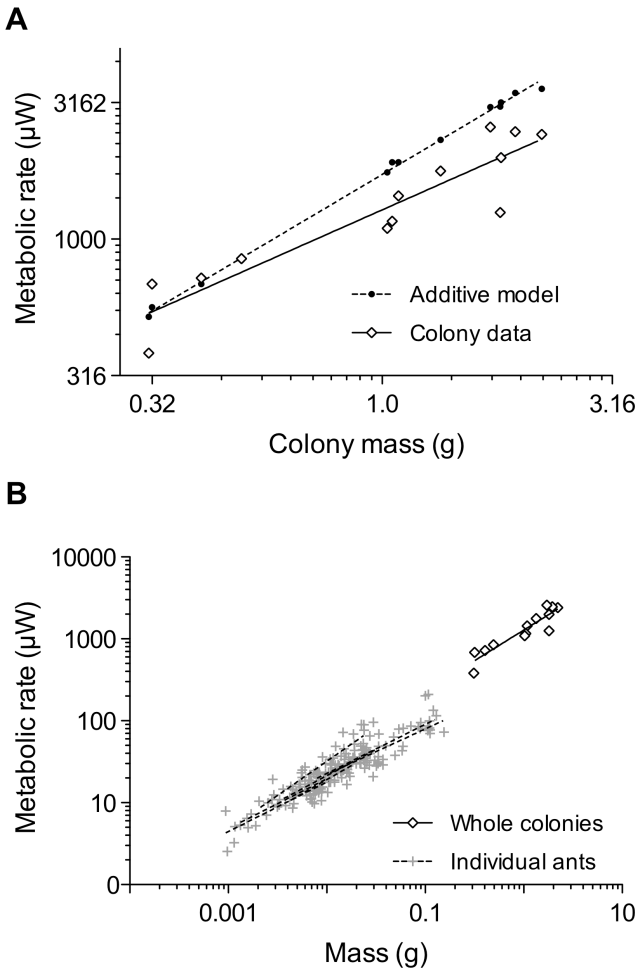

Figure 2.1. (A) Whole colony metabolic rate allometry plotted on double-log axes, with a hypometric slope (0.75) statistically less than the isometric slope (1.0) predicted by the additive model. (B) Intraspecific whole colony metabolic rates scale in essentially the same way as observed for intraspecific scaling of metabolic rate for individual ants, as seen on this plot with seven intraspecific negative metabolic rate allometries (data adapted from Chown et al. 2007) with slopes ranging from 0.56-0.84.

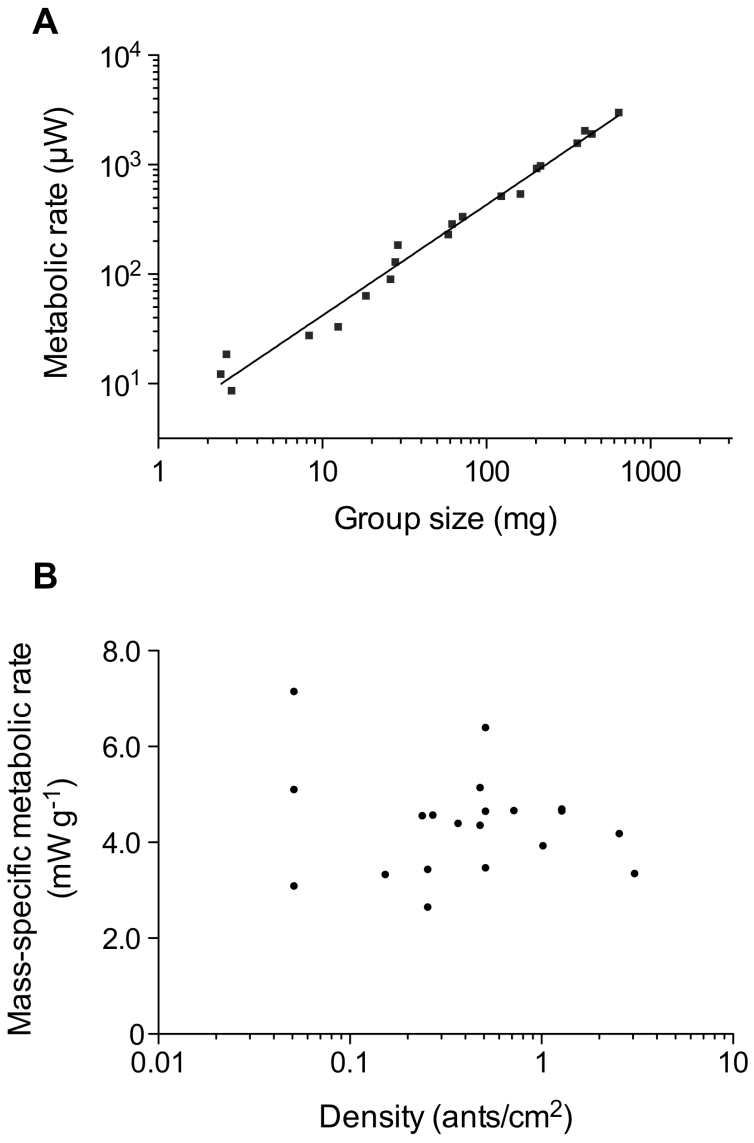

Figure 2.2. (A) Isometric scaling of metabolic rate among worker groups removed from the social environment of their colonies. (B) In the worker-group study, ant densities ranged greater than 60x, but showed no correlation with the mass-specific metabolic rates of the workers.

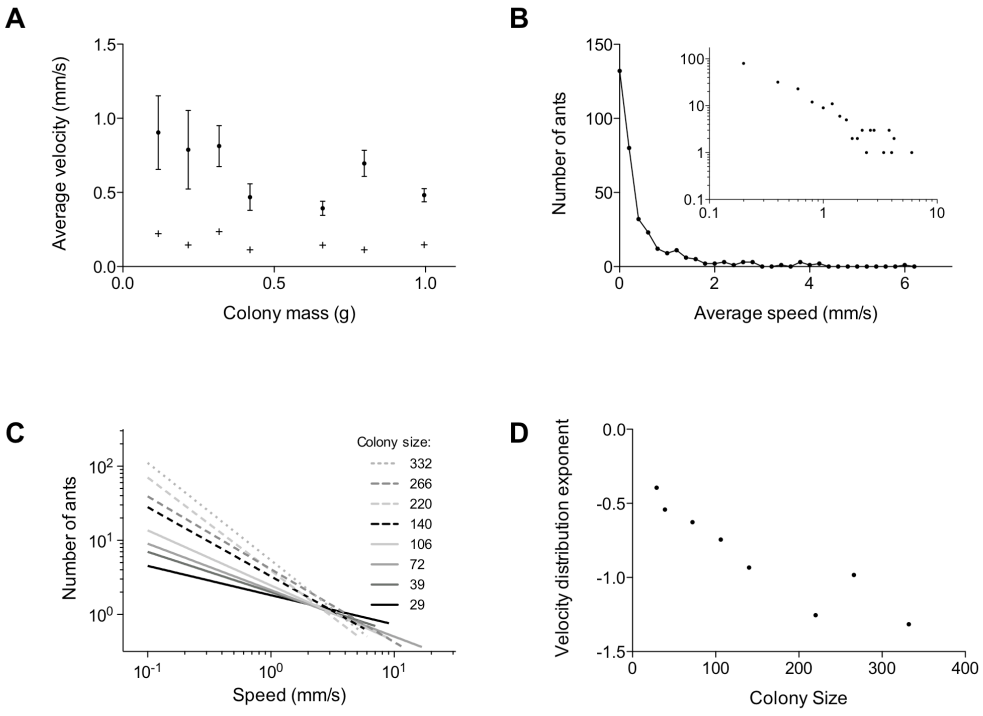

Figure 2.3. (A) Average ant velocity within a colony plotted as a function of colony size, error bars noting standard error. Crosses indicate median velocities for each colony. (B) This plot illustrates the frequency distribution of ant velocities within a colony having 332 workers. The inset displays the same data on double-logarithm axes. (C) Linear regressions of log-transformed velocity distributions for a range of colony sizes. (D) The slopes of the regressions in (C) are plotted here as the scaling exponents for the velocity distributions as a function of colony size.

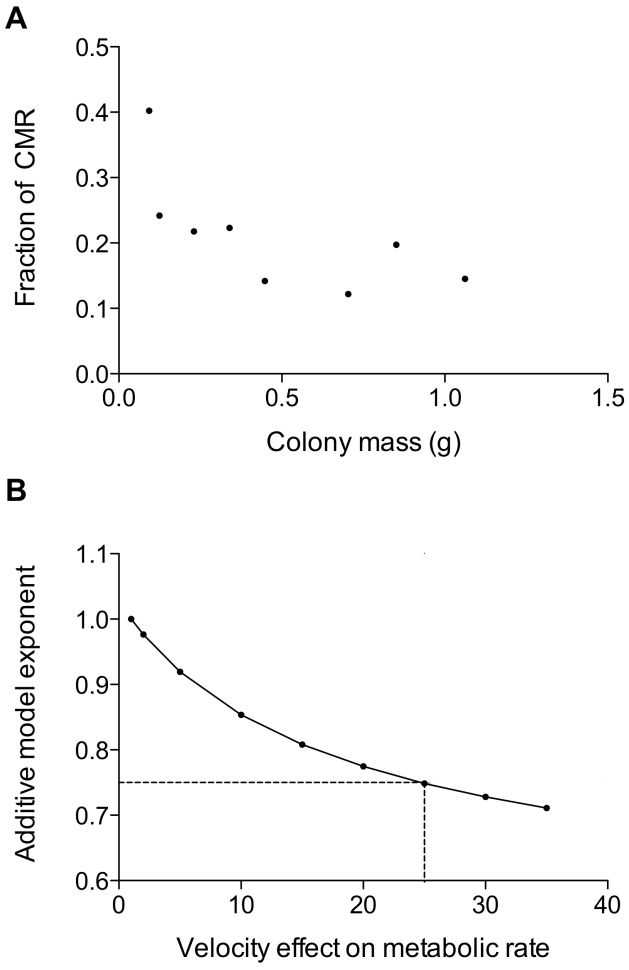

Figure 2.4. (A) The fraction of whole colony metabolic rate (CMR) estimated to be due to movement patterns decreases with increasing colony size. (B) This figure plots the estimated allometric exponent generated by the additive model modified to take into account both the effect of velocity on metabolic rate and the colony velocity distributions. If maximum running speed elevates individual metabolic rates by 25-times, then the additive model predicts metabolic rate scaling with mass$^{0.75}$.

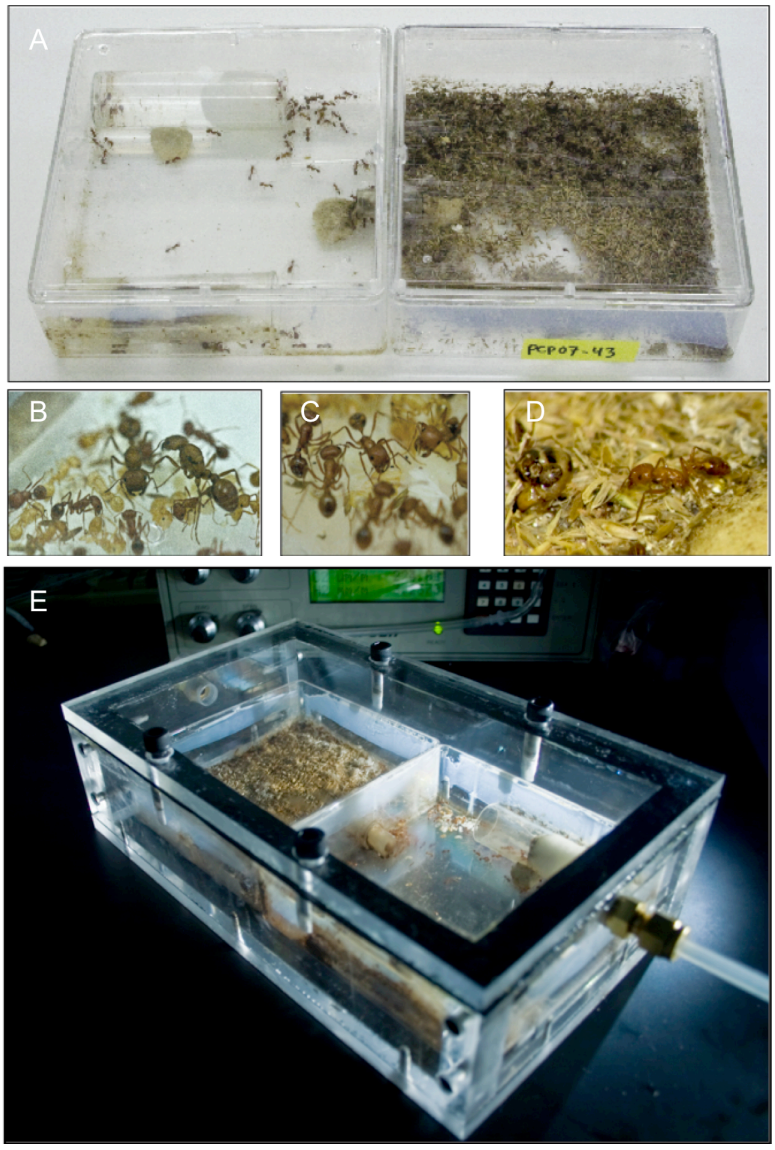

Figure 2.5. These photographs show (A) a colony of *Pogonomyrmex californicus* in its artificial nest enclosure, (B) queens, (C) workers tending to brood, (D) foraging for seeds, and (E) a colony nest enclosure within the flow-through respirometry chamber.

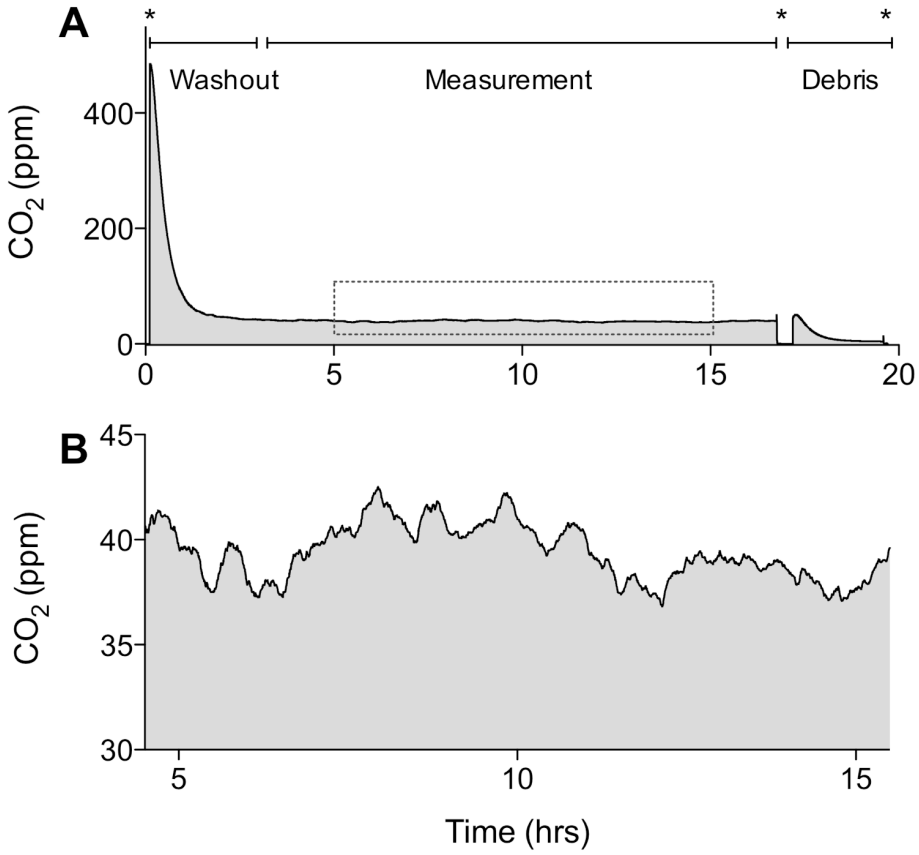

Figure 2.6. Representative trace of CO_2 recording during whole colony measurements. The entire recording graphed in (A) includes three baseline measurements as indicated by asterisks (*) and shows the excurrent airstream CO_2 concentration both for the whole colony measurement as well as after the ants had been removed so that the background CO_2 emission from debris could be measured. In (B), the CO_2 emission from the colony as illustrated by the dotted box in (A) is graphed for increased resolution.

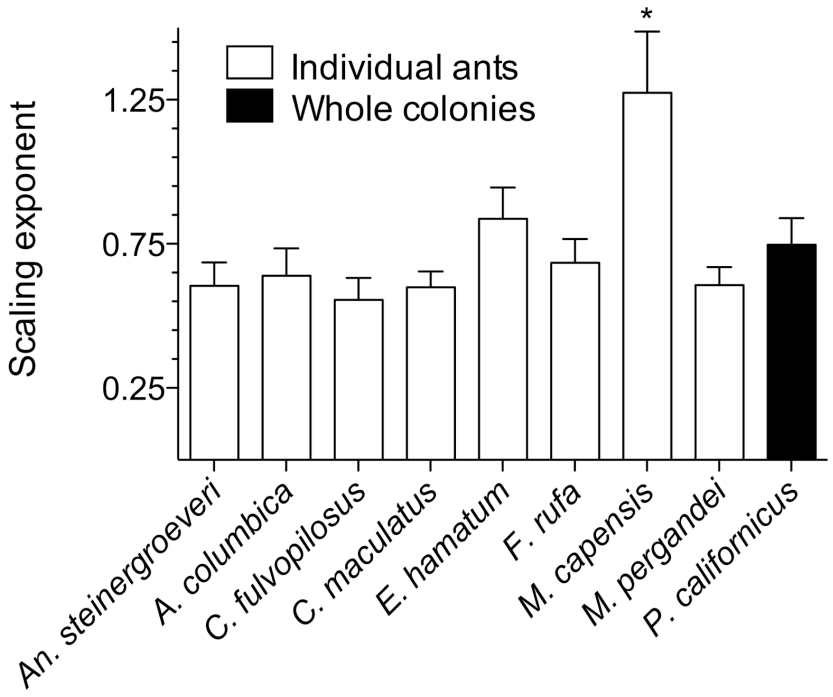

Figure 2.7. With the exception of *Messor capensis*, the homogenously hypometric intraspecific metabolic rate scaling allometries of individual ants (data from Chown et al. 2007), are not significantly different from the hypometric scaling allometry for whole colonies of *Pogonomyrmex californicus.*

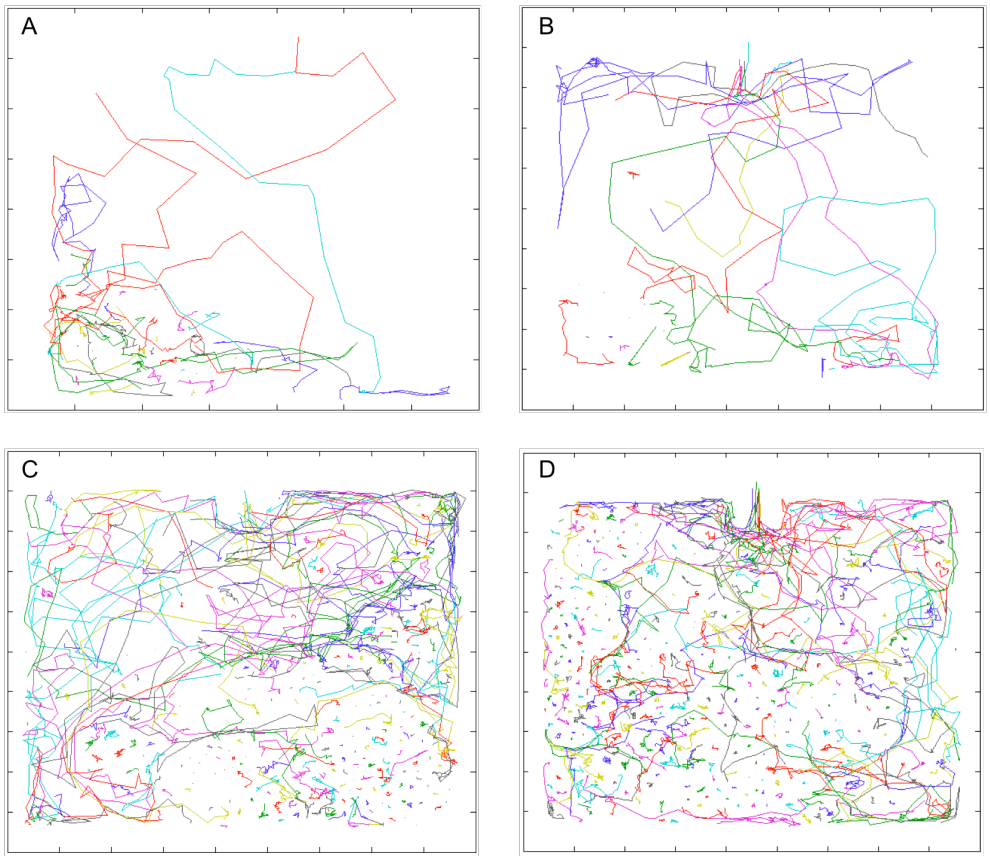

Figure 2.8. Digitized trajectories of ants in colonies with (A) 32, (B) 39, (C) 267, and (D), 332 workers. Each frame shows the trajectories of ants over a 60s period within the colony nest of width and height 11cm. Colors indicate different ants.

Table 2.1. Whole colony metabolic rate allometries.

Regression	Intercept (±SE)	Slope (±SE)	r^2	N	Range (g)
Additive model[1]	3.237 ± 0.004	1.000 ± 0.014	0.99	13	0.311-2.222
Additive model[2]	3.347 ± 0.001	1.001 ± 0.006	0.99	13	0.311-2.222
Additive model[3]	3.268 ± 0.005	0.980 ± 0.015	0.99	13	0.311-2.222
Colony measurements	3.107 ± 0.028	0.747 ± 0.093	0.85	13	0.311-2.222
Worker groups	3.468 ± 0.050	1.008 ± 0.033	0.98	20	0.003-0.641

Note: This table displays ordinary linear regression results for metabolic rate allometries based on $\log_{10}$-transformed data for the additive model predictions, whole colony metabolic rate measurements, and the worker group metabolic rate data, all standardized to 25°C. The three additive models were computed with scaling coefficients based on (1) *P. rugosus*, (2) general non-tick non-scorpion arthropods, and (3) estimated *P. californicus* mass-specific metabolic rates.

Table 2.2. Mass and metabolic rate data for whole colonies of *Pogonomyrmex californicus.*

Colony	Mass (g)	VCO2(ml/min)	Temperature (C)	Metabolic rate (µW at 25C)
1	2.2228	0.0091611	28.45	2416.22
2	1.0851	0.00546	28.45	1440.07
3	0.311	0.0013845	27.8	381.99
4	1.0518	0.004485	28.7	1162.59
5	1.947	0.0096603	28.88	2473.07
6	1.339	0.006474	27.87	1777.55
7	1.7183	0.010023	28.85	2571.26
8	1.8048	0.004719	28.37	1251.55
9	1.8124	0.007566	28.5	1988.61
10	0.3163	0.00273	29.18	684.51
11	0.4948	0.003159	28.2	847.74
12	1.0259	0.00249591	27.56	1094.03
13	0.404	0.0027222	28.4	720.47

TABLE 2.3. Colony census data at time of measurement.

	Queens		Workers		Pupae		Larvae	
Colony	#	mass (mg)	#	mass (mg)	#	mass (mg)	#	mass (mg)
1	1	12.8	405	1530	70	320	75	360
2	3	37.2	251	730	33	116.4	80	201.5
3	3	35.7	80	265.7	0	0	12	9.6
4	3	32.4	317	862	17	58.3	55	99.1
5	3	37.4	532	1613.4	36	136.2	88	160
6	3	36.4	400	1273.1	0	0	18	29.5
7	3	34.2	413	1247.8	57	224.4	124	211.9
8	2	24.5	503	1724.7	0	0	36	55.6
9	2	26.7	514	1654.7	0	0	82	131
10	2	24.6	92	260.4	0	0	19	31.3
11	2	24.8	120	391	19	65.5	9	13.5
12	1	11.6	260	888.8	0	0	55	125.5
13	3	30.8	105	350.6	0	0	16	23

Note: Data are presented for 10-month old whole colonies of *Pogonomyrmex californicus.* Note that the masses listed in each column are the measured masses of the total number of ants within that category, not average per-capita values.

Table 2.4. Mass and metabolic rate data for *Pogonomyrmex californicus* worker groups exhibiting isometric metabolic rate scaling.

Workers	Mass (g)	Temperature (C)	VO2 (mlO2/min)	Metabolic rate (µW at 25C)
1	0.0028	31.86	2.44E-05	5.38
1	0.0024	30.36	3.45E-05	8.45
1	0.0026	30.35	5.24E-05	12.83
3	0.0083	30.94	7.79E-05	18.32
5	0.0184	30.11	1.78E-04	44.39
5	0.0125	30.30	9.33E-05	22.94
10	0.0278	31.83	3.64E-04	80.47
10	0.0289	29.55	5.21E-04	134.85
10	0.026	30.06	2.54E-04	63.53
20	0.0585	31.83	6.48E-04	143.29
25	0.0717	29.91	9.48E-04	239.48
25	0.0618	31.55	8.10E-04	182.64
50	0.1232	29.81	1.45E-03	369.26
60	0.1612	30.30	1.52E-03	373.94
75	0.2024	31.86	2.60E-03	573.00
85	0.2139	30.13	2.75E-03	685.24
115	0.3584	30.11	4.44E-03	1104.81
150	0.4398	30.94	5.40E-03	1269.23
150	0.3985	31.34	5.77E-03	1320.01
225	0.6405	31.83	8.42E-03	1860.50

Chapter 3

INFORMATION PROCESSING IN SOCIAL INSECT NETWORKS

INTRODUCTION

Capturing the essence of biological networks is among the most important challenges facing modern science. Gene regulation, motor control, developmental specialization, and metabolic allometry all emerge as the result of integrated networks. These networks operate at different biological levels but all distribute and transform localized information into larger scale processes (Jeong et al., 2000; LaBarbera, 1990; Moses et al., 2008; Strogatz, 2001). However, not all biological networks develop or evolve around higher order function. Social networks, the broad class of networks characterizing human and animal social groups, are typically thought to exhibit global-structure consistent with the predictions of generative network models such as preferential attachment (Barabasi and Albert, 1999; Newman, 2010). In these systems, interactions benefit and reinforce an individual's own role within the network (Salganik et al., 2006), but at a potential cost to higher-level properties such as efficiency or resilience (Kaluza et al., 2008).

Although generally clustered into one category, social networks can describe many different types of complex systems from aggregations to cohesive social units. Network analyses show global similarities across social systems; they are generally decentralized and scale-free, with network structure emerging from local interactions in the absence of an external controller. However, the function

of interactions within social groups should vary with the evolutionary and ecological contexts in which the group evolves. The social interactions within, for example, a pod of dolphins (Lusseau, 2003; Lusseau and Newman, 2004) or extended family groups of ground squirrels (Wey et al., 2008), should serve very different functions than the communication networks among workers within a eusocial insect colony (Feigenbaum and Naug, 2010; Fewell, 2003; Mayack and Naug, 2009; Naug, 2008).

Social insect colonies are the hallmark of integrated social units, exhibiting some of the most awe-inspiring examples of complexity in the biological world. Nest architecture that promotes environmental stability (Penick and Tschinkel, 2008), division of labor that scales with colony size (Holbrook et al., 2011), and collective decision making (Sasaki and Pratt, 2011) all take place in the absence of hierarchical control (Wilson and Hölldobler, 1988). Social insect communication systems, which include such diverse modalities as direct individual contact, trophallaxis, and broadcast pheromonal signaling, show they are highly regulated units with coordinated individual behaviors that generate emergent effects which are beneficial to the group as a whole (Hölldobler and Wilson, 2009). If network structure reflects biological function, then the structure of a social insect colony should vary distinctly from that of social networks generated from associations based on individual success.

I investigated network motif profiles of seed harvester ant colony interaction networks to determine whether their antennation patterns are predominantly random, regulatory, or social in nature. Since the purpose of

antennation by ants is to obtain information, the structure of their communication networks is critical to how colonies function (Fewell, 2003). Motif analysis determines the predominant local interaction patterns (3-node directed subgraph motifs) making up a network (Milo et al., 2002) and has the potential to identify fundamental interaction signatures within networks of different size or context that may correspond to differences in functionality (Milo et al., 2004). Previous work by Milo and his colleagues (Milo et al., 2004; Milo et al., 2002; Shen-Orr et al., 2002) has shown that biological regulatory networks have predominant interaction patterns that move information directionally, while social networks develop bidirectionally-connected cliques as individuals mutually strengthen associations with their neighbors. I asked whether these different types of subgraph representation allow us to differentiate between networks selected for at the individual-level and networks that emerge as a result of group-level selection (Kaluza et al., 2008).

METHODS

Ant colonies

Whole colonies of *Pogonomyrmex californicus* were reared in the laboratory (Holbrook et al., 2011; Waters et al., 2010) in artificial nest enclosures (242 cm^2) containing separate nest and foraging arenas, water tubes, and foraging material including fruit flies, grass seeds, and finch seeds. All adult workers and queens within each of two colonies were uniquely marked. Color codes were applied to the dorsal surface of the ant head, mesosoma, and gaster with fine-tip

oil-based paint markers. Ants did not exhibit adverse reactions to the paint or increased mortality following paint marking.

After having been paint-marked, colonies were given two weeks to acclimate to their new markings and the experimental arena, a well-lit lab bench in an observation room maintained at 30 degrees C. A foam pad beneath the nest enclosures dampened vibrations and a sheet of transparent plastic was placed over the nest enclosures to prevent disturbance induced by experimenter exhalation. Fifteen minutes before video-recording, colonies were gently stimulated to engage in work (division of labor) with the addition of foraging items and debris through small openings in the nest enclosure lids. Following these methods, nearly all individuals within the colonies were visible from above and workers within the colonies were observed engaging in normal behaviors including foraging, brood care, food processing, refuse removal, policing, and allogrooming.

Video recording

I recorded digital video of colonies within nest enclosures to carefully observe the behaviors and patterns of interactions among individual ants (Movie S1). Video data were recorded using a CCD camera (Flea 2, Point Grey Research, Richmond, BC, Canada) and a 16mm fixed focal length lens (Edmund Optics, Barrington, NJ, USA) positioned on a copy stand above colony nest enclosures. Uncompressed AVI video (1624 x 800 pixels, 15 frames per second) was recorded using FlyCapture SDK (Point Grey Research, Richmond, BC, Canada). The arrangement of these components resulted in a resolution of 73.8

pixels per centimeter, more than sufficient to observe the fine-scale antennation patterns between interacting ants. I recorded each colony for a duration of two hours (approximately 550 GB for each recording).

Networks

To establish networks of directed contacts from the video recordings, each individual ant was tracked throughout the entire recording and her contacts with other ants manually recorded. Contact occurred if the ant stopped and placed both antennae onto another ant, orienting the head towards the contacted ant. Antennation was chosen as the focal behavior because it is a direct form of information exchange and can be clearly characterized ethologically. Networks of colony interactions were constructed as adjacency lists, each individual ant treated as a node, with their directional interactions supplying the network edges. A total of 12 networks were constructed, 5 for colony pcp07-40 and 7 for colony pcp07-35.

All social network data are snapshots of a system in time. For the data to be meaningful, they should be based on a time interval long enough to capture the behavior of the system at a point in time without being so long that behavioral variation over time averages and dampens away relevant interaction patterns. Data to populate the interaction networks in this study were based on the behaviors observed during 26-second subsets of the video recordings for each colony. Analyzing less time than this would have meant that the networks were highly fragmented (i.e., not connected). Preliminary data suggested that

reviewing 13-26 seconds of behavior would be sufficient to capture interactions for greater than 90% of the active individuals within the colonies. Of the 12 networks I analyzed, there was an average of 3.17 connected components per network and the largest connected cluster contained on average 92.96% of the nodes in each network. The effects of analysis and observation time on social network structure were investigated by cumulatively pooling networks. For each of the two colonies, I analyzed the network motif representation of networks based on 26, 52, 78, 104, and 130 seconds by combining observations to build sequentially larger networks.

Motif analysis

To test hypotheses about the mechanisms responsible for generating colony-level functionality, I analyzed the local-scale structure of interaction networks using triad motif analysis (Milo et al., 2004; Milo et al., 2002). The primary question addressed by motif analysis is whether particular subgraphs appear more often in an observed network than would be expected in similarly sized networks generated based on the assumptions of specific null models.

Using the implementation of motif analysis executed by Fast Network Motif Detection (FANMOD) (Wernicke and Rasche, 2006) I tested the structure of our networks against a network model that randomized the interactions between individuals. The null-model random graphs were generated with the same degree distribution as observed in the colonies to preserve global network structure. Nodes in the random networks also maintained the same number and

directionality of edges as in the respective observed networks. The frequencies of each of the 13 directed three-node subgraphs (Figure 3.4, Table 3.5) were calculated both for each observed network (N=12) and the simulated random graphs (N=10,000 per observed network).

The statistical significance of each subgraph representation within an observed network was calculated by comparing subgraph densities (the ratio of the number of occurrences of a specific subgraph to the total number of subgraphs within a network) between observed and random networks. I estimated bootstrapped p-values calculated as ratio of the number of randomized networks in which the subgraph density was higher than observed to the total number of randomized networks for each subgraph in each observed network. Significantly over-represented subgraphs ($p < 0.05$ and density > 0.01) are referred to as network motifs (Milo et al., 2002). It is possible that specific subgraphs are not generated within the randomized networks, resulting in cases for which the p-values are undefined. The only subgraph for which this occurred was ID=13, a subgraph identified in 5/12 networks, but with a instance count greater than one in only two networks and never with a subgraph density greater than 0.01.

Network visualizations and additional descriptive network statistics were generated in R using the igraph package (Csardi and Nepusz, 2006; R Development Core Team, 2011). Degree distributions for the nodes within a network can be modeled as power laws, $p(k) \propto k^{-alpha}$, where $p(k)$ is the fraction of vertices having degree k and *alpha* is the scaling exponent. I estimated the exponent associated with in-, out-, and total-degree distributions using the

methods of both ordinary least squares on log-transformed data and discrete maximum-likelihood estimation of the power-law distribution (Clauset et al., 2009; Dubroca, 2011). Unless described otherwise, data in the results section are presented as means ± standard errors.

RESULTS

Seed harvester colony interaction networks (Figure 3.1) developed at a rate of 4.86 ± 0.08 interactions per ant per minute. Networks were composed of an average of 89.17 ± 3.96 nodes and 191.5 ± 18 edges (Table 3.1). While differences in colony size affected the number of nodes ($F_{1,10}$=19.38) and edges ($F_{1,10}$=23.29), there were not significant differences in network topology. Across the 12 networks, the average in-degree power-law exponent was 1.93 ± 0.13 (Table 3.2) and the average out-degree power-law exponent was 2.03 ± 0.08 (Table 3.3). There was no significant effect of source colony on in-degree ($F_{1,10}$=0.152, p=0.71) or out-degree ($F_{1,10}$=1.77, p=0.21) exponents and there was also not a significant difference between these exponents ($F_{1,22}$=0.387, p=0.54). The exponents estimated by OLS were less than those estimated by maximum likelihood (in-degree: 3.18 ± 0.08, out-degree: 3.12 ± 0.09), but both sets of estimates are qualitatively consistent with right-skewed degree distributions characteristic of scale-free networks (Figure 3.4).

I used motif analysis to identify the relative significance of the thirteen possible directed subgraphs among every connected triad of ants within our recorded networks (Figure 3.2). Subgraphs were classified as significant motifs

when the frequency of a given subgraph was higher than expected compared to a null model of degree-preserved randomized interaction and its subgraph density was at least 0.01 (Table 3.4). Eight subgraphs (IDs: 1, 3, 6, 7, 9-12) were classified as motifs in at least one of the 12 observed networks, and one motif, the feed-forward loop (ID: 7), was present in 11/12 networks. The high frequency on significance for the feed-forward loop (i.e. significantly higher expected frequency in each network) indicates it to be a consistent network signature within the colonies I measured.

To evaluate the similarity of motif patterns across different networks and over time, I calculated the standardized Z-score for each subgraph (Milo et al., 2002) and constructed a triad significance profile (TSP) for each network (Figure 3.3). The TSP was consistent across all colony networks (Pearson's $r=0.58 \pm 0.03$, N=66 comparisons, median $p=0.03$). The motif distributions were also not significantly affected by the amount of time (26-130 s) used to populate interaction networks (Figure 3.6; Table 3.6).

When compared to the major network superfamilies (Milo et al., 2004), the combined motif signatures of our observed networks were somewhat more correlated with social networks ($r=0.68$, $p=0.009$) than the gene transcription ($r=0.48$, $p=0.09$) or the signal transduction ($r=0.60$, $p=0.03$) regulatory network superfamilies (Figure 3.3). Nevertheless, the correlation between colony and social networks was not significantly stronger than the correlation between colony and transcription networks ($\Delta r=0.20$, $n=13$, $p=0.49$). The fully connected triad (motif 13: the social-clique motif), which is a defining characteristic of the human

social network superfamily (Milo et al., 2004), was conspicuously uncommon in the *P. californicus* networks.

DISCUSSION

I compared the network motif profiles within social insect colony networks to the motif signatures for a range of technological and biological networks, including social networks. While the *P. californicus* networks exhibited scale-free structure and similarity with the general triad significance profile for the social network superfamily, the predominant motif within our colonies was the feed-forward loop. This interaction pattern is not typically identified with human social networks, but is involved in modulating information transmission in a range of regulatory networks across biological levels, including transcriptional regulation in *E. coli*, signal transduction between mammalian cells, and *C. elegans* synaptic wiring (Mangan and Alon, 2003; Mangan et al., 2006; Shen-Orr et al., 2002). In contrast, the social-clique motif, characteristic of social attachment networks (Milo et al., 2004; Shen-Orr et al., 2002), was absent in our *P. californicus* colony networks. The motif representation in *P. californicus* network structure supports the hypothesis that social network structure within these cohesive social groups has been selected to maximize colony-level function and/or efficiency rather than individual success. In other words, they are social regulatory networks, with key subgraph structures in common with regulatory networks across biological scales.

I suggest the motif signatures within social insect colonies may reflect selection for efficiency of directional information flow. Although all 13 subgraphs connect the same number of individuals, they vary in the costs of establishing and maintaining those connections. One way to compare efficiencies of interaction patterns is to evaluate the extent to which a particular subgraph maximizes the number of connected nodes (N) while minimizing costs of connectivity, in particular the number of edges as determined by interactions (I) and the resulting diameter (D) of the graph. In this way, subgraph efficiency (E) can be defined as E=N/(I*D). Applying this definition to the thirteen directed three-node subgraphs, calculated efficiencies range from 0.38 in motif 6, the motif of two mutual interactions, to 1.0 in motifs 7 and 8, the feed-forward loop and the three-cycle (Figure 3.2). The observation that the feed-forward loop is the characteristic motif signature among our colony networks suggests that efficiency of information transfer may be relevant to the patterns of connection among workers.

While this study has identified a number of intriguing features of communication patterns within social insect colonies, it also raises many new questions. One question to consider is how nest architectures may affect interaction dynamics. While the interaction patterns of individual ants may correlate with their spatial location within a nest (Pinter-Wollman et al., 2011), it is not clear whether location passively determines which type of interaction pattern individuals may be subjected to or engage in. Since ants tend to homeostatically regulate their densities (Holbrook et al., 2011) and exhibit spatial fidelity (Sendova-Franks et al., 2010), I do not expect spatial position to be a

causal factor influencing interaction patterns. However, given the substantial variation in labor-related specialization among workers within a colony, one factor that may be important is the extent to which individuals exhibit behavioral specialization for specific information-processing roles. An example of this kind of information-processing specialization has been identified in colonies of leaf-cutting ants, in which workers at the start of foraging may return to the nest unladen to increase the rate of information transmission to other workers within the nest (Bollazzi and Roces, 2011). By directly manipulating colony composition, I can empirically test hypotheses about the effects of spatial segregation and worker specialization. Additionally, by using different random models or generative network algorithms (Newman, 2010), the motif analysis method can be extended to test theoretical hypotheses about the temporal development and evolution of complex systems.

Animal groups exhibit an extreme range of social integration, from primarily solitary species that lack social cohesion to the complex interactions that shape superorganism species. To date there has been no network-based approach to separate out the very different mechanisms for network evolution across the diversity of social groups. Network motif analyses provide a new way to differentiate the interaction regimes under selection in social evolution. The markedly different subgraph characteristics of social insect and human societies open the field of network analysis for further exploration into the forces shaping social structure, function and evolution.

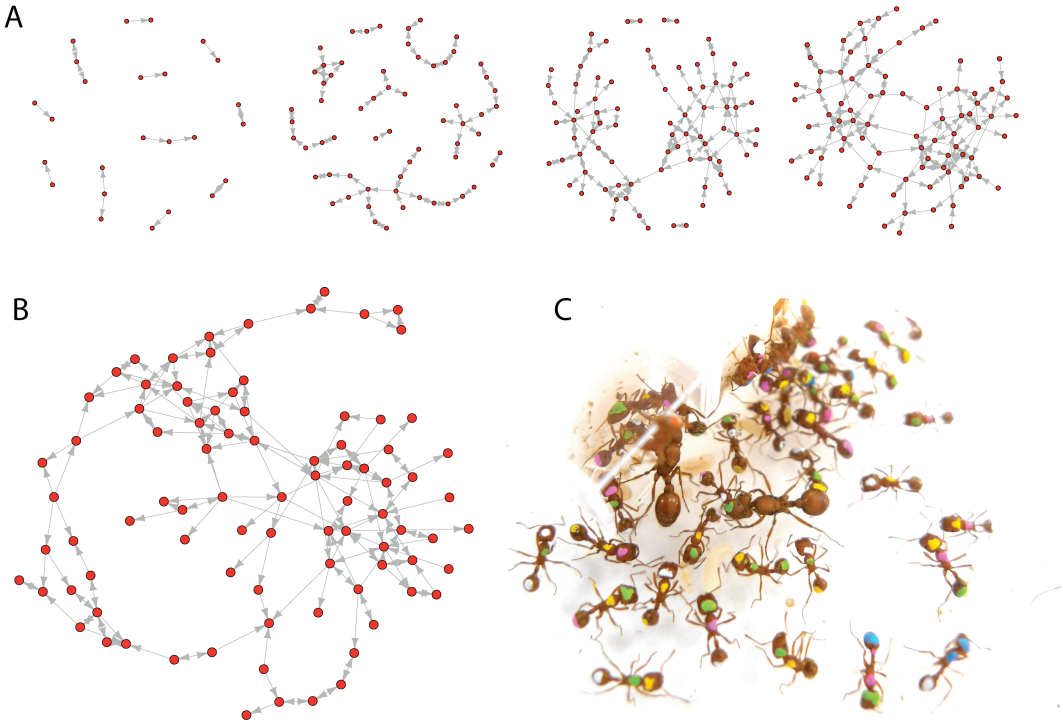

Figure 3.1. Ant colony interaction networks. **(A)** The development of a directed network of interactions between workers in a single *P. californicus* colony over a period of 60 s. Nodes represent individual workers or queens within a colony and arrows represent interactions between individuals. **(B)** Example *P. californicus* interaction network based on 26 s of colony behavior. **(C)** Photograph of queens and workers within a seed harvester colony; individuals have been painted with unique color combinations to track their interactions.

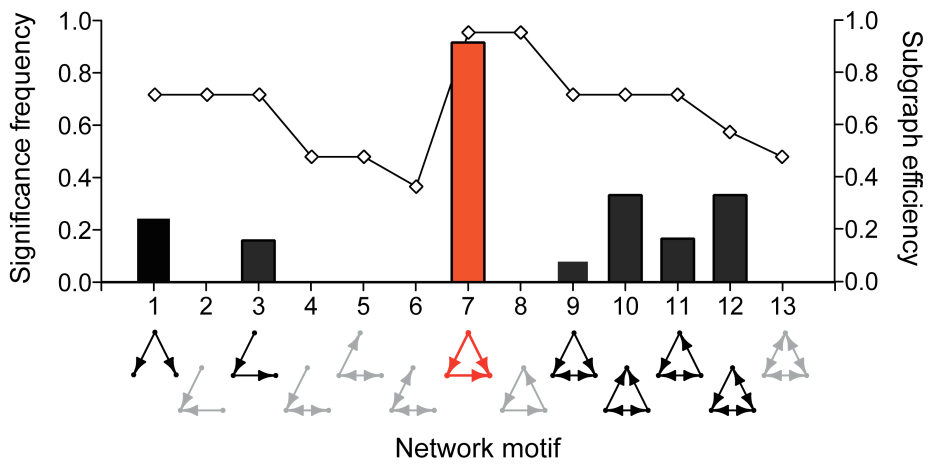

Figure 3.2. Distribution of network motifs. Network motif analysis deconstructs a network into its constituent subgraphs and determines whether any of these local-scale interaction patterns are represented more frequently than expected for a randomized network of the same size. The subgraphs that were identified as significant motifs in our analysis of social insect colony networks are plotted above in a summary histogram with relative frequencies on the left axis. The interaction efficiencies of each subgraph are plotted as a line with units along the right axis. One of the two subgraphs with the highest efficiencies, the feed-forward loop (motif 7), was also the most dominant motif observed across the *P. californicus* interaction networks. Gray subgraphs were not classified as network motifs, black indicates a subgraph identified as a motif within at least one network, and red indicates the only motif that was identified across the majority of networks.

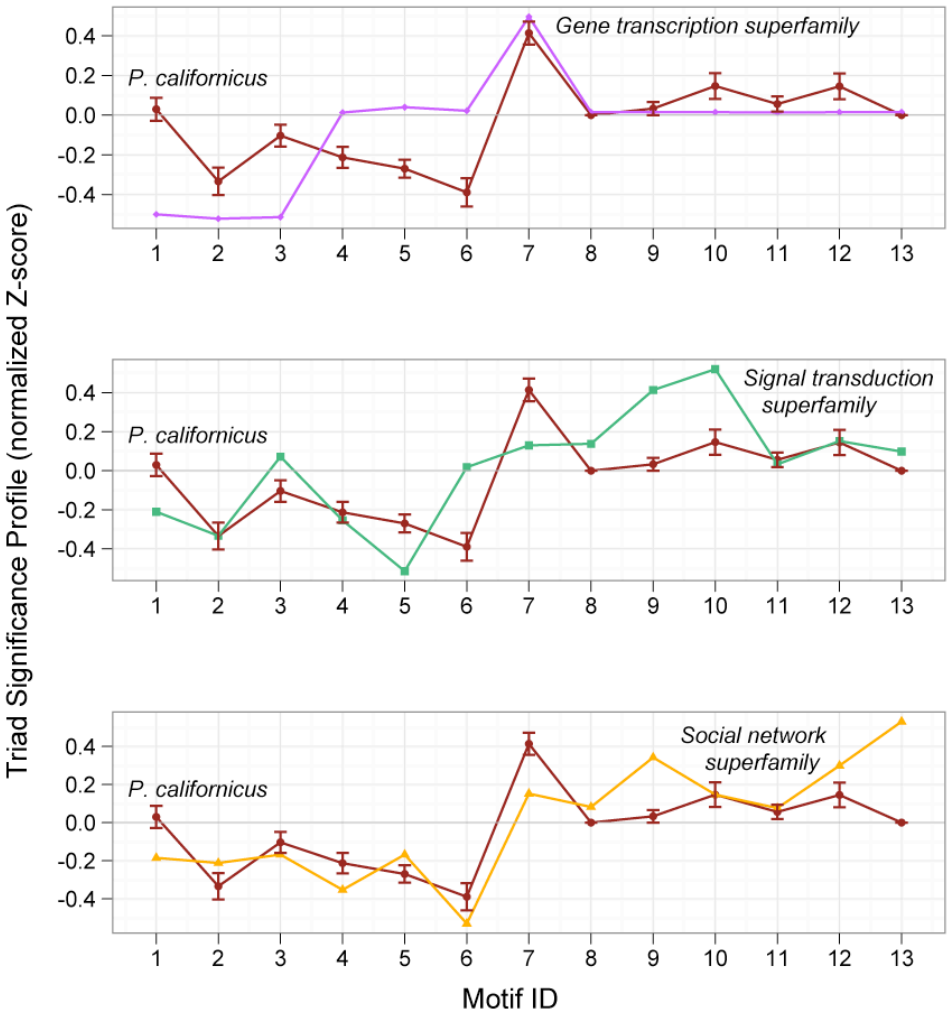

Figure 3.3. Social regulatory networks. Triad significance profiles compare the characteristic network motifs across a diverse range of network types and sizes by plotting standardized Z-scores which quantify the extent to which each subgraph is observed more or less frequently than expected in networks of a similar size and global structure but with randomized edge connections. The observed *P. californicus* social insect networks exhibit a distinct pattern of social regulatory structure combining elements found in previously identified major network superfamilies (Milo et al., 2004).

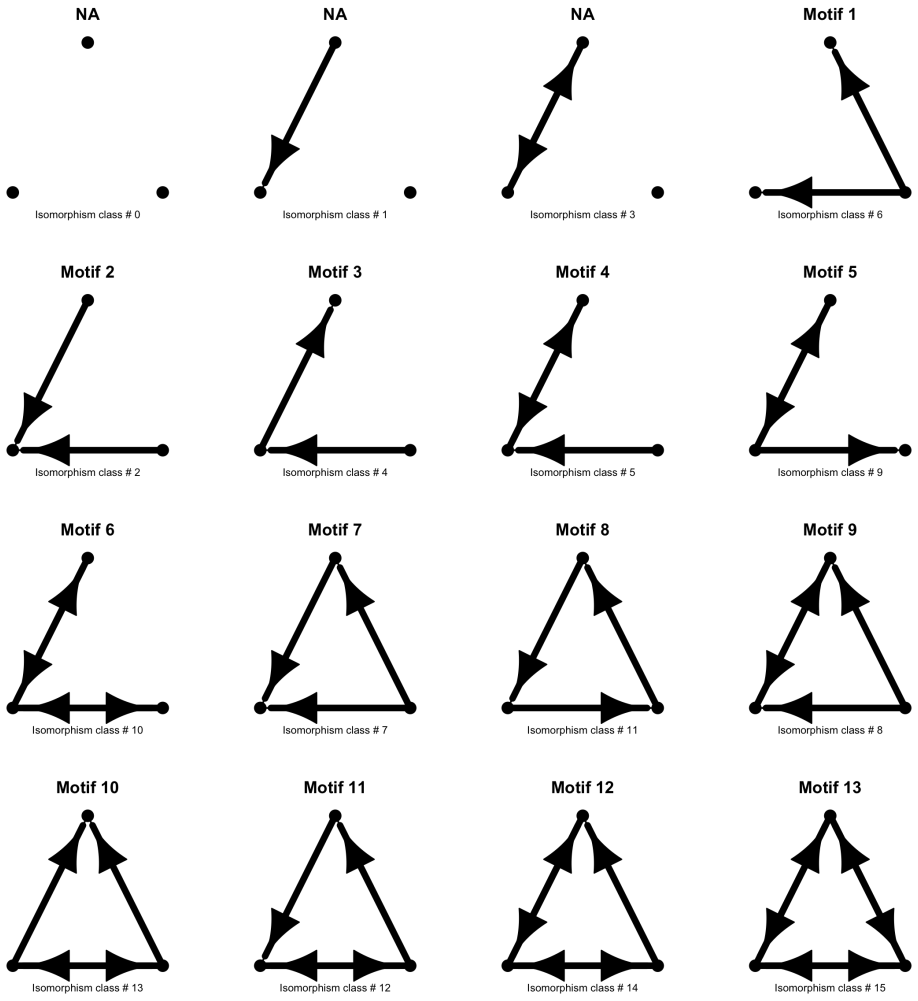

Figure 3.4. Isomorphism classes and network motifs. There are 16 isomorphism classes (#0-15) of three-node directed graphs. Note that there are only 13 of these graphs that connect all three nodes. Above, each of these is drawn and identified with the corresponding network motif ID.

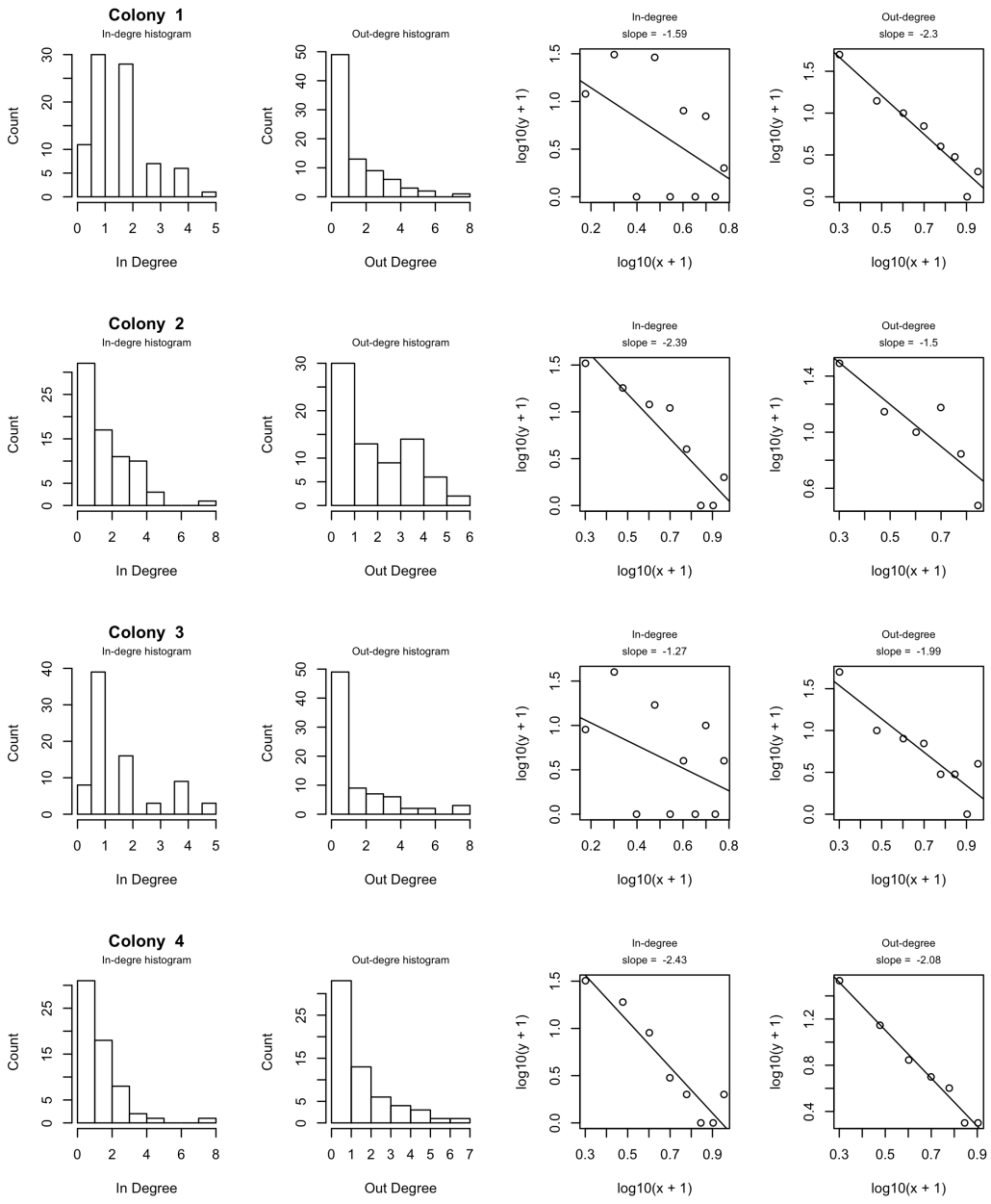

Figure 3.5a. Network degree distributions (networks 1-4). For each colony network, I present the histograms for in- and out-degree as well as the scatterplots associated with estimating the exponent by OLS-regression for the power-law distribution describing the in- and out-degree scaling in each colony.

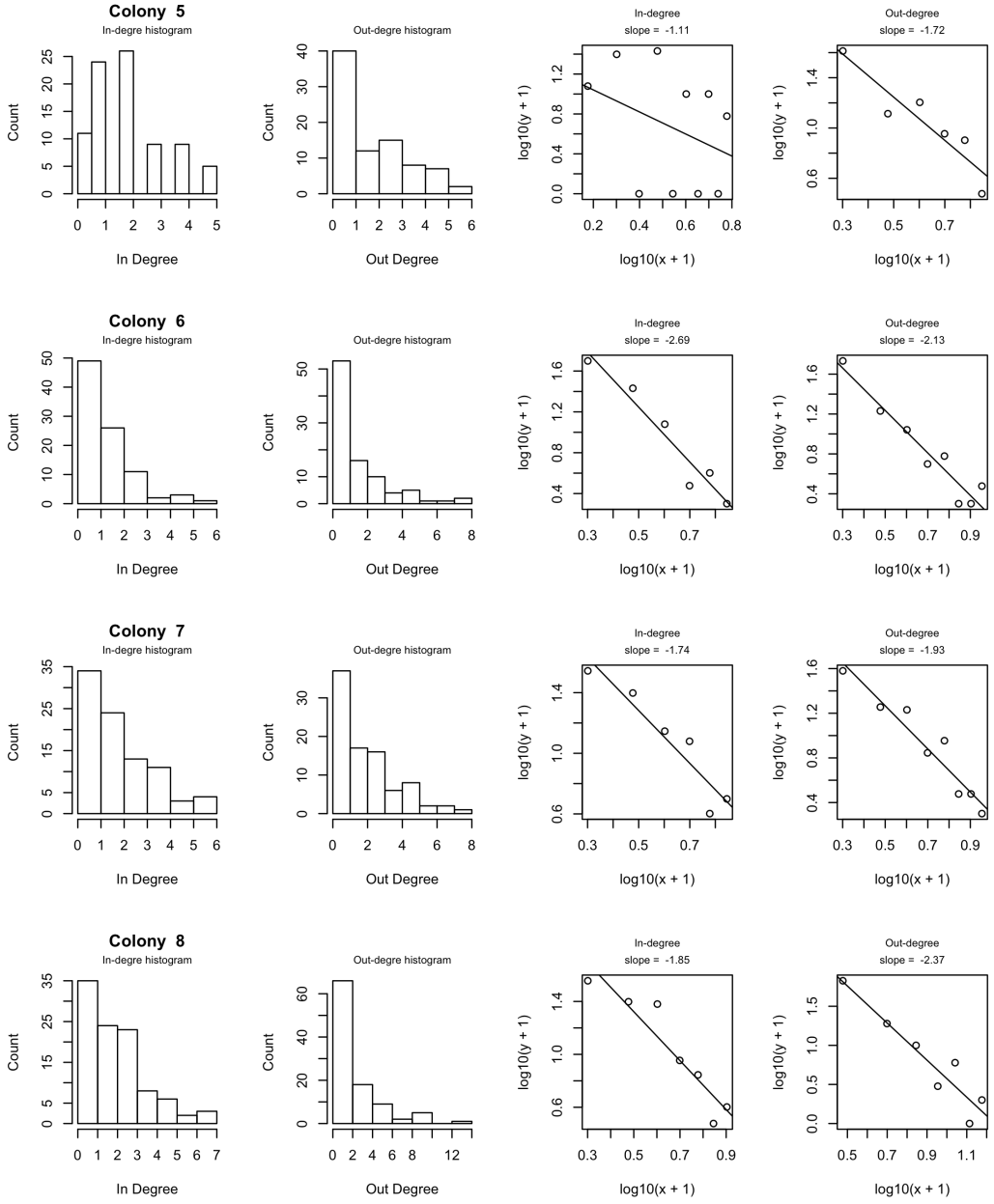

Figure 3.5b. Network degree distributions (networks 5-8). For each colony network, I present the histograms for in- and out-degree as well as the scatterplots associated with estimating the exponent by OLS-regression for the power-law distribution describing the in- and out-degree scaling in each colony.

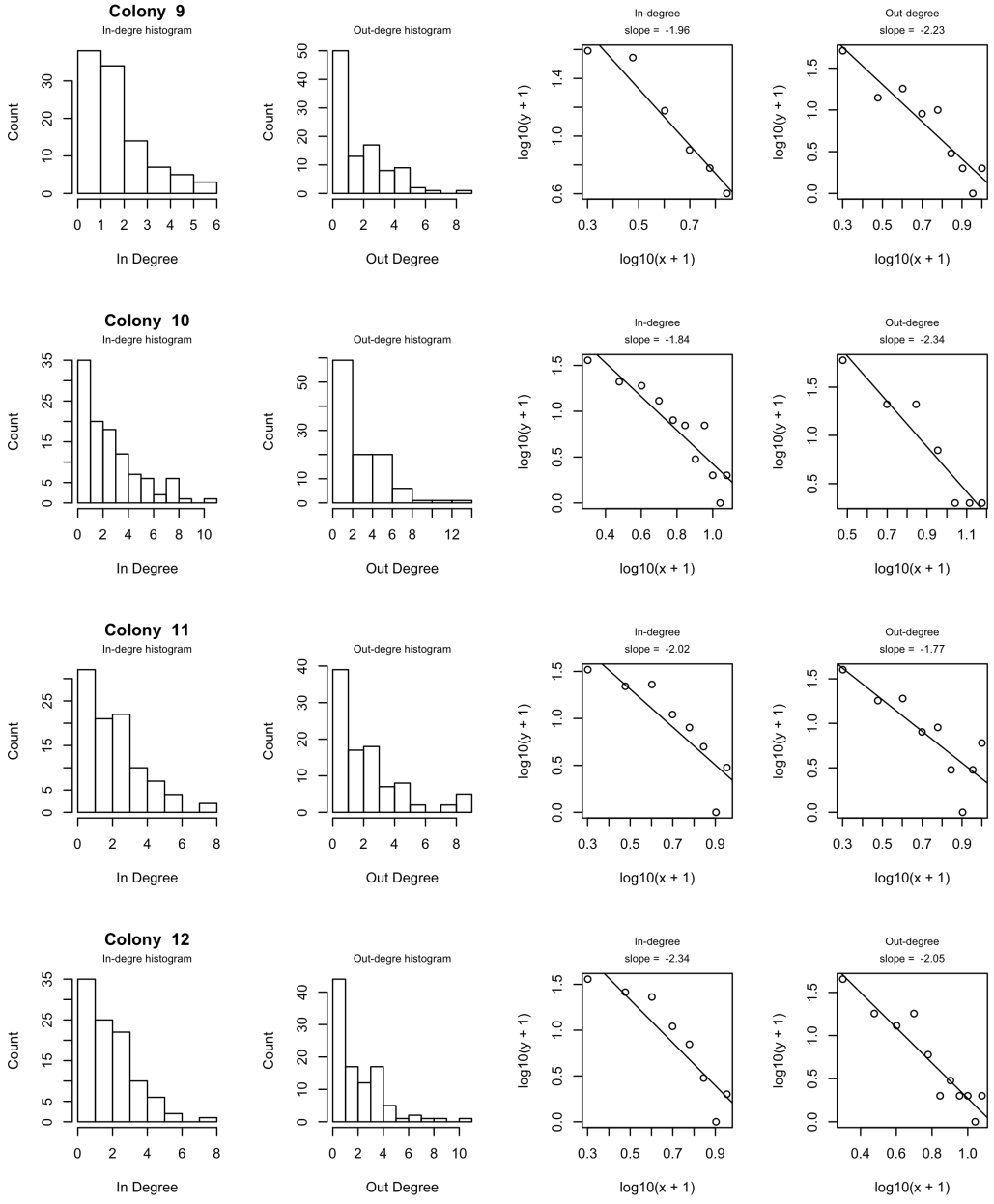

Figure 3.5c. Network degree distributions (networks 9-12). For each colony network, I present the histograms for in- and out-degree as well as the scatterplots associated with estimating the exponent by OLS-regression for the power-law distribution describing the in- and out-degree scaling in each colony.

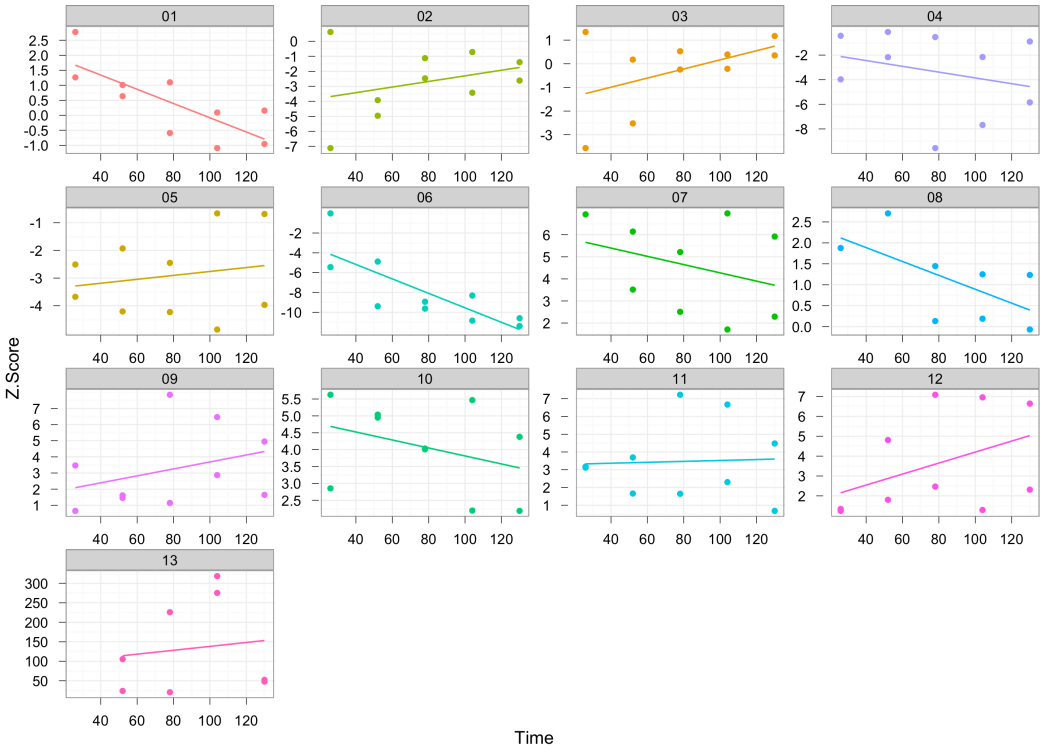

Figure 3.6. Effect of analysis time on subgraph Z-scores. The effect of analysis time on motif representation was examined by constructing cumulative networks spanning 30-130 seconds of whole-colony interaction. These networks exhibited a considerable range in size from 83 individuals and 136 interactions in a network based on 26 seconds of recorded behavior to 129 individuals engaging in 1117 interactions in a network based on 130 seconds of recorded behavior.

The Z-score is defined as the ratio of the difference in subgraph density between an observed network and its average density in a set of 10,000 randomized networks divided by the standard deviation of the subgraph's density in the randomized networks. Although there are visible trends in which the Z-scores associated with individual subgraphs (IDs 1-13) either increase or decrease

with the amount of time analyzed (and network size), none of the linear regressions were significant (p-values ranging from 0.20-0.99), suggesting that the method of motif analysis is robust with respect to the amount of time analyzed.

The figure above shows a scatterplot of the Z-scores for each subgraph as a function of the amount of time analyzed in constructing the interaction network. Table 3.6 gives the estimates and standard error for intercept and slope as well as t-score and p-value for the slope of each of the regression models fitting subgraph Z-score as a function of the amount of time used to construct the respective networks.

Table 3.1. Summary statistics for *P. californicus* interaction networks. This table summarizes global-scale network statistics for the twelve observed *P. californicus* interaction networks.

Network Statistic	Mean (N=12)	Standard Deviation
Nodes	89.167	13.730
Edges	191.5	62.372
Average Node Degree	4.213	0.824
Maximum Node Degree	13.333	2.964
Average Path Length	5.256	0.986
Diameter	14.75	2.261
Density	0.024	0.003

Table 3.2. Summary of out-degree scaling analysis.

Colony	Slope[1]	SE	R squared	P-value
1	-2.302233	0.2453528	0.9362024	0.0001
2	-1.495037	0.4009239	0.7766024	0.0203
3	-1.993387	0.397453	0.80741	0.0024
4	-2.076154	0.1107807	0.9859641	0
5	-1.718984	0.3488862	0.8585369	0.0079
6	-2.129866	0.2474018	0.9251065	0.0001
7	-1.93115	0.2274315	0.9231746	0.0001
8	-2.371344	0.3693494	0.8918231	0.0014
9	-2.230362	0.3129172	0.8788996	0.0002
10	-2.343456	0.3201249	0.9146595	0.0007
11	-1.773185	0.4323595	0.7061254	0.0046
12	-2.045588	0.2359468	0.8930656	0

(1) This is the OLS-estimated slope for the relationship describing how the number of nodes with a given number of out-degree edges scales with out-degree. The data (x) were transformed prior to regression according to $\log_{10}(x+1)$. The absolute value of the slope is an estimate for the degree distribution power law exponent (alpha).

Table 3.3. Summary out in-degree scaling analysis.

Colony	Slope[1]	SE	R squared	P-value
1	-1.589522	0.95259	0.258183	0.1337
2	-2.390163	0.4221644	0.8423322	0.0013
3	-1.27468	0.9519083	0.1831009	0.2173
4	-2.434398	0.335663	0.8976089	0.0003
5	-1.105925	1.0091694	0.1305242	0.305
6	-2.685515	0.3487973	0.936789	0.0015
7	-1.742611	0.3006386	0.8936109	0.0044
8	-1.849658	0.3015067	0.8827247	0.0017
9	-1.957485	0.2508555	0.9383577	0.0015
10	-1.838498	0.2517909	0.8555716	0
11	-2.018978	0.4390072	0.7790092	0.0037
12	-2.344854	0.4034605	0.8491615	0.0011

(2) This is the OLS-estimated slope for the relationship describing how the number of nodes with a given number of in-degree edges scales with in-degree. The data (x) were transformed prior to regression according to $\log_{10}(x+1)$. The absolute value of the slope is an estimate for the degree distribution power law exponent (alpha).

Table 3.4. Network motif analysis results.

Subgraph ID	Average Observed Density	Observed Networks[1]	Motifs (count > 1)[2]	Motifs (density > 1%)[3]
1	2.33E-01	12	3	3
2	1.25E-01	12	0	0
3	2.55E-01	12	2	2
4	1.17E-01	12	0	0
5	1.74E-01	12	0	0
6	4.07E-02	12	0	0
7	2.33E-02	11	11	11
8	4.43E-03	9	4	0
9	5.53E-03	11	4	1
10	9.62E-03	11	10	4
11	7.71E-03	11	7	2
12	8.21E-03	12	7	4
13	4.76E-03	5	2	0

This table summarizes the classification of subgraphs as network motifs. (1) The number of observed networks containing each respective subgraph. (2) The number of networks in which the observed density for a subgraph is significantly greater than its density in the random networks and in which the subgraph appears more than once in the observed network. (3) The number of networks in which the average observed density for a subgraph is significantly greater than its density in the random networks and in which the subgraph density is at least one percent in the observed network.

Table 3.5. Classification and identification of network motifs

Motif ID	Fanmod label	Isomorphism class number in R	Triad census name in R	Graph
1	6	6	021D	A<-B->C
2	36	2	021U	A->B<-C
3	12	4	021C	A->B->C
4	164	5	111D	A<->B<-C
5	14	9	111U	A<->B->C
6	78	10	201	A<->B<->C
7	38	7	030T	A->B<-C, A->C
8	140	11	030C	A<-B<-C, A->C
9	166	8	120D	A<-B->C, A<->C
10	46	13	120U	A->B<-C, A<->C
11	102	12	120C	A->B->C, A<->C
12	174	14	210	A->B<->C, A<->C
13	238	15	300	A<->B<->C, A<->C

Table 3.6. Effect of time on network motif Z-score summary statistics.

Subgraph	Intercept	Slope	t	Pr (>|t|)
1	2.289 ± 23.685	-0.024 ± 0.275	-0.086	0.9314
2	-6.459 ± 33.496	0.019 ± 0.275	0.068	0.9459
3	-4.050 ± 33.496	0.019 ± 0.275	0.07	0.9442
4	-3.791 ± 33.496	-0.024 ± 0.275	-0.086	0.932
5	-5.758 ± 33.496	0.007 ± 0.275	0.026	0.9795
6	-4.544 ± 33.496	-0.073 ± 0.275	-0.266	0.7911
7	3.856 ± 36.811	-0.019 ± 0.311	-0.06	0.9522
8	0.261 ± 39.061	-0.017 ± 0.330	-0.05	0.96
9	-0.759 ± 33.496	0.022 ± 0.275	0.078	0.9376
10	2.7078 ± 33.496	-0.012 ± 0.275	-0.043	0.9658
11	0.973 ± 33.496	0.003 ± 0.275	0.009	0.9925
12	-0.851 ± 33.496	0.028 ± 0.275	0.101	0.92
13	86.039 ± 44.022	0.499 ± 0.389	1.284	0.2022

Chapter 4

A MANIPULATIVE TEST OF THE SIZE-DEPENDENCE THEORY OF ANT COLONY METABOLIC ALLOMETRY

INTRODUCTION

The remarkable explanatory power of metabolic theory in ecology and evolutionary biology derives from the great diversity of life exhibiting a nonlinear scaling pattern in which metabolic rates are not proportional to mass, but rather exhibit a hypometric allometry (Calder, 1996; Ehnes et al., 2011; Peters, 1983; Schmidt-Nielsen, 1995). The central equation in metabolic theory (Robinson et al., 1983) may be used to predict an organism's metabolic rate, i.e. its oxygen consumption (VO_2), as the product of an allometric function of its mass (M) and an exponential function of its temperature (T):

$$\dot{V}O_2 = a\mathrm{M}^b \cdot \mathrm{e}^{c\mathrm{T}} \quad (1)$$

While the dependence of metabolism on temperature can be quite variable among taxa (Clarke, 2006; Irlich et al., 2009; Waters and Harrison, 2012), the mass scaling exponents (b) are generally constrained such that $0.5 < b < 1$ (Glazier, 2005; Hemmingsen, 1960; Robinson et al., 1983). Despite more than a century of empirical research and a recent deluge of theoretical models, the mechanistic basis for the hypometric relationship between mass and metabolic rate remains a major unresolved problem in biology (Agutter and Wheatley, 2004; Martinez del Rio, 2008). Perhaps more fundamentally, the relationship between mass and metabolic rate is almost entirely based on correlative data and only a

few studies have demonstrated a causal link between these factors (White et al., 2011; White and Seymour, 2004). If mass constrains or otherwise affects metabolism, then the mechanistic basis for this would have dramatic consequences throughout biology. If however, the relationship between mass and metabolism is due to another mechanistic factor (e.g., nutrient stoichiometry, population density, or evolutionary inertia) then this must be identified. To empirically test for an effect of mass on metabolic rate, it would be ideal to directly manipulate mass (Olsson et al., 2002; Sinervo and Huey, 1990; Sinervo et al., 1992) and measure any subsequent changes in metabolism. Alas, for the vast majority of organisms, the inability to manipulate mass without sacrificing critical tissues or otherwise inducing physiological trauma presents an imposing challenge to the experimentally evaluation of the mechanisms responsible for allometric scaling of metabolism.

Recent observational studies (Cao and Dornhaus, 2012; Nakaya et al., 2003; Shik, 2010; Vollmer and Edmunds, 2000; Waters et al., 2010) have reported that colonial organisms exhibit metabolic hypometry similar to the scaling pattern exhibited by unitary organisms. Manipulative tests of these scaling relationships have been performed with marine colonial organisms including ascidians (Nakaya et al., 2005) and encrusting bryozoans (White et al., 2011). In both cases, the reduction of colony size was associated with increased mass-specific metabolic rates. Using the framework of the Dynamic Energy Budgets theory (Kooijman, 2000; van der Meer, 2006) these increases in mass-specific metabolic rate can be explained by associated changes in energetic

allocation to growth as mediated by surface area (White et al., 2011). Due to physical connections between these modular organisms, the surface areas do not scale isometrically with the number of zooids in the colonies. In the insect colonies however, individuals are physically independent and any surfaces that exist (either in the arrangement of individuals or with respect to nest architecture) are the result of social interaction.

Among the eusocial insects, colony size strongly correlates with many life history characteristics, including reproductive allocation (Shik, 2008), fasting endurance (Kaspari and Vargo, 1995), division of labor (Dornhaus et al., 2008; Holbrook et al., 2011; Jeanson et al., 2007), foraging organization (Beekman et al., 2001), and information transmission (Blonder and Dornhaus, 2011). In some ant species, colony size is also associated with changes in the average body size of workers and in the composition of different physical castes within the colony (Tschinkel, 1993). The hypometric scaling of metabolic rate in colonies of *Pheidole dentata*, is hypothesized to be a result of changing caste composition with colony age; larger and older colonies have a greater number of supermajor workers, each of which exhibits a relatively low mass-specific metabolic rate (Shik, 2010). In same-aged colonies of the seed harvester ant, *Pogonomyrmex californicus*, metabolic rate scales similarly as *P. dentata*, however there is no corresponding scaling of morphological caste composition; instead it is hypothesized that metabolic allometry in this case may be due to decreases in demand for work as colony size increases (Waters et al., 2010). To test for a causal effect of colony size on metabolic rate, I conducted a size-manipulation

experiment on whole colonies of *P. californicus*. Considering colony metabolic rates standardized to a given temperature, it may be predicted that whole colonies of *P. californicus* would scale according to a simplified version of equation 1:

$$\dot{V}O_{2,colony} = a\mathrm{M}^{b} \quad (2)$$

Following the manipulation of colony size to half of its previous size, colony metabolic rates would scale according to:

$$\dot{V}O_{2,manipulation} = a\left(\tfrac{1}{2}M\right)^{b} \quad (3)$$

By considering the ratio of mass-specific metabolic rates (B) predicted by equations 2 and 3,

$$\frac{B_{manipulation}}{B_{colony}} = \frac{a\left(\frac{1}{2}M\right)^{b-1}}{a\left(M\right)^{b-1}} \approx \frac{\left(\frac{1}{2}M\right)^{-0.25}}{\left(M\right)^{-0.25}} = \tfrac{1}{2}^{-0.25} \quad (4)$$

it may be predicted that following size reduction, manipulated colonies would exhibit increases in mass-specific metabolic rates to approximately 1.2 times their previous rate as intact whole colonies.

METHODS

Rearing ant colonies

Queens of the California seed harvester ant, *Pogonomyrmex californicus*, were collected in Pine Valley, CA (32°49’20”N, 116°31’43”W, 1,136-m elevation) on July 2-3 2011. The queens had recently settled to the ground following mating flights and were collected as they were foraging or starting to

excavate new nests. This population of *P. californicus* exhibits cooperative pleometrotis (Johnson, 2004), so when the queens were returned to the laboratory, they were placed into artificial nest enclosures in foundress associations (n=3 queens per nest). Four sizes of artificial nest enclosures were used as colonies grew: a test tube (47.8 cm^2) was used until the first workers eclosed, a small plastic box was used until colonies were nine months old (209.5 cm^2; Pioneer Plastics, Inc., North Dixon, KY, USA), and a large plastic box (625 cm^2; Small Parts, Inc., Logansport, IN, USA) was used thereafter. Colonies were generously fed 1-2 times per week with grass seeds, frozen fruit flies, and droplets of Bhatkar, a synthetic diet for ants (Hölldobler and Wilson, 1990). Multiple small test tubes partially filled with water and plugged with cotton were also provided at all times. Colonies were reared in a dark incubator set to 32°C and observed in a laboratory in which the ambient room temperature ranges from 28-34°C.

Experimental design

The primary aim of this study was to determine whether size affects the average per-capita metabolism within ant colonies. Secondary aims included evaluating the extent to which activity, age, and consistent inter-colony differences influence metabolism within colonies. To address these aims, a series of measurements (including metabolic rates, colony masses, and activity estimates) were recorded at multiple time points (Figure 4.1A) across the development of a series of colonies (n=12). Colonies were measured in June-

August 2012 (size manipulation experiment), and in September 2012 (control measurements).

The Summer 2012 measurements included a repeated-measures experiment in which colonies were measured twice, once without manipulation and a second time following reduction in size. The schedule for this experiment (Figure 4.1B) involved acclimating colonies within a respirometry chamber for 24 hours, recording respirometry and video data for 16-24 hours, and then censusing the mass of the colony. Following the census, 50% of the worker, larvae, and pupae populations (by count, not by mass) were removed from the colony and set aside. The remaining (reduced size) colony was given five days to rest and was then returned to a respirometry chamber to acclimate for 24 hours before repeating the respirometry and video recording (7 days following the first measurement).

The measurements in September 2012 were designed to provide a control for the manipulation experiment (Figure 4.1C). It followed nearly the exact same protocol as the manipulation experiment; the only difference was that the workers, larvae, and pupae that were removed following the first measurement were returned to their colonies after 24 hours and five days before the second measurement. Since in many ways a colony's nest is part of its extended phenotype, for all of the repeated measurements in 2012, each colony was maintained within its own artificial nest enclosure.

Respirometry

Metabolic rates of whole colonies were estimated using flow-through respirometry (Lighton, 2008). To minimize disturbance, colonies were maintained within artificial nest enclosures which could be placed inside and sealed within a respirometry chamber, the lid of which was transparent to allow video recording of ant colony behavior simultaneous with respirometry (Figure 4.2A). The respirometry system was designed with push-mode plumbing (Figure 4.2B) with dry CO_2-free air supplied by a compressed air tank and regulated at constant flow rate (250 mL min^{-1}) with mass flow controllers (500 mL min^{-1} max; set to 50%). Air was passed through the reference cell of a CO_2 analyzer and into a multiplexer (RM-8; Sable Systems International, Las Vegas, NV, USA) to automate switching of measurement between baseline and chamber airflows (Figure 4.2B). The analyzer was calibrated using Nitrogen as a zero-CO_2 gas and 11.9 ppm and 298 ppm CO_2/N_2 balance gasses to set the span. Excurrent air was sequentially passed from the multiplexer through a Drierite column (Indicating Drierite, 10-20 mesh; W. A. Hammond Drierite Co. Ltd, Xenia, OH, USA) to remove water vapor, the sample cell of the CO_2 analyzer, a Drierite/Ascarite column (Ascarite II CO_2 Absorbent, 8-20 Mesh, Thomas Scientific, Swedesboro, NJ, USA) to scrub CO_2, and the fuel cell of an O_2 analyzer (FC-2; Sable Systems International). The flow rate of the excurrent air was periodically checked for accuracy and stability (SS-4, Sable Systems International). I also confirmed the lack of back-pressure by periodically disconnecting the flow downstream of the CO_2 analyzer and validating that there was no subsequent change in CO_2 concentration.

Temperature of the colony during each recording was estimated using with a thermistor fixed to the aluminum base of the respirometry chamber.

Each colony was given fresh food and water and placed into a respirometry chamber with ports disconnected from airflow but open to the room air 24 hours prior to the start of respirometry. Although all colonies were measured in chambers of the same size, our prior study has demonstrated that moderate variation in worker density does not explain patterns in colony metabolic rates (Waters et al., 2010). Data were converted from analog to digital (UI-2, Sable Systems International) and recorded at 1 Hz with Expedata version 1.1.18 (Sable Systems International). Colonies were measured for 16-24 hours with repeat-recording enabled so that a file was saved every 1851 seconds. The multiplexer was digitally controlled by Expedata to automate switching between baseline and respirometry chamber airflow measurements so that each recording included colony respirometry sandwiched between baseline data at the start and end of the recording. By programming markers to be saved at a sequence of time points during the recording, it was possible to automate the baseline and drift-correction analysis using a batch-processed macro within Expedata. Following this procedure, all of the files for a given colony's recording were appended in Expedata and exported as comma separated text for analysis in R v. 2.13.1 (R Development Core Team, 2011). Following each colony's respirometry run, the wet mass of the colony was censused, counting the total number of queens, larvae, pupae, and workers and weighing each group to the nearest 0.1 mg.

For six colonies at the start of the investigation, I measured the CO_2 production due to chamber debris. To do this, the debris and water tubes were removed, placed in a respirometry chamber, and measured using the same method as applied to the colony measurements. The fraction of whole colony CO_2 production attributable to the debris and water tubes averaged 0.0027 ± 0.0004 (range: 0.0011-0.0044). Since the measurement error attributable to debris was so small and since it did not scale with colony size ($F_{1,4}$=1.18, p=0.34), debris measurements were not incorporated into the subsequent measurements or analyses.

Colony activity

The activity patterns exhibited by the colonies in this study were analyzed by recording video of the colony nest enclosures and estimating the average per-capita walking speed of all of the workers within each colony. The video acquisition system, previously described (Waters and Fewell, 2012), enabled repeat recording of high quality uncompressed AVI video (2024 x 2024 pixels; 15 frames per second). The walking speeds of ants were estimated by manual tracking of all of the visibly moving ants within segments of video (30 s) which had been recorded at the end of respirometry (Meijering et al., 2012; Rasband, 1997-2012). Additionally, the size of the largest brood pile for each colony was measured in ImageJ by tracing the perimeter of these piles in frames of the video recordings of each colony.

Analysis of metabolic rate data

The data recorded by Expedata included CO_2 and O_2 concentrations of the excurrent airflow and the temperature of the respirometry chamber, saved as a sequence of baseline-corrected intervals (Figure 4.3). Reliable O_2 data (based on signal to noise ratios) were only available for a series of six colonies, so these recordings were used to estimate the colony respiratory quotient (0.86 ± 0.02 SE) and subsequent metabolic rate estimates were based on CO_2 data converted from units of ppm to Watts and standardized to 25°C assuming a Q_{10}=2.0 (Lighton, 2008). Standardization of metabolic rate data to a single temperature was necessary to account for variation in room temperature. Although 25°C is outside of the normal temperature range for these ants, its choice facilitates comparison across multiple data sets in the literature (Chown et al., 2007; Shik, 2010; Waters et al., 2010).

Statistical analyses

All statistical analyses were performed in R version 2.13.1 (R Development Core Team, 2011) and all graphs were plotted using ggplot2 version 0.8.9 (Wickham, 2009). Where scaling data exhibited heterscedasticity, estimates of the coefficient and exponent in the allometric equation (2) were calculated using ordinary least squares (Model I) and reduced major axis regression on $\log_{10}$ transformed data (Xiao et al., 2011). Reduced major axis (Model II, also known as standard major axis) regression was conducted using the lmodel2 package for R (Legendre, 2011). Paired comparisons were evaluated using the nonparametric

Wilcoxon signed rank test due to likely departure from normality and equal variance among comparisons with relatively small sample sizes (i.e., N=6-12 paired observations). In the results below, unless otherwise mentioned, estimates are presented as means ± standard error of the means.

RESULTS

Colony size and composition

Twelve colonies were censused before and after size manipulation in Summer 2012. Prior to manipulation, the average colony mass was 1.10 grams ± 0.12 SE and colony mass ranged from 0.32-1.70 grams. The age of the colonies, when measured prior to manipulation was 351-380 days (Collected 3 July 2011, measured 18 June 2012 – 17 July 2012).

The average colony prior to manipulation was composed of 2.4 ± 0.26 queens (12.2 ±0.4 mg each), 33.4 ± 6.3 larvae (2.9 ± 0.4 mg each), 33.9 ± 9.2 pupae (4.2 ± 0.2 mg each), and 255.3 ± 31.0 workers (3.5 ± 0.1 mg each). The number of individuals within a colony ranged from 86-452 (workers ranging from 70-400).

Queen mass was not correlated with colony mass ($r=0.21$, $p=0.53$), larvae mass was nearly correlated with colony mass ($r=0.56$, $p=0.06$), pupae mass was not correlated with colony mass ($r=0.21$, $p=0.52$) and worker mass was obviously very strongly correlated with colony mass ($r=0.90$, $p < 0.001$). The average per-capita masses of queens, larvae, pupae, and workers did not correlate with colony mass ($r=-0.20 – 0.31$, $p=0.26-0.92$).

The manipulated colonies had masses approximately 0.5 times their original size, though this fraction ranged from 0.46-0.52 depending on the colony; the variation was due to the fact that queen number was not manipulated, there were occasionally odd numbers of ants, and there was occasional loss of worker escapees during manipulation. There was however, no general trend of manipulation fraction depending on colony size ($F_{1,10} = 0.369$, $p=0.56$).

Stabilization time for metabolic rates

Although colonies were given 24 hours to rest after their nests were placed in the respirometry chamber, they exhibited increased activity following the start of flow-through respirometry; this increase in activity (i.e. walking/running) tapered off after 2-4 hours (Figure 4.3D). To determine more accurately the time period after which CO_2 emission stabilized, I fit a series linear regression models to the time series respirometry data. As the model was fit to data truncated to sequentially later start times, the significance of the negative slope estimated by the model decreased. Based on this analysis, I concluded that the respirometry traces had stabilized after approximately 8.7 hours (Figure 4.4). To avoid pseudo-replication in all subsequent analyses, a single metabolic rate was estimated for each colony recording based on the average of data collected between 8.7-14.4 hours (Figure 4.4).

Metabolic rate allometry of unmanipulated and reduced-size colonies

Colonies and reduced-size colonies exhibited a hypometric relationship with metabolic rate (Figure 4.5). The exponent, estimated as the slope of a line fit by OLS regression on log transformed data (including unmanipulated and reduced-size colonies), was 0.79 ± 0.06 SE (95% CI: 0.66-0.92; R-squared: 0.8883). By comparison, the reduced major axis model estimated the exponent as 0.84 (95% CI: 0.72-0.97). For just the unmanipulated colonies, the OLS-derived exponent is 0.87 ± 0.11 SE (95% CI: 0.62-1.12; R-squared: 0.8582); these data were not significantly different from an isometric scaling relationship. For just the post size-reduction colonies, the exponent was 0.75 ± 0.11 SE (95% CI: 0.51-0.98; R-squared: 0.8293); this was a significant hypometric scaling relationship. Modeling the data in an ANCOVA design, there was not a significant improvement to the base model by accounting for different intercepts ($p=0.67$) or different slopes ($p=0.43$) for the measurements before and after manipulation.

The average mass-specific metabolic rates after reducing colony size was significantly higher than before colony sizes manipulation (Wilcoxon signed rank test, N=12 paired observations, V=11, $p=0.023$, Figure 4.6A). The size manipulation lead to an increase in mass-specific metabolic rate in nine of twelve colonies, with post-manipulation metabolic rates on average 1.21 times higher than pre-manipulation metabolic rates.This effect size matches almost perfectly the theoretical prediction (1.20) based on equation 4 and is significantly greater than the alternative isometric prediction (95% CI: 1.07-1.35).

Control experiment testing for a possible effect of colony manipulation on metabolic rate

The control experiment was conducted using the six colonies that showed the greatest increases in mass-specific metabolic rate after colony size reduction. There was not a significant change in the mass-specific metabolic rate of colonies following the removal of 50% of the colony for 24 hours and its subsequent replacement (Figure 4.6B; Wilcoxon signed rank test, N=6 paired observations, V=17, p=0.218). Visual inspection of the respirometry traces (Figure 4.7) for each colony before and after the control experiment reinforced this result and suggests that repeatability of metabolic rates was relatively high despite the handling of the workers.

Following the control experiment, six whole colonies had been measured a total of three times each, so I analyzed the repeatability of these metabolic rate estimates (Figure 4.8). The repeated measures analysis of variance (Table 1) identified a strong effect of mass ($p < 0.003$), and there was not a significant effect of measurement period ($p > 0.26$), indicating good repeatability in metabolic rates within same-sized individual colonies.

The control data can also be used to confirm the repeatability of metabolic allometry across time as the control measurements were conducted on colonies that had been previously measured (Figure 4.8). Considering the six pairs of repeated measures together (N=12), the method of ordinary least squares regression on log10 transformed data predicts a scaling exponent of 0.63±0.08 SE (95% CI: 0.44-0.81; R-squared: 0.8548). Considering just the first set of

measurements during the control (N=6), the scaling exponent was 0.53±0.08 SE (95% CI: 0.32-0.75; R-squared: 0.9208). Considering just the second set of measurements during the control (N=6), the scaling exponent was 0.76±0.10 SE (95% CI: 0.48-1.04; R-squared: 0.9348).

Behavior

The walking speeds of all ants (N=2,116 workers) visible within eight colonies during the first measurement of the size manipulation experiment were estimated by manually tracking individual positions across a 30-second video recording (Figure 4.9). The distribution of walking speeds within each colony was strongly skewed to the right (positive skew) with average walking speeds for each colony at least twice the median walking speed. While there was not a significant effect of colony size on mean walking speed (linear regression, $F_{1,6}$=1.26, p=0.31), there was a significant effect of colony size on median walking speed ($F_{1,6}$=6.74, p=0.04) with the median speed decreasing sharply with increasing colony mass (Figure 4.10). Additionally, the fraction of the colony moving less than 1.0 mm s^{-1} increased with colony mass ($F_{1,6}$=9.56, p=0.02), but there was not a significant trend of the fraction of the colony moving greater than 15.0 mm s^{-1} ($F_{1,6}$=0.14, p=0.72). Following experimental size manipulation, the walking speeds (for a sample of N=5 colonies) showed no significant change relative to the walking speeds prior to manipulation (Figure 4.11).

DISCUSSION

Two alternative hypotheses could explain the metabolic hypometry observed for *P. californicus* colonies (Waters et al., 2010). Smaller colonies might have higher metabolic rates per gram due to their smaller size. Alternatively, colonies might achieve larger sizes partly because they possess an intrinsically lower mass-specific metabolic rate. The results of the current size manipulation experiment strongly support the hypothesis of a size-dependence of metabolism. Reducing colonies to half of their size generated an increase in mass-specific metabolic rates to 1.21 times their rates as larger colonies, nearly exactly as predicted by equation 4. If intrinsic differences among colonies in metabolic intensity were responsible for smaller colonies having higher metabolic rates, then no change in mass-specific metabolic rates would be expected following reduction of colony size.

Our prior study (Waters et al., 2010) also showed that larger colonies had a higher fraction of workers inactive (not walking). Again, this could be due to a direct effect of colony size, or it could be a function of the larger colonies achieving their large size partly by greater division of labor. Our examination of locomotory activity patterns across colony size were generally consistent with our prior study. I found that activity patterns of intact colonies scaled with colony size so that larger colonies were composed of slower-moving ants and a greater fraction of inactive ants compared to smaller intact colonies. However, the walking speeds of ants did not change significantly following the experimental

reduction of colony size, suggesting that the variation in walking speeds I have observed across colony sizes is not due to effects of colony size per se.

Why might larger colonies have lower metabolic rates per gram but have workers walking with similar speeds as smaller colonies? One possible explanation is that factors in addition to locomotory behavior (such as reproductive and growth rates) are likely to be important in determining whole-colony metabolic rates. Our previous calculations suggest that variation in walking rates is unlikely to completely explain variation in colony metabolism (Waters et al., 2010). Another possibility is that compensatory mechanisms may be triggered by the size-reduction experiment. For example, the removal of nurse workers may have triggered DNA methylation changes in foragers that returned to performing nurse-related tasks (Herb et al., 2012). Alternatively, the manipulation may have stimulated colonies to up-regulate growth processes in response to the reduction in size, stimulating workers to work more closely with brood piles.

Although the difference was not statistically significant, I observed that nearly two months following the experimental size reduction, colonies were producing more brood than they had previously been (Figure 4.12). This is consistent with the observation that brood production scales hypometrically with colony size, i.e., the number of brood produced per worker is greater in smaller colonies than larger colonies (Cao and Dornhaus, 2012; Michener, 1964). Although our behavioral analyses did not detect an increase in per-capita speed following the experimental size manipulation, it is possible that the large fraction

of stationary workers were in fact doing more work within the colony with respect to processing food and tending to the queen and brood, causing the higher mass-specific metabolic rates in the reduced-size colonies.

Previous size-manipulation studies examining metabolic rate allometries in marine colonial organisms have identified surface areas necessary for growth as a critical factor in generating metabolic hypometry in these modular organisms (Nakaya et al., 2003; Nakaya et al., 2005; White et al., 2011). Based on these observations, I might consider what the analogous surface areas are in social insect colonies and what effect the size manipulation had on these surfaces. One possible surface area of importance is the surface around the piles of larvae. Workers frequently pile larvae into clusters, but the specific reasons why they create these brood piles are not clear. However, there are potentially important consequences to the shape of these brood piles if the larvae are not well mixed within, namely, the size of the pile affects the ease with which workers may interact with larvae. Larger piles make relatively fewer larvae accessible and this may reduce their ability to communicate the demand for work to the rest of the colony. Thus, I predicted that the surface to volume ratios for brood piles would decrease with colony size and that following the experimental size reduction, the surface area to volume ratio of brood piles should increase. Since the brood piles are effectively two-dimensional, I measured the perimeter of the piles as a proxy for their surface area and counted the number of larvae as a proxy for pile volume. Consistent with the predictions, the perimeter per larva ratio decreased with colony size ($F_{1,22}$=8.93, p=0.006, Figure 4.13A), the perimeter scaled

hypometrically with the number of larvae ($F_{1,22}$=8.93, p=0.006, Figure 4.13B), and the perimeter per larva ratio increased following the experimental reduction of colony size (Wilcoxon sign rank test, V=14, N=12 pairs, p=0.052, Figure 4.13C). The perimeter per larva ratio in reduced size colonies was on average 1.52±0.12 times greater than the perimeter per larva ratio in whole colonies. Conceivably, greater access to brood could stimulate effort by the workers, leading to higher mass-specific metabolic rates in reduced-size (or simply smaller) colonies.

How is colony size perceived by the workers within a social insect colony? The hydrocarbon profiles of eggs laid by the queens can communicate information about colony size across development (Moore and Liebig, 2010). Additionally, nutritional feedback between workers, larvae, and the queen may be critical in establishing growth patterns (Tschinkel, 1988). The common theme to both of these mechanisms is that perception of colony size relies on physical interaction among the individuals within a social insect colony. In whole *P. californicus* colonies, the interactions among workers exhibit a predominance of regulatory patterns not expected by animal social network models (Waters and Fewell, 2012). Examining the dependence of these networks to colony size and their responsiveness to perturbation will make it possible to develop an integrated and mechanistic model for the hypometric relationship between colony size and metabolic rate in social insect colonies.

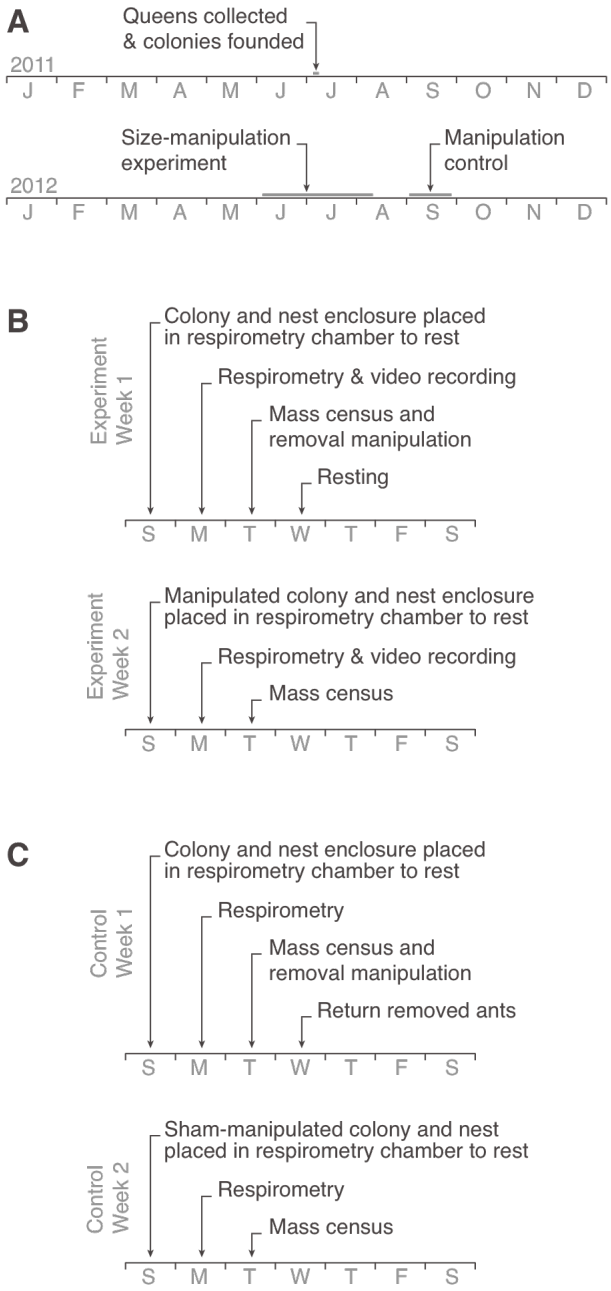

Figure 4.1. Protocol and timeline of experiments. (A) A two-year timeline indicating the sequence of events reported in this manuscript. (B) For each colony, the manipulation experiment spanned two weeks with sequential

recordings one week apart. The days identified above are for conceptual purposes only; since I constructed two respirometry chambers, it was possible to run colonies continuously and sequentially, always having one colony being measured while the next colony was resting in the second chamber in preparation for being measured the following day. (C) The control experiment followed nearly the same protocol as the manipulation, except the ants that were removed following the first measurement were returned to the colony one day later.

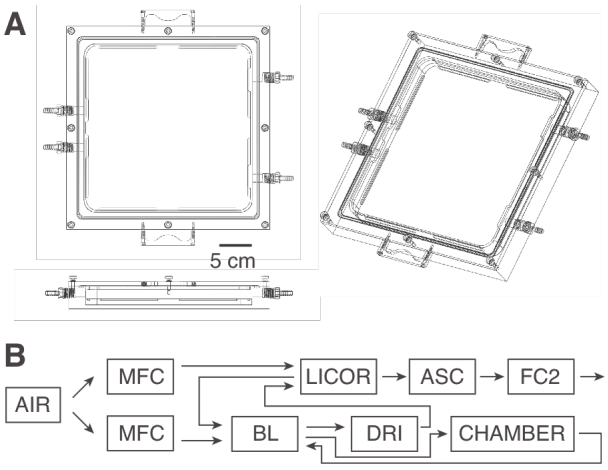

Figure 4.2. Respirometry chamber and system design schematic. (A) The respirometry chamber was constructed with an aluminum base, plexiglass lid, rubber o-ring, and multiple inlet/outlet ports. It holds an artificial nest enclosure made up of a square petri dish (25 cm x 25 cm) with mesh-covered holes on the side placed to align with the respirometry chamber inlet/outlet ports. (B) The airflow was plumbed as a push-model flow-through respirometry system with mass flow controllers (MFC), a baseline multiplexer (BL), CO_2 analyzer (LICOR), Drierite (DRI) and Ascarite (ASC) columns, and an O_2 analyzer (FC2). The baseline multiplexer switches the flow of air into the gas analyzers between the airflow coming from the chamber and a baseline air stream. While the analyzers are baselining, the multiplexer maintains a continuous flow of air into the respirometry chamber from the second mass flow controller avoiding repeatedly disturbing the colony with changes in flow regime.

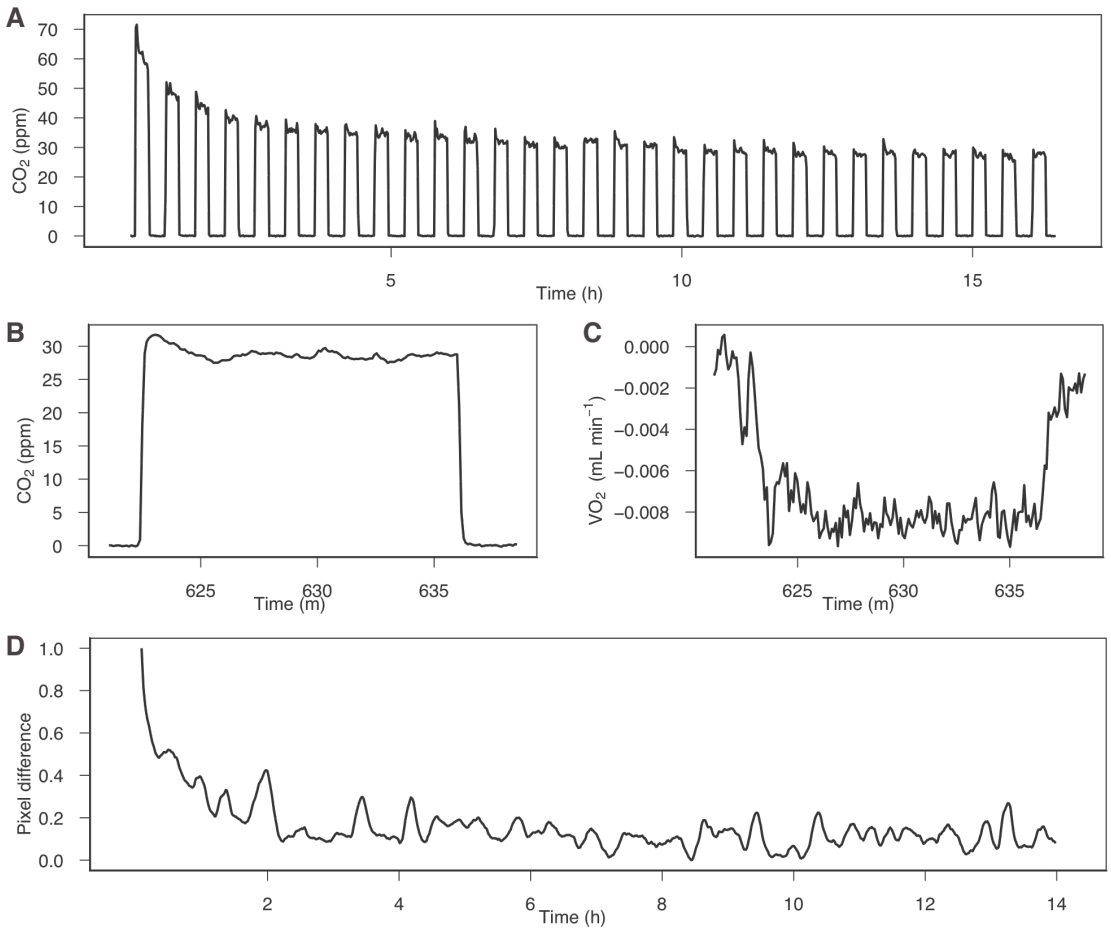

Figure 4.3. Whole-colony flow-through respirometry and activity. (A) A representative sixteen hour respirometry recording, showing alternating baseline and chamber recordings. (B) A single 10 minute CO_2 recording. (C) A single 10 minute O_2 recording. (D) Normalized bulk activity metric based on analyzing pixel changes in sequential video frames.

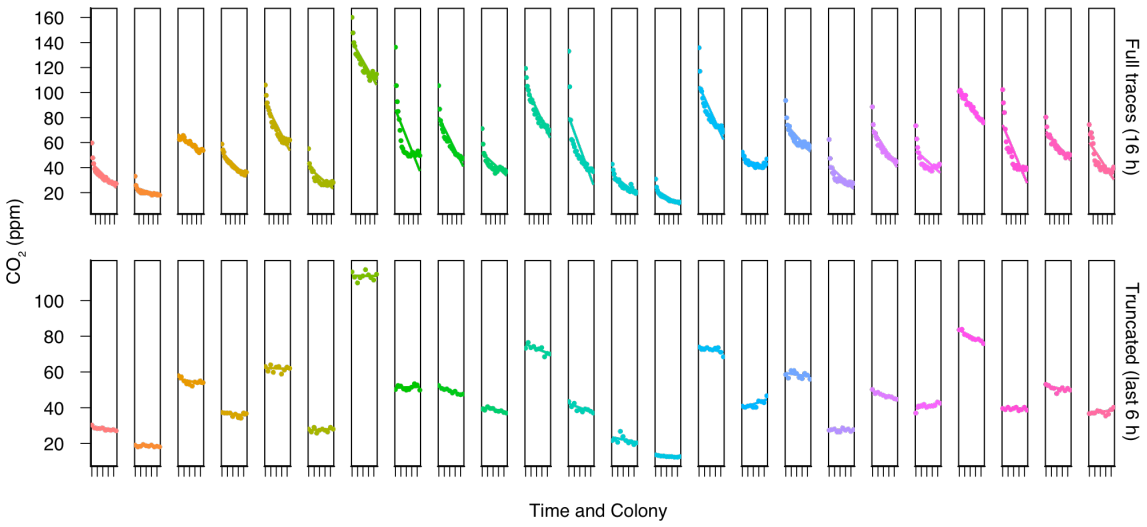

Figure 4.4. Settling period and respirometry data over time. The two sets of 24 panels above display the complete respirometry data from the manipulation experiment. Each pair of sequential columns represents a single colony, before and after size manipulation. The x-axis for the 24 top panels spans 16 hours of respirometry; for the bottom panels it spans only the last 6 hours of respirometry.

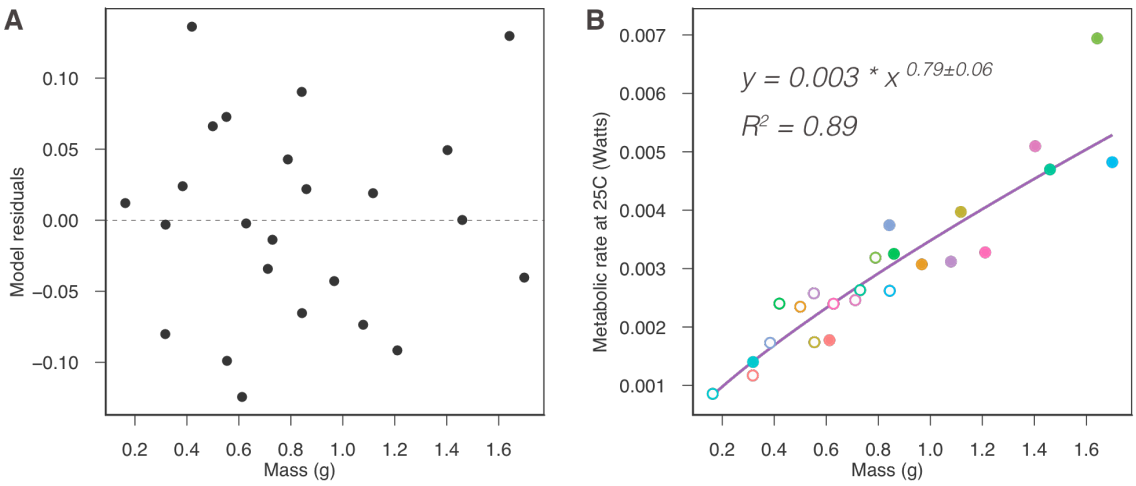

Figure 4.5. Modeling metabolic rate allometry. (A) Since the variance in metabolic rate data increases with mass, the data were $\log_{10}$ transformed to establish homoscedasticity as can be observed by the plot of residuals of an ordinary least squares linear regression model fit to the $\log_{10}$ transformed data. (B) On linear axes, mass and metabolic rate are plotted (solid circles represent colony metabolic rates prior to manipulation; open circles represent colony metabolic rates after size manipulation) and the power law equation is plotted with coefficient and exponent determined by back-calculating their values from the OLS regression on $\log_{10}$ transformed data.

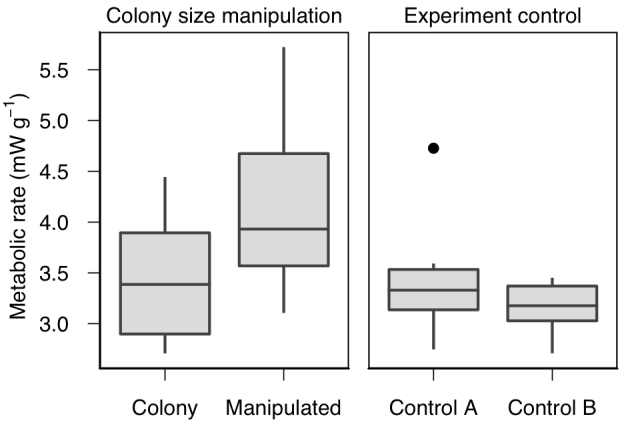

Figure 4.6. Testing for a direct effect of colony size on metabolic rate. (A) The experimental size reduction (N=12 colonies, repeated measures) lead to a significant increase in mass specific metabolic rates. (B) There was not a significant effect of the sham manipulation on colony metabolic rate in the experimental control (N=6 colonies, repeated measures).

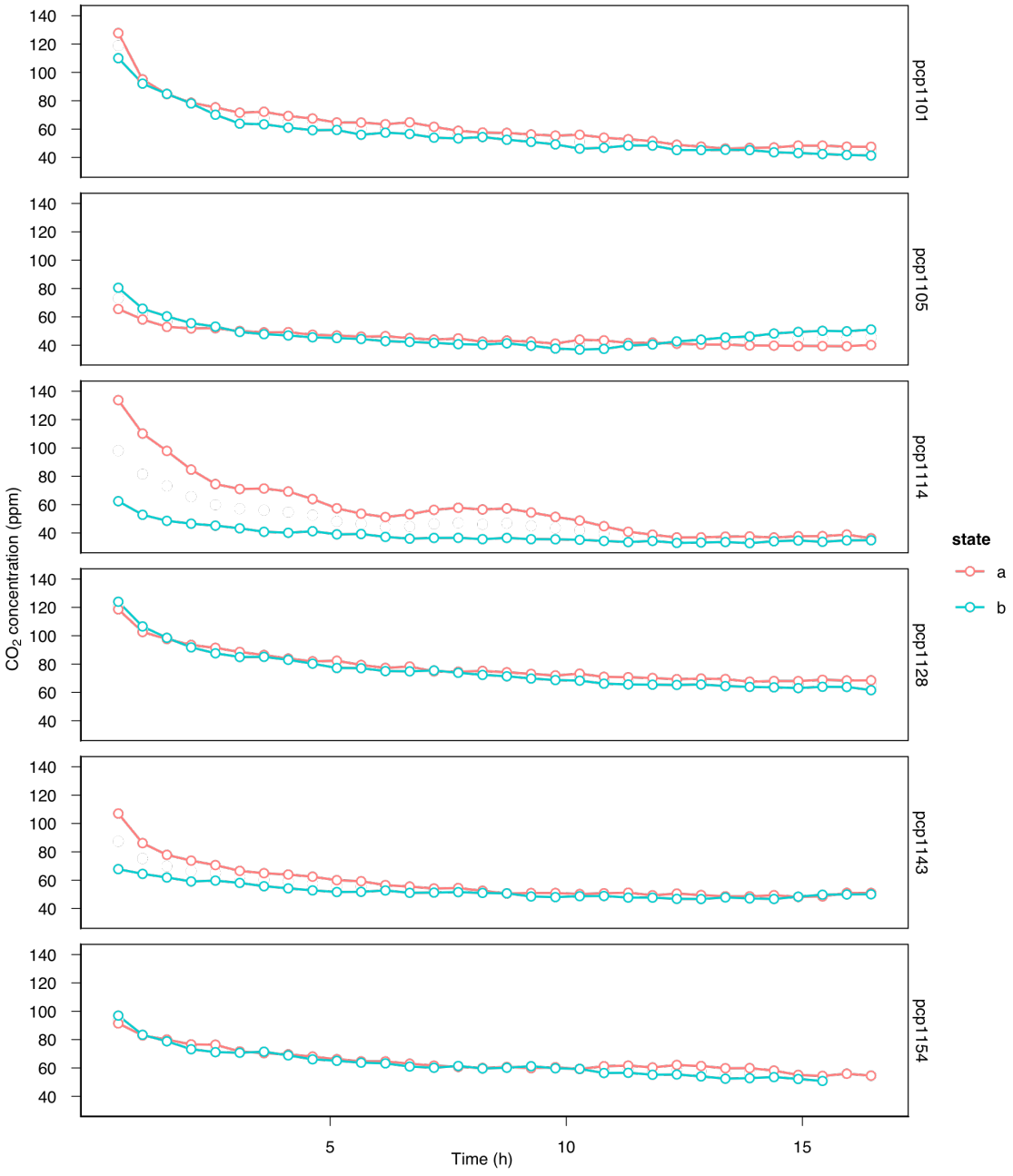

Figure 4.7. Control experiment respirometry traces. States "a" and "b" refer to the two repeated measures during this control experiment, before and after a 24-hour removal of 50% of the colony mass.

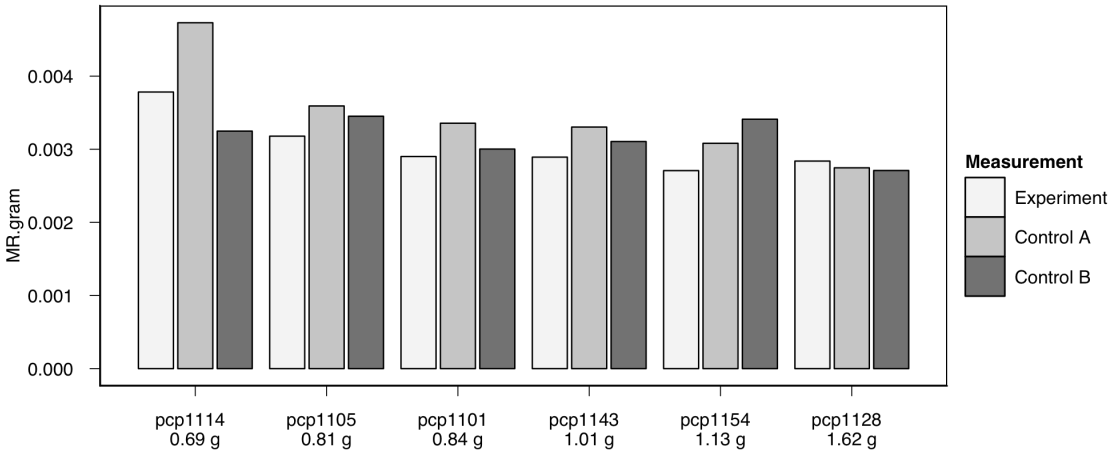

Figure 4.8. Repeated measures of metabolic rates on a set of six colonies. These colonies were measured first during the size manipulation experiment (labeled above as "Experiment") and then twice during the control experiment ("Control A" and "Control B"). Data are plotted along the x-axis grouped by colony and sorted by average mass across the three measurement periods.

Figure 4.9. Trajectories of ants in a *P. californicus* colony. (A) A still-frame from the video recording of a colony within its artificial nest and sealed within a respirometry chamber during flow-through respirometry. Two clusters of brood are located near water tubes toward the bottom of the frame; the lid of a small petri dish containing food and debris is located toward the top-center of the frame. (B) In this image, the track of each ant's movement within the nest is identified with a different color line. The positions of each ant visibly moving were tracked every 5 frames across a 451 frame recording (30 s). In this colony, I tracked a total of 161 workers; an additional 78 additional workers were present but they were not moving (e.g., standing over brood or stationary within a water tube).

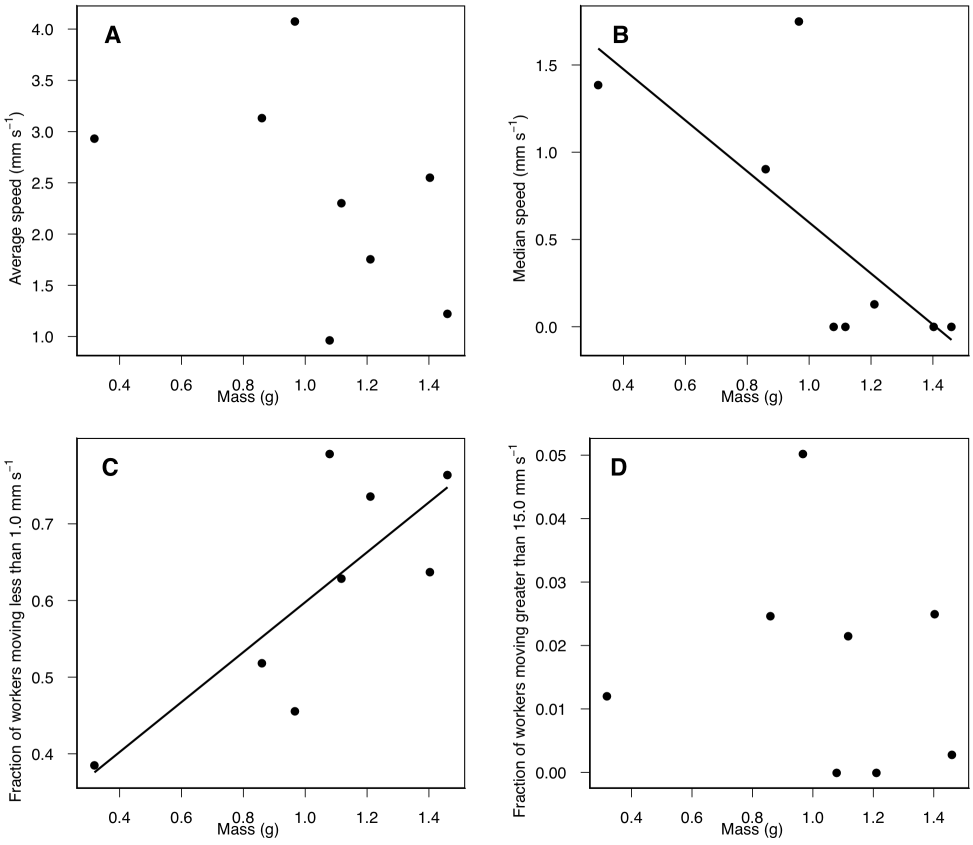

Figure 4.10. Analysis of walking/running behavior in *P. californicus* colonies. I tracked 995 ants in 8 colonies (a total of 90,545 manually digitized coordinates) to determine how walking speeds scaled with colony size. Generally, as colonies get larger, there is a greater fraction of inactive ants. This can be seen above by (B) the significant decrease in median walking speed with colony size and in (C) the significant increase in the fraction of workers moving less than 1.0 mm s^{-1}.

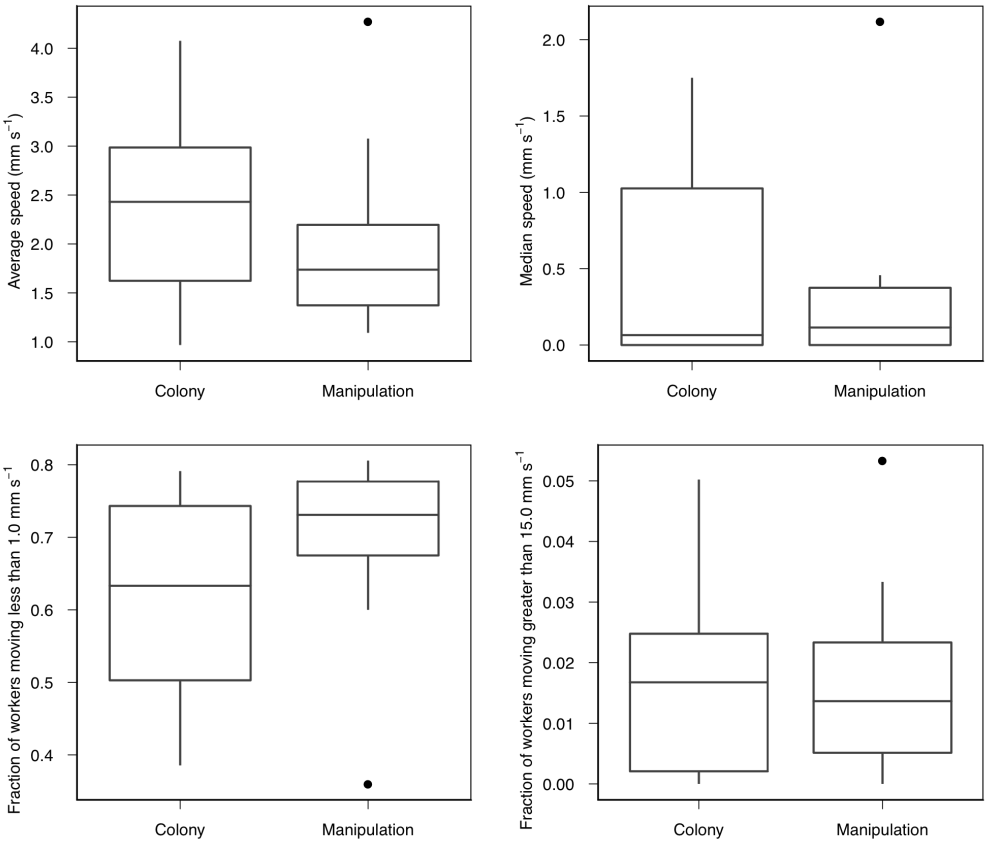

Figure 4.11. Analysis of walking/running behavior in *P. californicus* colonies before and after size manipulation (N=8 pairs). Although walking speeds exhibited a strong correlation with colony size and mass-specific metabolic rates, the experimental size manipulation did not affect the average, median, or distribution of walking speeds.

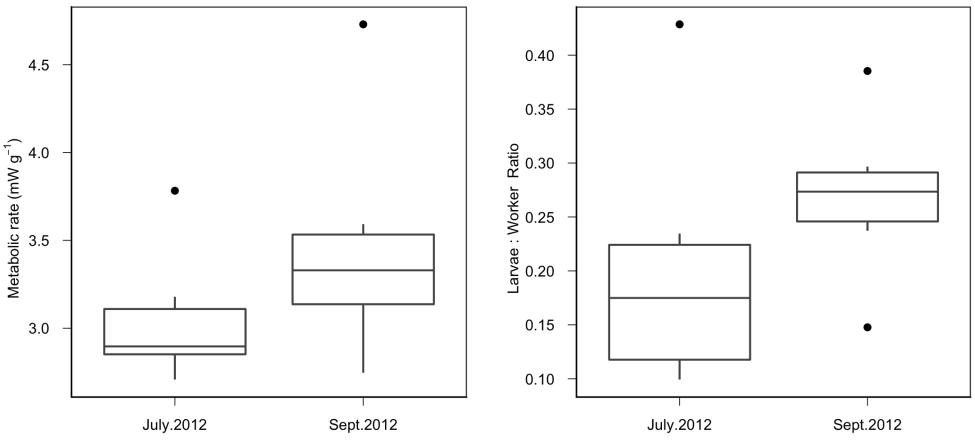

Figure 4.12. Changes in colony composition following size manipulation and differences in mass specific metabolic rate. From July to September 2012, the average number of larvae per colony increased. At the same time, mass specific metabolic rates tended to increase.

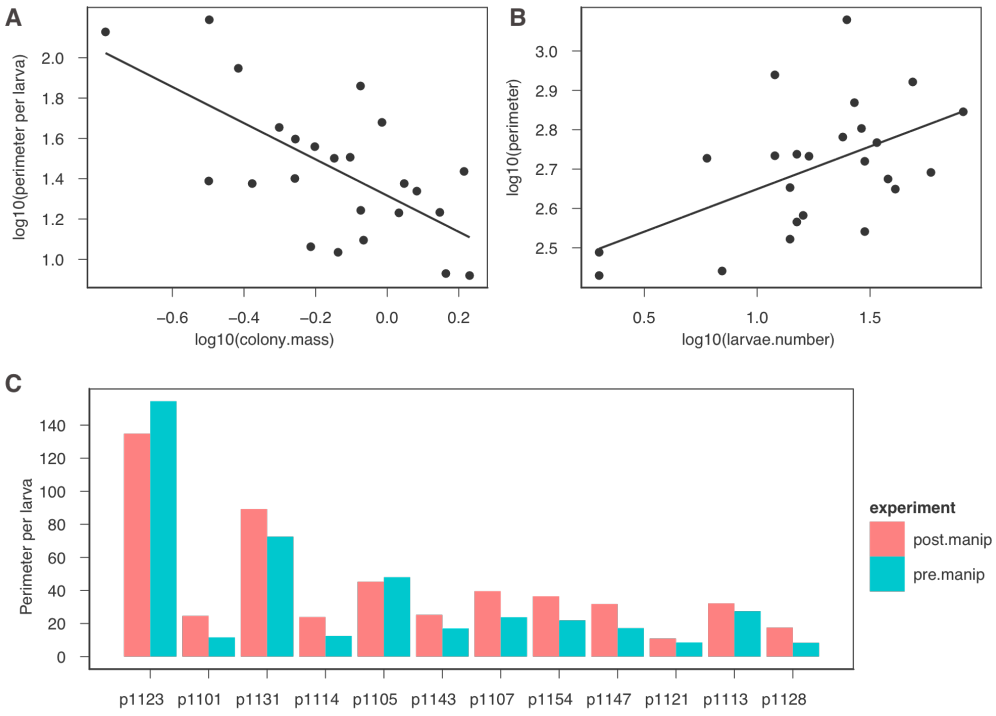

Figure 4.13. The geometry of brood piles in social insect colonies. Brood piles contain a number of larvae which may be accessed by workers along the edge of the pile. Are these piles spread out so that all of the larvae can be well-accessed by workers, or do they cluster? (A) The perimeter to larva ratio decreased with colony size, scaling with colony mass$^{-0.90\pm0.21}$ (95% CI: -1.35 – -0.44). (B) The perimeter of brood piles scaled hypometrically with larvae number$^{0.22\pm0.07}$ (95% CI: 0.07-0.37). (C) Following the experimental size manipulation, which reduced the number of workers, larvae, and pupae by 50%, there was an increase in perimeter per larva ratio.

Repeated measures ANOVA

*formula = Watts ~ Mass * Measurement.Period + Error(Colony.ID/Measurement.Period)*

Error: Colony.ID

	df	SS	MS	F	P
Mass	1	7.33E-06	7.33E-06	237.157	0.00419
Mass:Measurement.Period	2	1.72E-07	8.62E-08	2.7904	0.26383
Residuals	2	6.18E-08	3.09E-08		

Error: Colony.ID:Measurement.Period

	df	SS	MS	F	P
Mass	1	1.50E-06	1.50E-06	20.8486	0.002586
Measurement.Period	2	2.34E-07	1.17E-07	1.6279	0.262697
Mass:Measurement.Period	2	1.13E-07	5.67E-08	0.7872	0.491614
Residuals	7	5.04E-07	7.20E-08		

Table 4.1. Results of a repeated measures analysis of variance modeling colony metabolic rate (Watts) as dependent on colony mass, measurement period, and colony. While there was a strong effect of mass, there was not a significant effect of measurement period.

Chapter 5

TOWARD A NETWORK MODEL OF METABOLIC REGULATION IN SOCIAL INSECT COLONIES

Size and metabolism

Size is among the most important factors in determining the biology of an individual animal (Bonner, 2006; McMahon and Bonner, 1983; Went, 1968). Characteristics that correlate with body size include lifespan, metabolism, and growth (Calder, 1996; Peters, 1983; Schmidt-Nielsen, 1995). Despite the significance of these factors for fields ranging from ecology to human medicine, scientists have not yet been able to explain the mechanism that generates these patterns throughout nature (Chown et al., 2007; Glazier, 2005; Savage et al., 2008). Recent studies have demonstrated that similar patterns related to size occur in entire societies such as marine colonial organisms and social insect colonies, broadening the scope of these unexplained patterns (Fonck and Jaffe, 1996; Nakaya et al., 2003; White et al., 2011). The focus of this dissertation has been to develop the use of social insect colonies as model organisms to test hypotheses about the mechanistic basis for the observed allometric scaling of metabolic rate with colony size.

The metabolic rates of all animals, including insects, can be highly plastic, and are extremely dependent on behavior. Animal behaviors require time and energy (Cuthill and Houston, 1997), and measurements of metabolic rate integrate both of these variables. In social insect colonies, as with individual animals, the

rates of biological processes and the budgets for energy supply and demand scale hypometrically with body size, meaning that larger animals have predictably lower mass-specific metabolic rates (Calder, 1996; Hou et al., 2010; Oster and Wilson, 1978; Peters, 1983; Schmidt-Nielsen, 1995; Waters et al., 2010). While one common theory suggests that the supply of energy limits metabolic rates in larger animals, being a major constraint to animal physiology and behavior (Brown et al., 2004; West et al., 1997), an alternative hypothesis is that demand for energy is lower in larger organisms, with behavioral regulation providing the mechanistic basis for patterns such as the ¾-power scaling of metabolic rate with body size (Reinhold, 1999; Ricklefs, 2003; Secor and Diamond, 1998).

Metabolic allometry in social insect colonies

It has long been hypothesized that since social insect colonies behave in many ways as functionally integrated superorganisms, they should likewise benefit from an economy of scale (Emerson, 1939; Wheeler, 1911). A number of early studies examined whether or not a "group effect" influenced the metabolic rate of social insects. In some ant species, such an effect was identified (Fonck and Jaffe, 1996; Galle, 1978), while in others it was not (Brian, 1973; Lighton and Bartholomew, 1988; Lighton, 1989). Honeybees exhibit striking effects of group size, with metabolic rates scaling hypometrically in swarm clusters (Heinrich, 1981a; Heinrich, 1981b) and entire nests (Southwick, 1982), apparently because these colonies use metabolic heat to thermoregulate, and mass-specific heat loss rates decrease as colony surface area to volume ratio decreases in larger colonies.

As described in Chapters 2 and 4, colonies of the seed-harvester ant, *Pogonomyrmex californicus*, consistently exhibit metabolic hypometry, with metabolic rates scaling with colony mass$^{0.77\pm0.06}$ (Figure 5.1). This scaling relationship was robust to different experimental protocols, nest enclosures, experimental size manipulation, and colony age. The scaling exponents of colonies before and after size-manipulation were statistically indistinguishable (ANCOVA, $F_{1,20}$=0.64, p=0.435) as were their scaling coefficients (ANCOVA, $F_{1,21}$=0.19, p=0.67). The colonies measured in 2010 (Chapter 2) were approximately three years old and the colonies measured in 2012 (Chapter 4) were approximately one year old; both exhibited statistically indistinguishable scaling exponents (ANCOVA, $F_{1,21}$=0.63, p=0.436). The persistence of a relatively constrained and hypometric mass-scaling exponent strongly suggests that colony size is a critical factor in predicting the pace of life in social insect colonies.

While the effect of size on colony metabolic rates remained similar across years, there were strong differences in the absolute metabolic rates. The mass-specific metabolic rates of the colonies measured in 2012 were on average three times greater than the mass-specific metabolic rates of colonies measured in 2010. These colony cohorts exhibited similar colony compositions in terms of queen number, larvae and worker composition, and average body size, suggesting such parameters did not explain these differences. However, average walking-speeds of workers and colony growth rates correlated with the metabolic variation across years. The 2010 cohort exhibited average walking speeds between 0.3-1.0 mm s^{-}

^{1}, while the average walking speed for workers in 2012 ranged from 1.0-4.0 mm s^{-1}. Additionally, the colonies in 2012 were younger than the ones in 2010, and they exhibited significantly greater net effective growth rates, defined as the ratio of their wet mass at the time of measurement to their age (Welch two sample t-test, $t=5.23$, $df=16.6$, $p < 0.001$; Figure 5.2). It should be noted that these calculated net effective growth rates may not reflect variation in colonial growth rates over shorter time periods. The higher metabolic rates, net effective growth rates and walking speeds of the 2012 colonies support the hypothesis that colony growth and worker behavior are strong determinants of colonial metabolic rates.

One of the predictions of the supply-limitation hypothesis of metabolic allometry is that as metabolic rates become increasingly constrained with size, growth rates should scale accordingly. The data presented here for *P. californicus* colonies do not match this prediction. To the contrary, the largest colonies exhibited relatively high growth rates and relatively low metabolic rates (Chapter 2). These scaling patterns, together with the fact that colonies in all studies were generously supplied with food, water, and space, suggest that differences in colony size may be associated with variation in metabolic demand.

Integrating metabolism and behavior

The central hypothesis of this dissertation is that increases in colony size are associated with changes in behavioral organization that reduce the mass-specific demand for work which then decreases the mass-specific metabolic rate.

There are a number of (non-mutually exclusive) mechanisms which may plausibly operate to generate the observed metabolic and locomotory scaling patterns:

1. **Ergonomic optimization and the division of labor.** As colonies grow and the supply of resources into the colony increases, there is the potential for increased variance in worker size, morphology, task specialization, and spatial fidelity. These factors may directly contribute to the development of a division of labor and improve the energetic efficiency of colony operations (Oster and Wilson, 1978).
2. **Scaling of work capacity relative to production and reproduction.** Since much of the work performed by workers is related to care for and provisioning of larvae, the organization of this work depends on queen egg-laying rates and how these scale with colony size. Although the number of workers increases with the size of the colony, queen number does not. Furthermore, queen egg-laying rates in a number of species do not depend on colony size (Brian, 1989; Porter and Tschinkel, 1985); in others it increases but not as fast as the supply of workers (Endler et al., 2006). As a consequence, the capacity for work within social insect colonies may scale faster than the demand for work imposed by the number of larvae, leading to the potential for a growing surplus of relatively idle individuals, a reserve workforce, as colony size increases.
3. **Work capacity scaling and the division of labor.** The response-threshold model for the division of labor is based on the theory that workers vary in

the stimulus intensities required for them to engage in particular behaviors (Beshers and Fewell, 2001). Individuals with relatively high response thresholds for a given task are more likely to be available for other tasks (or simply idle) as long as there is a sufficient supply of other individuals with lower response thresholds. Thus, if the supply for work increases faster than its demand, larger colonies are more likely to establish a division of labor than smaller colonies (Jeanson et al., 2007). Indeed, the division of labor increases in colonies of *P. californicus* both with size and age (Holbrook et al., 2011).

4. **Social geometry.** A number of social behaviors may affect the demand for work as colony size increases. While workers have a tendency to gather brood into piles, thus securing them from predators, preventing loss, and centralizing their care near that of the queens, the piles themselves insulate larvae on the interior from access to workers and may act as barriers to the communication of larval growth demands (Brian, 1956). As such, there may be aspects of colony geometry that are affected by colony size. For example, larger brood piles, which have a lower surface-to-volume ratio (Figure 4.13), may lead to lower brood feeding rates and growth. Worker access to the queen may be similarly affected by increased crowding as colony size increases, with possible effects on her feeding, transmission of her fertility signal, and her ease of mobility within the nest. Geometric considerations such as these may play a role not only in driving down metabolic demand with increasing colony size,

but they may also play a central role in generating Michener's paradox (Michener, 1964), the observation that the effective productivity of a colony decreases with its size (Brian, 1953; Shik, 2008).

5. **Network structure and the efficiency of task-allocation.** One common element of each of mechanisms described above is that they all depend on interaction between the individuals within a colony. Foraging workers need to interact with nurse workers to provision for the larvae, nurse workers interact with the queen and the larvae, some workers may conduct policing behavior among each other, and idle workers may remain inactive until stimulation by interaction with passing workers engages their response threshold. Just as the nervous and cardio-pulmonary systems in vertebrates serve to transmit information about an animal's environment and energetic state, so too might the interaction networks within social insect colonies serve as the conduits for information about energetic supply and demand. Intriguingly, the communication networks in social insect colonies may serve as both the conduits for the transmission of information as well as the mechanism for behavioral regulation at the colony-level if the structure of these networks affected the allocation and distribution of work. Since the potential for network complexity scales exponentially with colony size (the total number of possible interactions, I, depends on colony size, N, according to $I \sim N^2$), it is possible that there may be barriers to efficient communication as colony size increases (Blonder and Dornhaus, 2011). However, observations on the net

effective growth rates in *P. californicus* (Chapter 2 & 4) suggest that while larger colonies had lower mass-specific energetic demands, they also grew more than smaller colonies. These observations suggest a novel mechanism for the hypometric scaling of metabolic demand with colony size, i.e. that metabolic demand may be proportional to the rate of information flux through a network. As colony size increases, information may be transmitted more slowly across the whole colony while local information transmission rate either stays constant or increases due to density. As a consequence, larger colonies may be more able to buffer transient stimuli than smaller colonies and this may lead to a more efficient allocation of work with increasing colony size.

Social insect colony interaction networks

In 1988, E. O. Wilson and Bert Hölldobler described the organization of communication within social insect societies as "dense heterarchies" in which feedback patterns among highly connected individuals and task groups generate emergent complexity (Wilson and Hölldobler, 1988). Among the most important foundations of social insect societies, communication provides the basis for the division of labor and its regulation (Hölldobler and Wilson, 1990; Hölldobler and Wilson, 2009). Although individuals within colonies may communicate in many ways, from acoustic to chemical, direct physical interactions are hypothesized to play a central role in the organization of social insect colonies (Anderson and McShea, 2001; Gordon, 2007). One way to study the patterns of physical

interaction is to aggregate sequences of observed interactions as a network model for communication. The structure of social interaction networks has been demonstrated to correlate with colony decision, immunity, and resource distribution (Dussutour and Simpson, 2009; Naug, 2008; Naug, 2009; Sendova-Franks et al., 2010). By uniquely marking individuals, recording their behavior, and tracking their interactions with other individuals within a colony, patterns of communication in *P. californicus* colonies were studied by examining the frequency of interaction and the topological structure of their interaction networks (Chapter 3).

Since workers engage in tasks dependent on information received through interactions with other individuals within the colony, the structure of these interaction networks is hypothesized to influence the distribution and efficient allocation of work. In a small colony, workers may be in direct contact with a relatively larger fraction of the colony than workers from a large colony, and as such, they would be exposed to a relatively greater amount information and stimulus, leading to task redundancy and a poor distribution of work. As colony size increases, enhanced communication networks may distribute more work effectively leading to a larger reserve workforce and a relatively smaller proportion of individuals actively engaged in colony labor, thus reducing mass-specific metabolic rates compared to smaller colonies.

Investigating the topology of *P. californicus* interaction networks (Figure 5.3) revealed a number of intriguing features. Similar to scale-free networks, the degree distribution was strongly right-skewed with a few workers engaging in

many interactions and most workers engaging in fewer interactions (Figure 3.5 and Figure 5.8). There was also a preponderance of regulatory feed-forward loop subgraphs present in the colony networks (Chapter 3). The density of feed-forward loop did not scale with colony mass ($p=0.18$) or worker number ($p = 0.44$), but did increase as a fraction of behavioral triads as the number of larvae increased ($F_{1,4}=15.21$, $p=0.02$, $R^2=0.80$; Figure 5.4).

The feed-forward loop involves three ants and three directional interactions. Adapting terminology from the transcriptional regulation literature (Shen-Orr et al., 2002), I may name the three ants as A, B, and C. Ant A interacts with both B and C; ant B also interacts with ant C. In this way, information is transmitted in a directional way from A and B to C and it is efficient in the directional transmission of information in that there are no mutual or negative feedback interactions. One plausible hypothesis for the dominance of the feed-forward loop is that use of this pattern provides increased reliability in the decision-making behavior of the receiving ant (ant C), since a change in its behavior may require a pair of coherent interactions from the other two individuals (A and B). The feed-forward loop is a characteristic subgraph within metabolic and gene-transcription networks in which gene expression may be regulated only in response to persistent changes in an environment (Mangan and Alon, 2003; Mangan et al., 2006). The subgraph most associated with animal social interactions, the mutually-connected clique triad (Milo et al., 2004), was absent from the majority of *P. californicus* interaction networks (Waters and Fewell, 2012).

Within a social insect colony, larvae are the only individuals that grow, and thus most demand for food comes from the larvae. In *Solenopsis invicta*, a larval metabolic caste processes nutrients that are fed to the queen by workers thus generating a feedback cycle in which social interactions regulate egg-laying rate (Tschinkel, 1988). In *Lasius niger*, workers forage for resources with different stoichiometric intake targets depending on the larval composition within the colony (Dussutour and Simpson, 2008; Dussutour and Simpson, 2009). Thus, larval growth rate may be a principal factor in setting the metabolic demands for a colony, demands that drive the patterns of interaction and behavior of workers that forage for the resources to supply the growing larvae.

The interaction and feedback between the larvae and worker populations may play a central role in regulating the scaling of work in social insect colonies. Wilson and Hölldobler (Wilson and Hölldobler, 1988) predicted that feedback loops such as this would be important in establishing emergent patterns of colony-level organization and Fewell developed this concept further within the framework of a functional network operating with differential feedback between the task groups within a colony (Fewell, 2003). While the behavior and metabolic rates of workers are ultimately influenced by their interactions with each other, their interactions with larvae may provide the mechanism to integrate the relative abundance of energetic supply and metabolic demand within the colony.

A major long-term goal of research in this area should be to test these various proposed mechanisms for the hypometric scaling of colonial metabolic rates and behavior. Doing so would be facilitated by development of models that

incorporate the network interactions, as it seems unlikely that colonial scaling can be explained by autonomous individual behavior. One obvious null model for network interactions in colonies is a diffusion model, in which workers are hypothesized to interact randomly. While I know that this is not the case, if scaling patterns exhibited by such null models match the empirically observed patterns, this might allow determination of the specific aspects of colonial geometry, behavior distribution, or interaction pattern that explains hypometric scaling. I have begun tests of such a null model, but these remain preliminary (Appendix A). Nonetheless, these preliminary tests suggest that such random models likely do not explain the scaling of colonial behavior. Future directions will include extending the response-threshold model for the division of labor (Beshers and Fewell, 2001; Jeanson et al., 2007) so that its predictions may be assessed based on different network models for connectivity within a colony. It will also be possible to experimentally manipulate the social geometry of a colony, such as by redistributing brood piles or the area for interaction between individuals to determine how these factors specifically contribute to the metabolic regulation and behavioral integration of whole colonies.

Appendix: A diffusion model for predicting the scaling of interaction rates

Understanding how colony size might affect interaction networks among ants requires the development of mathematical models of worker interactions that can include factors such as ant size, speed and nest size. A null model for the interactions within a social insect colony is that they proceed randomly in a manner similar to molecular diffusion, with interactions mathematically explicable by worker velocities and density. To explore this hypothesis, I developed a kinetic model for ant interaction frequencies based on the collision probabilities of randomly diffusing particles. An alternative explanation for interaction patterns is that there is a functional basis to the interactions between workers. These models are not mutually exclusive and there are data supporting each perspective. *Pogonomyrmex barbatus* workers tend to interact more with each other at nest entrances, a spatially deterministic feature consistent with the diffusion model (Pinter-Wollman et al., 2011). *Acromyrmex heyeri* foragers engage in significantly different interaction rates depending on whether they are in the initial or established phase of foraging, a difference with a functional basis in the need to communicate information about new resources early in foraging (Bollazzi and Roces, 2011).

To estimate the collisional frequency of a single particle (or ant), the area of the nest's surface it crosses may be estimated and the number of other ants' paths it may intersect in a given time interval may be calculated based on ant density. The area covered by a single ant on its trajectory may be calculated as the product of the distance traveled and the effective diameter of its interaction

with other ants. The distance traveled by an ant may be found by taking the product of its average speed ($\bar{v}_i$) and the duration (Δt) of its travel. The effective diameter (d_i), within which it is likely to interact with nearby ants, depends on body size and may be approximated as close to 5.0 mm for an average-sized *P. californicus* worker. Thus, the area of the nest surface occupied by an ant on its journey is given by:

$$Area_i = \bar{v}_i \cdot \Delta t \cdot d_i$$

The number of times this ant collides with another depends on how many other ants' paths it crosses, which depends on the density of ants within the nest enclosure (given by the ratio of the total number of ants, N, to the total area, A_{total}). Thus, the collisional rate (Z_i) of a single ant may be found by:

$$Z_i = \frac{N \cdot Area_i}{A_{total} \cdot \Delta t}$$

The total collisional rate for the entire colony is one-half of the sum of all ants' collisional rates (to avoid double-counting each interaction):

$$Z_{ii} = \tfrac{1}{2} \cdot Z_i \cdot N$$

This model predicts that per capita interaction rates should increase linearly with colony size, and total net interactions should increase exponentially with colony size (Fig. 5.5A). This effect occurs due to the increase in ant density with colony size.

Modifying the diffusion model for to match worker behavior

Two major results of the kinematic analysis of worker walking speeds (Chapter 4) were that larger colonies tended to have more slowly walking workers and more workers "standing around." Median walking speed decreased with colony size (Figure 4.10B). There was also an increase in the relative proportion of stationary ants with increasing colony size (Figure 4.10C).

To consider how these changes in walking speed across colony size might alter a diffusion model, I parameterized the model so that average worker speed inversely proportional to colony size, as described in Chapter 4. With these parameters, the model predicted a highly nonlinear relationship between per-capita interaction rate and colony size (Figure 5.5B).

While the random diffusion model assumed that ants are uniformly distributed throughout the nest and that density increases with colony size, these assumptions may not be accurate. A previous study identified that even as colony size increases within a fixed enclosure, the workers maintain a relatively constant effective density by adjusting how much of the nest box they occupy (see Chapter 2). If walking speeds are constant and density is held constant across colony sizes, per capita interactions do not change with size (data not shown). Revising the model so that density is held constant with respect to colony size (and speeds decrease with increasing colony size as before), the per-capita interaction rate is predicted to decrease with colony size (Figure 5.6F).

The fact that predictions of the diffusion model regarding the scaling of per capita interaction rate vary dramatically with assumptions indicates that

verification of the model's parameters is critical in order to assess whether such a model can have utility in the describing the scaling of colony network interactions.

Scaling of interaction rates with colony size and comparisons with the various diffusion models

During the respirometry recordings conducted in 2012 (Chapter 4), video recordings of colony behavior were saved and used to explore the relationship between colony size, walking speeds, and interaction patterns between workers. Although data are available for both pre- and post- size-manipulated colonies, the data analyzed so far were for video recordings of colonies prior to the size manipulation. The methods for these analyses were similar to those previously described in Chapter 3 (Waters and Fewell, 2012), with the only difference being that individuals were not paint-marked but rather digitally marked and manually tracked using the MTrackJ plugin for ImageJ (Meijering et al., 2012; Rasband, 1997-2012).

How did per capita interaction rates change with colony size? The slower velocities and increased number of stationary workers led to no net change in per capita interaction rates across a range of colony sizes, despite the greater number of ants and the higher densities of ants (Figure 5.6A, $F_{1,3}=0.54$, $p=0.516$). If one considers only the ants that engage in interactions, the per capita interaction rate increased with the size of the group, suggesting that the effect of increasing ant density outweighed the slower velocities in larger colonies (Figure 5.5B,

$F_{1,3}$=12.38, p=0.04). As a scaling relationship, the whole-colony interaction rate scaled with the number of interacting ants$^{1.24\pm0.05}$ ($F_{1,3}$=572.5, p < 0.001; 95% CI: 1.08-1.41).

Are the diffusion models useful for predicting the scaling of interactions across colony size? Inclusion of additional colonies is probably necessary to answer this question, since it is very difficult to test against nonlinear models with such a low sample size. However, a number of factors suggest that the scaling of interactions in ant colonies is not well-predicted by a diffusion model. First, the decline in velocities in large colonies is not predicted by such random models. Second, the decline in velocities only applied to the colony as a whole, considering only the ants that were walking, there were not significant differences in walking speeds between colonies. Similarly, the decrease in the fraction of ants walking in larger colonies does not fit with a diffusion model. Even if the decline in walking speed with colony size is incorporated into the diffusion model, the highly nonlinear pattern predicted by the model (Fig. 5E) does not seem to fit the observed data (Fig. 5A). More data are needed to reject such models with statistical power, but the data to date suggest that these simple diffusion models are not good descriptors of ant interactions in our colonies, perhaps because I lack good measures of actual ant density, or perhaps because workers seek or avoid each other in a manner not predicted by a diffusion-type model.

The diffusion model for per-capita collision rates assumes that all of the ants within a colony move at the same speed, and as such, all individuals within

the colonies are predicted to exhibit the same per-capita interaction rate. In reality, the distribution of walking speeds (Chapter 4) and interactions (Figure 5.7) is far from uniform or normal, but rather is highly right-skewed. The number of interacting ants increases with colony size, but larger colonies may have a larger fraction of relatively inactive ants that do not engage in interactions. Thus in large colonies, a few ants have many interactions, while many ants have very few interactions, similar to the pattern observed for walking speeds for which larger colonies had more skewed speed distributions (Chapter 2). This result is consistent with the observation that larger colonies have an increased division of labor in which a few ants are doing most of the walking and communicating (Holbrook et al., 2011).

Some other predictions of the diffusion models do fit with the empirical data. Per-capita interaction rates (among individuals engaged in interactions) did increase linearly with individual ant walking speeds (Figure 5.7). The overall (pooling all colonies) correlation between interaction rate and walking speed was significantly positive ($r=0.32$, $p < 0.001$). The relationship was also significant ($p < 0.05$) in five of six colonies examined (Fig. 5.6). However, even for the 5 colonies in which the relationship is significant, walking speed explained only a small fraction of the variation in per-capita interaction rate (average $R^2=0.16 \pm 0.07$). Individuals with the most interactions tended to exhibit not the highest speeds but relatively moderate speeds, again suggesting that a diffusion-type model is not predictive of ant interactions. Observations of ant interactions also suggest that these are not random. Interactions tend to make ants stop and

frequently result in their changing direction and/or speed, strongly suggesting that information exchange occurs, producing non-random walking patterns.

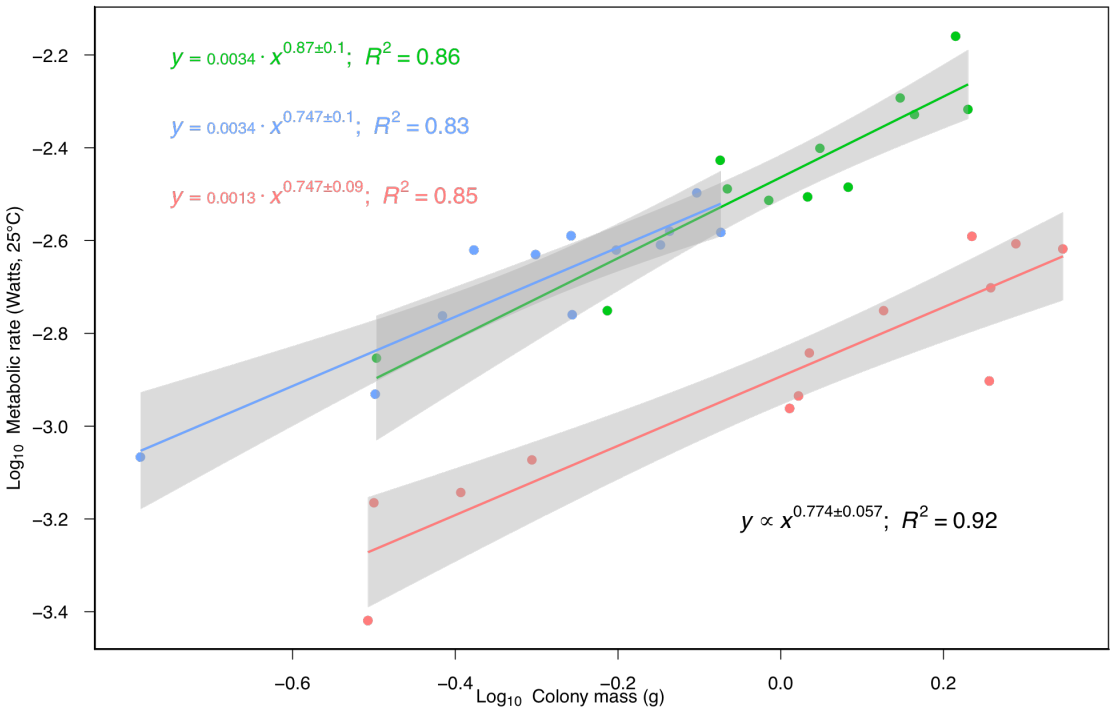

Figure 5.1. Metabolic allometry of *P. californicus*. The figure above shows the metabolic rate allometries of three sets of measurements of seed-harvester colonies. In red are the data collected in 2010 and described in Chapter 2 (Waters et al., 2010) and the green and blue colors indicate the pre-manipulation and post size-manipulation data collected in 2012, described in Chapter 4. Although there is a significant difference in the metabolic elevation (the 2012 measurements are approximately three times higher than in 2010), the equation at the bottom right indicates the common scaling exponent shared by the three allometries.

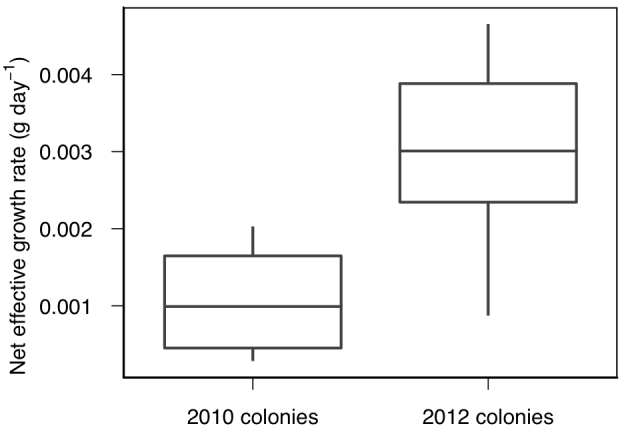

Figure 5.2. Growth rates of colonies measured in 2010 (approximately three years old) and 2012 (approximately one year old). The 13 colonies measured in 2010 exhibited net effective growth rates of 0.0011±0.00017 g day^{-1}; the 12 colonies measured in 2012 exhibited net effective growth rates of 0.003 ± 0.00033 g day^{-1}

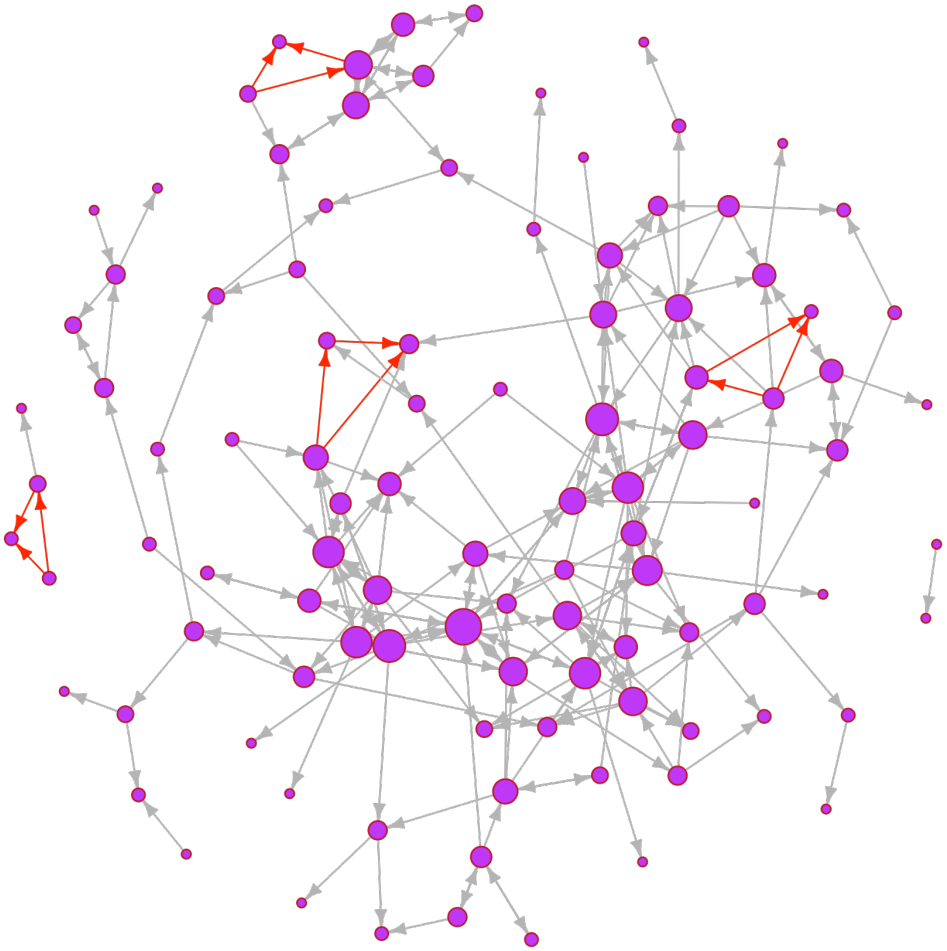

Figure 5.3. Social insect colony interaction network. This network was constructed based on recording the antennal interactions between workers in a *P. californicus* colony across 30 s of video recorded simultaneously with flow-through respirometry. The network is composed of 102 nodes or vertices (each representing a unique worker) and 222 directional edges (representing interactions between the workers). In this visualization, the nodes are scaled proportional to their degree (i.e., the sum of their in- and out-interactions). The network can be

deconstructed into 703 distinct triads (subgraphs of three connected nodes), 3.13% of which are topologically identical to the feed-forward loop motif (four of which are highlighted above in red). By contrast, when a similarly sized network (i.e., one preserving the local-degree distribution) is modeled with random interactions, it is only expected to exhibit the feed-forward loop in 0.72 ± 0.003% (SD) of the network triads (N=10,000 simulated randomized networks).

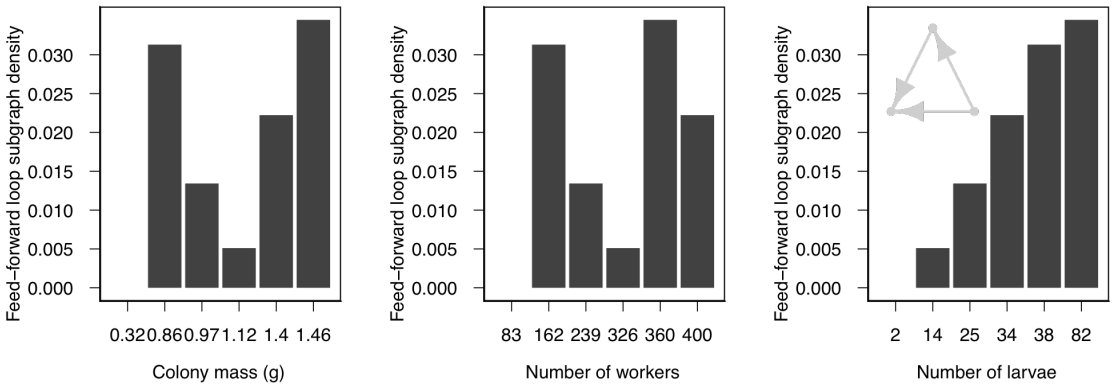

Figure 5.4. Scaling of regulatory network structure. The feed forward loop was identified as a subgraph within 5/6 *P. californicus* interaction networks measured using the video recorded during the analysis of respirometry in Chapter 4. In each of these cases, the subgraph density was significantly higher than expected given its density in the random models. While there was not a trend of this subgraph's density scaling with colony mass ($p=0.18$) or worker number ($p=0.44$), there was a strong trend of the feed-forward loop subgraph density increasing with the number of larvae ($F_{1,4}=15.21$, $p=0.02$, $R^2=0.80$).

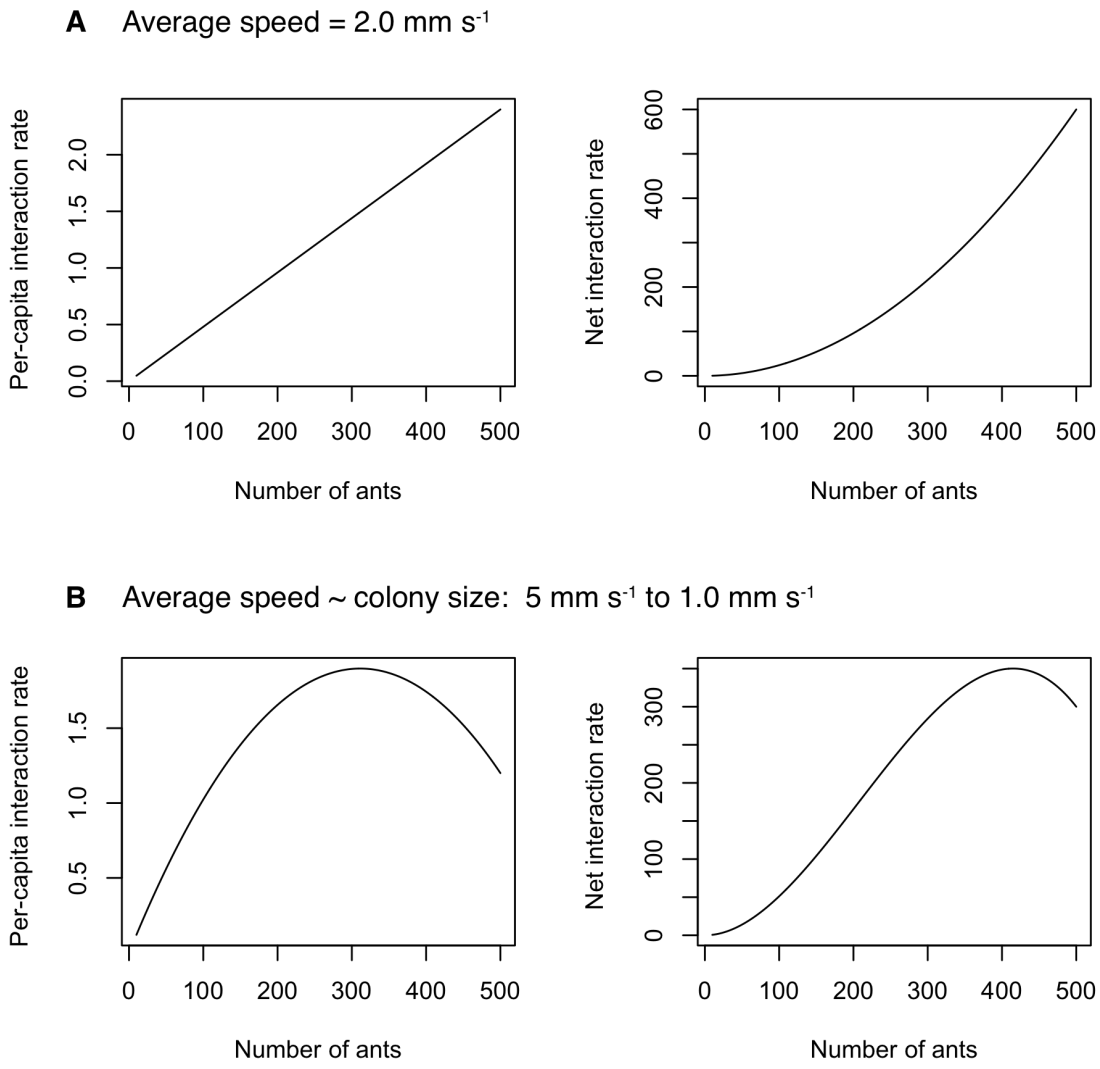

Figure 5.5. Predictions of the diffusion model for ant colony interaction/collision patterns. (A) If average speed is constant across a range of colony sizes, the per-capita interaction rates are predicted to increase linearly with colony size (density) and net interaction rates should increase with the square of colony size. (B) If average speed decreases with increasing colony size according to the observed empirical pattern, then over a lower range of sizes per capita and net total interactions increase due to the effect of increased ant density, but at

higher ranges of colony size the effect of decreasing speed predominates, leading to a fall in per capita and total net interactions. the relationship between interaction rate and colony size becomes nonlinear. This is because of a tradeoff as colony size increases between density increasing the probability of collision and speed decreasing the probability of collision.

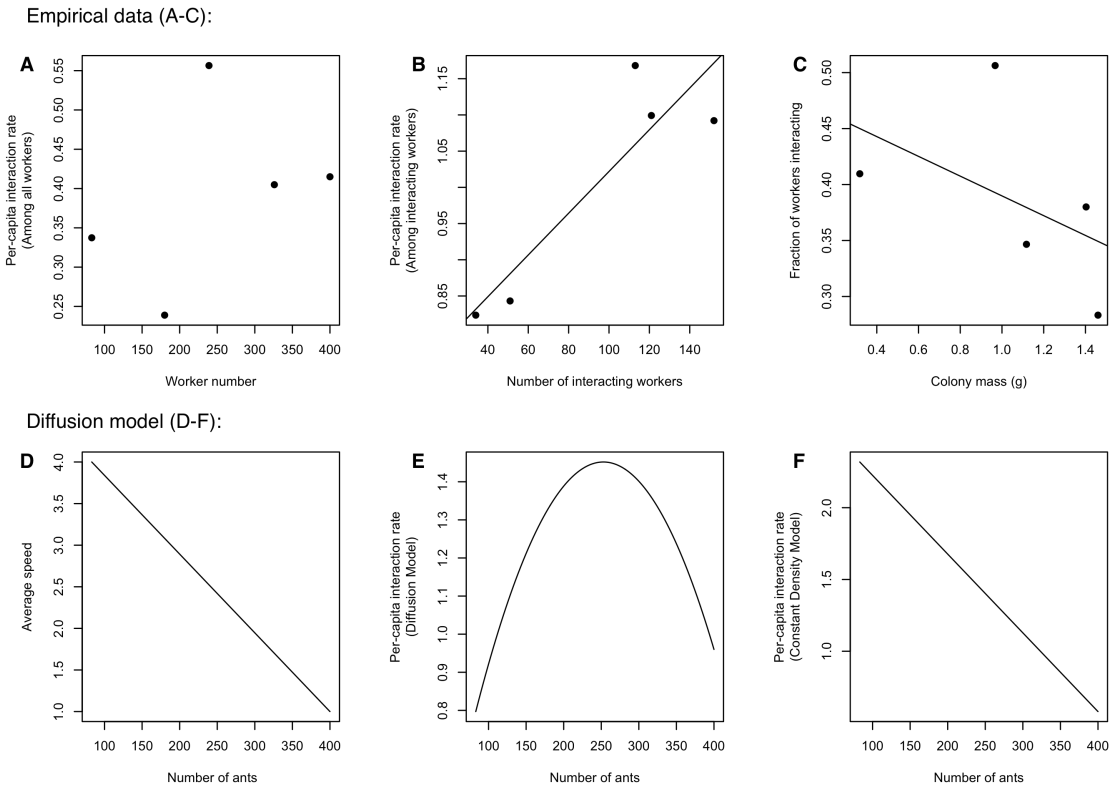

Figure 5.6. Empirical data (A-C) and model estimates (D-F) for the scaling of per-capita interaction rates. (A) There was no trend of per-capita interaction rates increasing with colony size when considered based on the total number of workers. (B) There was a trend of per-capita interaction rates increasing with colony size when considered based on the number of actively interacting workers. (C) The fraction of a colony's worker population actively involved with interacting with each other decreased with colony size. (D) The model was

parameterized so that larger colonies were composed of ants moving slower. (E) The random diffusion model predicts a nonlinear scaling of per-capita interaction rates because the density is increasing with colony size (tending to increase collision frequency) but the speeds are decreasing (tending to decrease collision frequency). (F) If the model is modified so that density is preserved, per-capita interaction rates are expected to decrease with colony size.

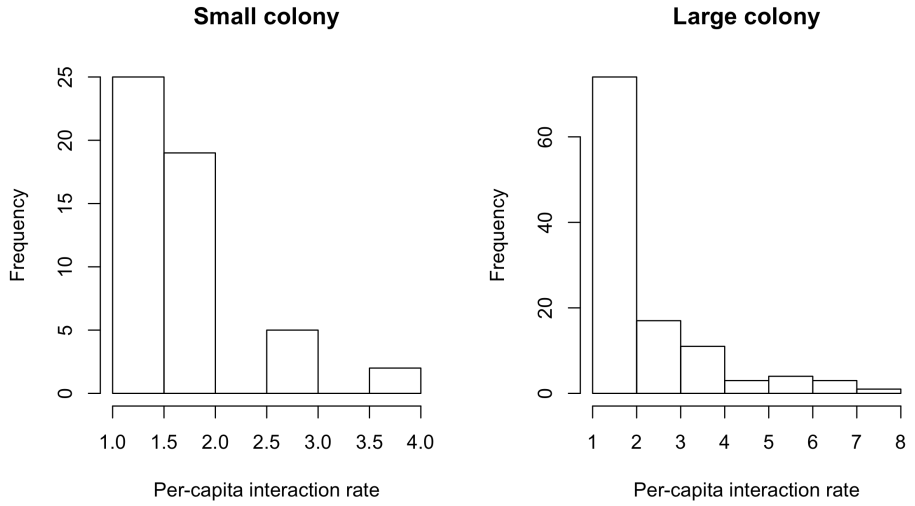

Figure 5.7. Degree distribution and colony size. The degree distribution is a probability distribution of worker interaction rates. Shown above are the degree distribution for a small colony (180 workers) and a large colony (326 workers). Random-graph networks are characterized by normal shaped degree distributions. The observed interaction rates are not normally distributed among the workers within their colonies. In this example, as colony size increases, this distribution becomes increasingly skewed, reflecting an increase in the variance in the per-capita interaction rates; larger colonies may have a greater disparity between the number of individuals doing the most active communicating and those doing the least.

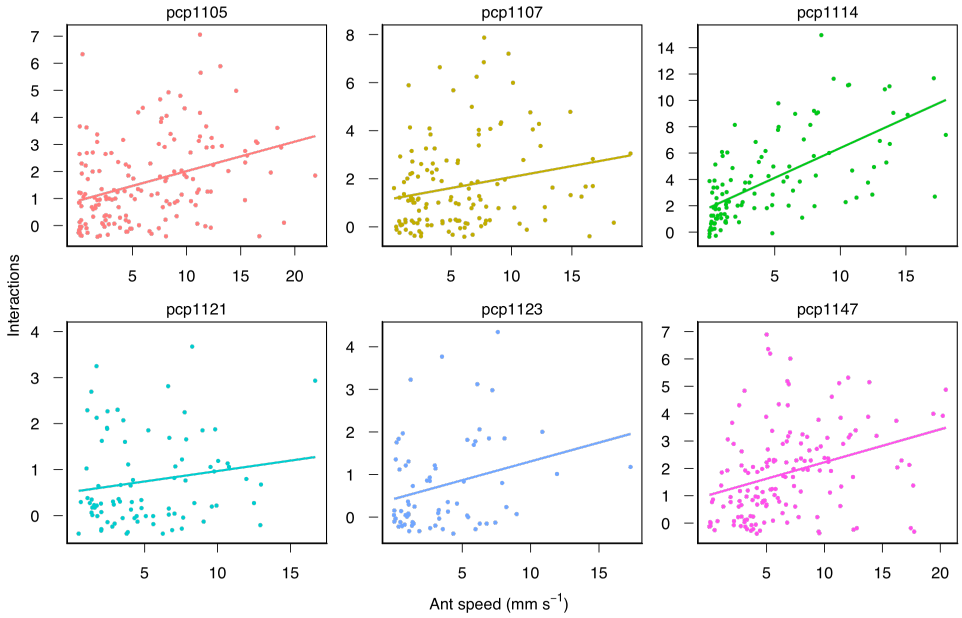

Figure 5.8. Per-capita interaction rate and walking speed on the individual-level. There is a correlation between per-capita interaction rate and walking speed. In six of the *P. californicus* colonies investigated in Chapter 4, individual-level kinematic data were compared with the corresponding individual's social interaction pattern. The figures above plot the relationship between each ant's average walking speed and their network degree (the sum of in- and out-interactions they exhibited).

LITERATURE CITED

Agutter, P. S. and Wheatley, D. N. (2004). Metabolic scaling: consensus or controversy? *Theoretical Biology and Medical Modelling* **1**, 13.

Alleyne, M., Chappell, M. A., Gelman, D. B. and Beckage, N. E. (1997). Effects of parasitism by the braconid wasp *Cotesia congregata* on metabolic rate in host larvae of the tobacco hornworm, *Manduca sexta*. *Journal of Insect Physiology* **43**, 143-154.

Andersen, A. N. and Lonsdale, W. M. (1990). Herbivory by Insects in Australian Tropical Savannas: A Review. *Journal of Biogeography* **17**, 433-444.

Anderson, C. and McShea, D. W. (2001). Individual versus social complexity, with particular reference to ant colonies. *Biological Reviews* **76**, 211-237.

Anderson, C., Ratnieks, F. and Feener Jr, D. (1999). Task partitioning in insect societies. I. Effect of colony size on queueing delay and colony ergonomic efficiency. *The American Naturalist* **154**, 521-535.

Auerswald, L. and Gäde, G. (2000). Metabolic changes in the African fruit beetle, *Pachnoda sinuata*, during starvation. *Journal of Insect Physiology* **46**, 343-351.

Balderrama, N. M., Almeida, L. O. B. and Núñez, J. A. (1992). Metabolic rate during foraging in the honeybee. *Journal of Comparative Physiology B: Biochemical, Systemic, and Environmental Physiology* **162**, 440-447.

Barabasi, A.-L. and Albert, R. (1999). Emergence of scaling in random networks. *Science* **286**, 509-512.

Bartholomew, G. A. and Casey, T. M. (1977). Body temperature and oxygen consumption during rest and activity in relation to body size in some tropical beetles. *J. Thermal Biology* **2**, 173-176.

Bartholomew, G. A., Vleck, D. and Vleck, C. (1981). Instataneous measurements of oxygen consumption during pre-flight warm-up and post-flight cooling in sphingid and saturnid moths. *Journal of Experimental Biology* **90**, 17-32.

Beekman, M., Sumpter, D. and Ratnieks, F. (2001). Phase transition between disordered and ordered foraging in Pharaoh's ants. *Proceedings of the National Academy of Sciences* **98**, 9703.

Beshers, S. N. and Fewell, J. (2001). Models of division of labor in social insects. *Annual Review of Ecology and Systematics* **46**, 413-440.

Blatt, J. and Roces, F. (2001). Haemolymph sugar levels in foraging honeybees (*Apis mellifera carnica*): dependence on metabolic rate and *in vivo* measurement of maximal rates of trehalose synthesis. *Journal of Experimental Biology* **204**, 2709-2716.

Blonder, B. and Dornhaus, A. (2011). Time-Ordered Networks Reveal Limitations to Information Flow in Ant Colonies. *PLoS ONE* **6**, e20298.

Bollazzi, M. and Roces, F. (2011). Information needs at the beginning of foraging: grass-cutting ants trade off load size for a faster return to the nest. *PLoS ONE* **6**, e17667.

Bonabeau, E., Theraulaz, G., Deneubourg, J., Aron, S. and Camazine, S. (1997). Self-organization in social insects. *Trends in Ecology & Evolution* **12**, 188-193.

Bonner, J. T. (2006). Why Size Matters: From Bacteria to Blue Whales. Princeton: Princeton University Press.

Bouwma, A., Nordheim, E. and Jeanne, R. (2006). Per-capita productivity in a social wasp: no evidence for a negative effect of colony size. *Insectes Sociaux* **53**, 412-419.

Bradley, T. J., Brethorst, L., Robinson, S. and Hetz, S. (2003). Changes in the Rate of CO2 Release following Feeding in the Insect *Rhodnius prolixus*. *Physiological And Biochemical Zoology* **76**, 302-309.

Brian, M. V. (1953). Brood-Rearing in Relation to Worker Number in the Ant Myrmica. *Physiological Zoology* **26**, 355-366.

Brian, M. V. (1956). Group Form and Causes of Working Inefficiency in the Ant *Myrmica rubra* L. *Physiological Zoology* **29**, 173-194.

Brian, M. V. (1973). Feeding and Growth in Ant Myrmica. *Journal of Animal Ecology* **42**, 37-53.

Brian, M. V. (1989). Social factors affecting queen fecundity in the ant *Myrmica rubra*. *Physiological Entomology* **14**, 381-389.

Brown, J. H., Gillooly, J. F., Allen, A. P., Savage, V. M. and West, G. B. (2004). Toward a metabolic theory of ecology. *ECOLOGY* **85**, 1771-1789.

Buck, J. (1962). Some physical aspects of insect respiration. *Annual Reviews of Entomology* **7**, 27-56.

Calder, W. A. I. (1996). Size, function and life history. Mineola, NY: Dover Publications.

Camazine, S., Deneubourg, J., Franks, N., Sneyd, J., Theraula, G. and Bonabeau, E. (2003). Self-organization in biological systems: Princeton Univ Pr.

Cao, T. and Dornhaus, A. (2008). Ants under crowded conditions consume more energy. *Biology Letters* **4**, 613.

Cao, T. T. and Dornhaus, A. (2012). Larger laboratory colonies consume proportionally less energy and have lower per capita brood production in Temnothorax ants. *Insectes Sociaux*, 1-5.

Casey, T. (1977). Physiological responses to temperature of caterpillars of a desert population of *Manduca sexta* (Lepid: Sphingidae). *Comparative Biochemistry and Physiology Part A: Physiology* **57**, 53-58.

Casey, T. and Ellington, C. (1989). Energetics of insect flight. *Energy Transformations in Cells and Organisms*, 258-272.

Casey, T. M. and Hegel-little, J. R. (1987). Instantaneous oxygen consumption and muscle stroke work in *Malacosoma Americanum* during pre-flight warm-up. *Journal of Experimental Biology* **127**, 389-400.

Casey, T. M. and Knapp, R. (1987). Caterpillar thermal adaptation: behavioral differences reflect metabolic thermal sensitivities. *Comparative Biochemical Physiology* **86**, 679-682.

Chappell, M. and Rogowitz, G. (2000). Mass, temperature and metabolic effects on discontinuous gas exchange cycles in eucalyptus-boring beetles (Coleoptera: cerambycidae). *J Exp Biol* **203**, 3809-3820.

Chappell, M. A. (1983). Metabolism and thermoregulation in desert and montane grasshoppers. *Oecologia* **56**, 126-131.

Chappell, M. A. (1984). Temperature regulation and energetics of the solitary bee *Centris pallida* during foraging and intermale mate competition. *Physiological Zoology* **57**, 215-225.

Chown, S. and Nicolson, S. W. (2004). Insect physiological ecology: mechanisms and patterns: Oxford University Press, USA.

Chown, S. L., Addo-Bediako, A. and Gaston, K. J. (2003). Physiological diversity: listening to the large-scale signal. *Functional Ecology* **17**, 568-572.

Chown, S. L., Marais, E., Terblanche, J. S., Klok, C. J., Lighton, J. R. B. and Blackburn, T. M. (2007). Scaling of insect metabolic rate is inconsistent with the nutrient supply network model. *Functional Ecology* **21**, 282-290.

Clarke, A. (2006). Temperature and the metabolic theory of ecology. *Functional Ecology* **20**, 405-412.

Clauset, A., Shalizi, C. R. and Newman, M. E. J. (2009). Power-law distributions in empirical data. *SIAM Review* **51**, 661-703.

Contreras, H. L. and Bradley, T. J. (2009). Metabolic rate controls respiratory pattern in insects. *Journal of Experimental Biology* **212**, 424-428.

Csardi, G. and Nepusz, T. (2006). The igraph software package for complex network research. *InterJournal, Complex Systems* **1695**, http://igraph.sf.net.

Cummins, K. W. and Wuycheck, J. C. (1971). Caloric equivalents for investigations in ecological energetics. Stuttgart: E. Schweizerbart.

Cuthill, I. and Houston, A. (1997). Managing time and energy. *Behavioral Ecology*, 97-120.

Davis, A. L. V., Chown, S. L., McGeoch, M. A. and Scholtz, C. H. (2000). A comparative analysis of metabolic rate in six *Scarabaeus* species (Coleoptera : Scarabaeidae) from southern Africa: further caveats when inferring adaptation. *Journal of Insect Physiology* **46**, 553-562.

Davis, A. L. V., Chown, S. L. and Scholtz, C. H. (1999). Discontinuous gas-exchange cycles in *Scarabaeus* dung beetles (Coleoptera : Scarabaeidae): Mass-scaling and temperature dependence. *Physiological And Biochemical Zoology* **72**, 555-565.

DeLong, J. P. and Hanson, D. T. (2009). Density-dependent individual and population-level metabolic rates in a suite of single-celled eukaryotes. *The Open Biology Journal* **2**, 32-37.

Dillon, M. E., Wang, G. and Huey, R. B. (2010). Global metabolic impacts of recent climate warming. *Nature* **467**, 704-706.

Dornhaus, A., Holley, J.-A., Pook, V., Worswick, G. and Franks, N. (2008). Why do not all workers work? Colony size and workload during emigrations in the ant *Temnothorax albipennis*. *Behavioral Ecology and Sociobiology* **63**, 43-51.

Downs, C. J., Hayes, J. P. and C. R. Tracy. (2008). Scaling metabolic rate with body mass and inverse body temperature: a test of the Arrhenius fractal supply model. *Functional Ecology* **22**, 239-244.

Dubroca, L. (2011). plfit.r. Retrieved from http://tuvalu.santafe.edu/~aaronc/powerlaws/plfit.r.

Dussutour, A. and Simpson, S. J. (2008). Carbohydrate regulation in relation to colony growth in ants. *Journal of Experimental Biology* **211**, 2224-2232.

Dussutour, A. and Simpson, S. J. (2009). Communal nutrition in ants. *Current Biology* **19**, 740-744.

Ehnes, R. B., Rall, B. C. and Brose, U. (2011). Phylogenetic grouping, curvature and metabolic scaling in terrestrial invertebrates. *Ecology Letters*, 993-1000.

Emerson, A. E. (1939). Social Coordination and the Superorganism. *American Midland Naturalist* **21**, 182-209.

Endler, A., Liebig, J. and H√∂lldobler, B. (2006). Queen fertility, egg marking and colony size in the ant Camponotus floridanus. *Behavioral Ecology and Sociobiology* **59**, 490-499.

Feigenbaum, C. and Naug, D. (2010). The influence of social hunger on food distribution and its implications for disease transmission in a honeybee colony. *Insectes Sociaux* **57**, 217-222.

Fewell, J. H. (1988). Energetic and Time Costs of Foraging in Harvester Ants, *Pogonomyrmex occidentalis*. *Behavioral Ecology and Sociobiology* **22**, 401-408.

Fewell, J. H. (2003). Social Insect Networks. *Science* **301**, 1867-1870.

Fielden, L. J., Krasnov, B. R., Khokhlova, I. S. and Arakelyan, M. S. (2004). Respiratory gas exchange in the desert flea Xenopsylla ramesis (Siphonaptera: Pulicidae): response to temperature and blood-feeding. *Comparative Biochemistry and Physiology - Part A: Molecular & Integrative Physiology* **137**, 557-565.

Fittkau, E. J. and Klinge, H. (1973). On biomass and trophic structure of the central Amazonian rain forest ecosystem. *Biotropica* **5**, 2-14.

Fonck, C. and Jaffe, K. (1996). On the energetic cost of sociality. *Physiology & Behavior* **59**, 713-719.

Forsman, A. (2000). Some like it hot: intra-population variation in behavioral thermoregulation in color-polymorphic pygmy grasshoppers. *Evolutionary Ecology* **14**, 25-38.

Full, R. J. (1997). Invertebrate Locomotor Systems. In *Handbook of Physiology Section 13: Comparative Physiology*, vol. II (ed. W. H. Dantzler), pp. 853-930. New York: Oxford University Press.

Galle, L. (1978). Respiration as one of the manifestations of the group effect in ants. *Acta Biologica Szeged* **24**, 111-114.

Gaston, K. J. (1991). The Magnitude of Global Insect Species Richness. *Conservation Biology* **5**, 283-296.

Gillooly, J., Brown, J., West, G., Savage, V. and Charnov, E. (2001). Effects of size and temperature on metabolic rate. *Science* **293**, 2248.

Gillooly, J. F., Allen, A. P., Savage, V. M., Charnov, E. L., West, G. B. and Brown, J. H. (2006). Response to Clarke and Fraser: effects of temperature on metabolic rate. *Functional Ecology* **20**, 400-404.

Giraud, T., Pedersen, J. and Keller, L. (2002). Evolution of supercolonies: the Argentine ants of southern Europe. *Proceedings of the National Academy of Sciences of the United States of America* **99**, 6075.

Glazier, D. S. (2005). Beyond the '3/4-power law': variation in the intra- and interspecific scaling of metabolic rate in animals. *Biol Rev Camb Philos Soc* **80**, 611-62.

Gnaiger, E. and Kuznetsov, A. V. (2002). Mitochondrial respiration at low levels of oxygen and cytochrome c. *Biochemical Society Transactions* **30**, 252-258.

Goldsworthy, G. and Coupland, A. (1974). The influence of the corpora cardiaca and substrate availability on flight speed and wing beat frequency inLocusta. *Journal of Comparative Physiology A: Neuroethology, Sensory, Neural, and Behavioral Physiology* **89**, 359-368.

Gordon, D. (2007). Control without hierarchy. *Nature* **446**, 143.

Gouveia, S. M., Simpson, S., Raubenheimer, D. and Zanotto, F. P. (2000). Patterns of respiration in Locusta migratoria nymphs when feeding. *Physiological Entomology* **25**, 88-93.

Greenlee, K. and Harrison, J. (2004a). Development of respiratory function in the American locust *Schistocerca americana* I. Across-instar effects. *Journal of Experimental Biology* **207**, 497.

Greenlee, K. and Harrison, J. (2004b). Development of respiratory function in the American locust *Schistocerca americana*: II. Within-instar effects. *Journal of Experimental Biology* **207**, 509.

Greenlee, K. and Harrison, J. (2005). Respiratory changes throughout ontogeny in the tobacco hornworm caterpillar, *Manduca sexta*. *Journal of Experimental Biology* **208**, 1385-1392.

Greenlee, K., Nebeker, C. and Harrison, J. (2007). Body size-independent safety margins for gas exchange across grasshopper species. *The Journal of Experimental Biology* **210**, 1288.

Greenlee, K. J. and Harrison, J. F. (2004c). Development of respiratory function in the American locust Schistocerca americana I. Across-instar effects. *Journal of Experimental Biology* **207**, 497-508.

Greenlee, K. J., Henry, J. R., Kirkton, S. D., Westneat, M. W., Fezzaa, K., Lee, W. K. and Harrison, J. F. (2009). Synchrotron imaging of the grasshopper tracheal system: morphological and physiological components of tracheal hypermetry. *American Journal of Physiology- Regulatory, Integrative and Comparative Physiology* **297**, R1343.

Grimaldi, D. and Engle, M. S. (2005). Evolution of the Insects. New York: Cambridge University Press.

Guppy, M. and Withers, P. (1999). Metabolic depression in animals: physiological perspectives and biochemical generalizations. *Biological Reviews* **74**, 1-40.

Hahn, D. A. and Denlinger, D. L. (2010). Energetics of Insect Diapause. *Annual Review of Entomology* **56**, 103-121.

Harrison, J. F. (1997). Ventilatory mechanism and control in grasshoppers. *American Zoologist* **37**, 73-81.

Harrison, J. F. and Fewell, J. H. (2002). Environmental and genetic influences on flight metabolic rate in the honey bee, *Apis mellifera*. *Comparative Biochemistry and Physiology* **133**, 323-333.

Harrison, J. F., Fewell, J. H., Anderson, K. E. and Loper, G. M. (2006a). Environmental physiology of the invasion of the Americas by Africanized honeybees. *Integrative and Comparative Biology* **46**, 1110-1122.

Harrison, J. F., Frazier, M. R., Henry, J. R., Kaiser, A., Klok, C. J. and Rascon, B. (2006b). Responses of terrestrial insects to hypoxia or hyperoxia *Respiratory Physiology & Neurobiology* **154**, 4-17.

Harrison, J. F., Kaiser, A. and VandenBrooks, J. M. (2010). Atmospheric oxygen level and the evolution of insect body size. *Proceedings of the Royal Society B: Biological Sciences* **277**, 1937.

Harrison, J. F., LaFreniere, J. J. and Greenlee, K. J. (2005). Ontogeny of tracheal dimensions and gas exchange capacities in the grasshopper, *Schistocerca americana*. *Comparative Biochemistry and Physiology Part A: Molecular and Integrative Physiology* **141**, 372-380.

Harrison, J. F. and Lighton, J. R. B. (1998). Oxygen-sensitive flight metabolism in the dragonfly *Erythemis simplicicollis*. *Journal of Experimental Biology* **201**, 1739-1744.

Harrison, J. F. and Roberts, S. P. (2000). Flight respiration and energetics. *Annual Review of Physiology* **62**, 179-205.

Harshman, Hoffmann and Clark. (1999). Selection for starvation resistance in *Drosophila melanogaster*: physiological correlates, enzyme activities and multiple stress responses. *Journal Of Evolutionary Biology* **12**, 370-379.

Heinrich, B. (1980a). Mechanisms of body temperature regulation in honeybees, *Apis mellifera* I. Regulation of head temperature. *Journal of Experimental Biology* **85**, 61-72.

Heinrich, B. (1980b). Mechanisms of body temperature regulation in honeybees, *Apis mellifera* II. Regulation of thoracic temperature at high air temperatures. *Journal of Experimental Biology* **85**, 73-87.
Heinrich, B. (1981a). Energetics of honeybee swarm thermoregulation. *Science* **212**, 565-566.

Heinrich, B. (1981b). The mechanisms and energetics of honeybee swarm temperature regulation. *Journal of Experimental Biology* **91**, 25-55.

Heinrich, B. (1992). The Hot-Blooded Insects. Cambridge: Harvard University Press.

Hemmingsen, A. (1960). Energy metabolism as related to body size and respiratory surfaces, and its evolution. *Reports of the Steno Memorial Hospital and the Nordisk Insulinlaboratorium* **9**, 7-110.

Herb, B. R., Wolschin, F., Hansen, K. D., Aryee, M. J., Langmead, B., Irizarry, R., Amdam, G. V. and Feinberg, A. P. (2012). Reversible switching between epigenetic states in honeybee behavioral subcastes. *Nat Neurosci* advance online publication.

Herreid, C. F., Full, R. J. and Prawel, D. A. (1981). Energetics of cockroach locomotion. *Journal of Experimental Biology* **94**, 189-202.

Hetz, S. K. and Bradley, T. J. (2005). Insects breathe discontinuously to avoid oxygen toxicity. *Nature* **433**, 516-519.

Holbrook, C. T., Barden, P. M. and Fewell, J. H. (2011). Division of labor increases with colony size in the harvester ant *Pogonomyrmex californicus*. *Behavioral Ecology* **22**, 960-966.

Hölldobler, B. and Wilson, E. O. (1990). The Ants. Cambridge, Mass.: Belknap Press.

Hölldobler, B. and Wilson, E. O. (2009). The superorganism : the beauty, elegance, and strangeness of insect societies. New York: W.W. Norton.

Hou, C., Kaspari, M., Vander Zanden, H. and Gillooly, J. (2010). Energetic basis of colonial living in social insects. *Proceedings of the National Academy of Sciences* **107**, 3634-3638.

Hulbert, A. and Else, P. (2004). Basal metabolic rate: history, composition, regulation, and usefulness. *Physiological And Biochemical Zoology* **77**, 869-876.

Hulbert, A. J. and Else, P. L. (2000). Mechanisms underlying the cost of living in animals. *Annual Review of Physiology* **62**, 207-235.

Irlich, U. M., Terblanche, J. S., Blackburn, T. M. and Chown, S. L. (2009). Insect Rate-Temperature Relationships: Environmental Variation and the Metabolic Theory of Ecology. *The American Naturalist* **174**, 819-835.

Janzen, D. H. (1987). Insect diversity of a Costa Rican dry forest: why keep it, and how? *Biological Journal of the Linnean Society* **30**, 343-356.

Jeanson, R., Fewell, J., Gorelick, R. and Bertram, S. (2007). Emergence of increased division of labor as a function of group size. *Behavioral Ecology and Sociobiology* **62**, 289-298.

Jeong, H., Tombor, B., Albert, R., Oltvai, Z. N. and Barabasi, A. L. (2000). The large-scale organization of metabolic networks. *Nature* **407**, 651-654.

Johnson, R. A. (2004). Colony founding by pleometrosis in the semiclaustral seed-harvester ant *Pogonomyrmex californicus* (Hymenoptera: Formicidae). *Animal Behaviour* **68**, 1189-1200.

Joos, B., Lighton, J. R. B., Harrison, J. F., Suarez, R. K. and Roberts, S. P. (1997). Effects of ambient oxygen tension on flight performance, metabolism and water loss of the honeybee. *Physiological Zoology* **70**, 167-174.

Kaiser, A., Klok, C. J., Socha, J. J., Lee, W. K., Quinlan, M. C. and Harrison, J. F. (2007). Increase in tracheal investment with beetle size supports hypothesis of oxygen limitation on insect gigantism. *Proceedings of the National Academy of Sciences of the United States of America* **104**, 13198-13203.

Kaluza, P., Vingron, M. and Mikhailov, A. S. (2008). Self-correcting networks: Function, robustness, and motif distributions in biological signal processing. *Chaos: An Interdisciplinary Journal of Nonlinear Science* **18**, 026113-17.

Kaspari, M. and Vargo, E. L. (1995). Colony Size as a Buffer Against Seasonality: Bergmann's Rule in Social Insects. *The American Naturalist* **145**, 610-632.

Kirkton, S. D., Niska, J. A. and Harrison, J. F. (2005). Ontogenetic effects on aerobic and anaerobic metabolism during jumping in the American locust, *Schistocerca americana*. *Journal of Experimental Biology* **208**, 3003-3012.

Klok, C. J. and Chown, S. L. (2005). Temperature- and body mass-related variation in cyclic gas exchange characteristics and metabolic rate of seven weevil species: Broader implications. *Journal of Insect Physiology* **51**, 789-801.

Klok, C. J. and Harrison, J. F. (2009). Atmospheric hypoxia limits selection for large body size in insects. *PLoS ONE* **4**, e3876.

Klok, C. J., Kaiser, A., Lighton, J. R. B. and Harrison, J. F. (2010). Critical oxygen partial pressures and maximal tracheal conductances for *Drosophila melanogaster* reared for multiple generations in hypoxia or hyperoxia. *Journal of Insect Physiology* **56**, 461-469.

Kooijman, S. A. L. M. (2000). Dynamic energy and mass budgets in biological systems: Cambridge University Press.

Korb, J. (2003). Thermoregulation and ventilation of termite mounds. *Naturwissenschaften* **90**, 212-219.

LaBarbera, M. (1990). Principles of design of fluid transport systems in zoology. *Science* **249**, 992-1000.

Lachenicht, M. W., Clusella-Trullas, S., Boardman, L., Le Roux, C. and

Terblanche, J. S. (2010). Effects of acclimation temperature on thermal tolerance, locomotion performance and respiratory metabolism in *Acheta domesticus* L. (Orthoptera: Gryllidae). *Journal of Insect Physiology* **56**, 822-830.

Lalouette, L., Williams, C., Hervant, F., Sinclair, B. and Renault, D. (2010). Metabolic rate and oxidative stress in insects exposed to low temperature thermal fluctuations. *Comparative Biochemistry and Physiology-Part A: Molecular & Integrative Physiology*.

Legendre, P. (2011). lmodel2: Model II Regression. R package version 1.7-0., http://CRAN.R-project.org/package=lmodel2.

Lighton, J., Weier, J. and Feener Jr, D. (1993a). The energetics of locomotion and load carriage in the desert harvester ant *Pogonomyrmex rugosus*. *Journal of Experimental Biology* **181**, 49.

Lighton, J. R. and Bartholomew, G. A. (1988). Standard energy metabolism of a desert harvester ant, *Pogonomyrmex rugosus*: Effects of temperature, body mass, group size, and humidity. *Proc Natl Acad Sci U S A* **85**, 4765-4769.

Lighton, J. R. B. (1989). Individual and whole-colony respiration in an African formicine ant. *Functional Ecology* **3**, 523-530.

Lighton, J. R. B. (1991). Ventilation in Namib desert tenebrionid beetles: mass scaling and evidence of a novel quantized flutter-phase. *Journal of Experimental Biology* **159**, 249-268.

Lighton, J. R. B. (2008). Measuring Metabolic Rates : A Manual For Scientists. Oxford ; New York: Oxford University Press.

Lighton, J. R. B., Bartholomew, G. A. and Feener, D. H. (1987). Energetics of Locomotion and Load Carriage and a Model of the Energy Cost of Foraging in the Leaf-Cutting Ant *Atta colombica* Guer. *Physiological Zoology* **60**, 524-537.

Lighton, J. R. B. and Berrigan, D. (1995). Questioning paradigms: caste-specific ventilation in harvester ants, *Messor pergandei* and *M. Julianus* (Hymenoptera:Formicidae). *Journal of Experimental Biology* **198**.

Lighton, J. R. B., Brownell, P. H., Joos, B. and Turner, R. J. (2001). Low metabolic rate in scorpions: implication for population biomass and cannibalism. *The Journal of Experimental Biology* **204**, 607-613.

Lighton, J. R. B., Fukushi, T. and Wehner, R. (1993b). Ventilation in *Cataglyphis bicolor*: regulation of carbon dioxide release from the thoracic and abdominal spiracles. *Journal of Insect Physiology* **39**, 687-699.

Lighton, J. R. B. and Lovegrove, B. G. (1990). A temperature-induced switch from diffusive to conective ventilation in the honeybee. *Journal of Experimental Biology* **154**, 509-516.

Lipp, A., Wolf, H. and Lehmann, F.-O. (2005). Walking on inclines: energetics of locomotion in the ant Camponotus. *Journal of Experimental Biology* **208**, 707-719.

Loveridge, J. P. and Bursell, E. (1975). Studies on the water relations of adult locusts (*Orthoptera: Acrididae*). I. Respiration and the production of metabolic water. *Bull. Ent. Res.* **65**, 13-20.

Lucas, J. (1985). Metabolic rates and pit-construction costs of two antlion species. *Journal of Animal Ecology* **54**, 295-309.

Lusseau, D. (2003). The emergent properties of a dolphin social network. *Proceedings of the Royal Society of London. Series B: Biological Sciences* **270**, S186.

Lusseau, D. and Newman, M. (2004). Identifying the role that animals play in their social networks. *Proceedings of the Royal Society of London. Series B: Biological Sciences* **271**, S477.

Mangan, S. and Alon, U. (2003). Structure and function of the feed-forward loop network motif. *Proceedings of the National Academy of Sciences of the United States of America* **100**, 11980-11985.

Mangan, S., Itzkovitz, S., Zaslaver, A. and Alon, U. (2006). The incoherent feed-forward loop accelerates the response-time of the gal system of *Escherichia coli. Journal of Molecular Biology* **356**, 1073-1081.

Marron, M., Markow, T., Kain, K. and Gibbs, A. (2003). Effects of starvation and desiccation on energy metabolism in desert and mesic Drosophila. *Journal of Insect Physiology* **49**, 261-270.

Martin, M. M. and Van't Hof, H. M. (1988). The cause of reduced growth of Manduca sexta larvae on a low-water diet: Increased metabolic processing costs or nutrient limitation? *Journal of Insect Physiology* **34**, 515-525.

Martinez del Rio, C. (2008). Metabolic theory or metabolic models? *Trends Ecol Evol* **23**, 256-60.

Matsura, T. (1981). Responses to starvation in a mantis, *Paratenodera angustipennis* (S.). *Oecologia* **50**, 291-295.

Mayack, C. and Naug, D. (2009). Energetic stress in the honeybee Apis mellifera from *Nosema ceranae* infection. *Journal of Invertebrate Pathology* **100**, 185-188.

McGaughran, A., Redding, G. P., Stevens, M. I. and Convey, P. (2009). Temporal metabolic rate variation in a continental Antarctic springtail. *Journal of Insect Physiology* **55**, 129-134.

McMahon, T. A. and Bonner, J. T. (1983). On Size and Life. New York: Scientific American Books, Inc.

Medrano, J. F. and Gall, G. A. E. (1976). Food Consumption, Feed Efficiency, Metabolic Rate And Utilization Of Glucose In Lines Of Tribolium Castaneum Selected For 21-Day Pupa Weight. *Genetics* **83**, 393-407.

Meijering, E., Dzyubachyk, O. and Smal, I. (2012). Methods for cell and particle tracking. *Methods Enzymol* **504**, 183-200.

Michener, C. D. (1964). Reproductive efficiency in relation to colony size in hymenopterous societies. *Insectes Soc* **4**, 317-342.

Miller, P. L. (1966). The supply of oxygen to the active flight muscles of some large beetles. *Journal of Experimental Biology* **45**, 285-304.

Miller, P. L. (1981). Ventilation in active and in inactive insects. In *Locomotion and Energetics in Arthropods*, eds. C. F. Herreid and C. F. Fourtner), pp. 367-390. New York: Plenum Press.

Milo, R., Itzkovitz, S., Kashtan, N., Levitt, R., Shen-Orr, S., Ayzenshtat, I., Sheffer, M. and Alon, U. (2004). Superfamilies of evolved and designed networks. *Science* **303**, 1538.

Milo, R., Shen-Orr, S., Itzkovitz, S., Kashtan, N., Chklovskii, D. and Alon, U. (2002). Network Motifs: Simple Building Blocks of Complex Networks. *Science* **298**, 824-827.

Minelli, A., Maruzzo, D. and Fusco, G. (2010). Multi-scale relationships between numbers and size in the evolution of arthropod body features. *Arthropod Structure and Development*.

Moore, D. and Liebig, J. (2010). Mechanisms of social regulation change across colony development in an ant. *BMC Evolutionary Biology* **10**, 328.

Morgan, K. R., Shelley, T. E. and Kimsey, L. S. (1985). Body temperature regulation, energy metabolism and foraging in light-seeking and shade-seeking robber flies. *Journal of Comparative PHysiology B* **155**, 561-570.

Moses, M. E., Forrest, S., Davis, A. L., Lodder, M. A. and Brown, J. H. (2008). Scaling theory for information networks. *Journal of The Royal Society Interface* **5**, 1469-1480.

Nagy, K. A. (2005). Field metabolic rate and body size. *Journal of Experimental Biology* **208**, 1621-1625.

Nakaya, F., Saito, Y. and Motokawa, T. (2003). Switching of metabolic-rate scaling between allometry and isometry in colonial ascidians. *Proceedings of the Royal Society of London Series B-Biological Sciences* **270**, 1105-1113.

Nakaya, F., Saito, Y. and Motokawa, T. (2005). Experimental allometry: effect of size manipulation on metabolic rate of colonial ascidians. *Proc Biol Sci* **272**, 1963-9.

Naug, D. (2008). Structure of the social network and its influence on transmission dynamics in a honeybee colony. *Behavioral Ecology and Sociobiology* **62**, 1719-1725.

Naug, D. (2009). Structure and resilience of the social network in an insect colony as a function of colony size. *Behavioral Ecology and Sociobiology* **63**, 1023-1028.

Nespolo, R., Lardies, M. and Bozinovic, F. (2003). Intrapopulational variation in the standard metabolic rate of insects: repeatability, thermal dependence and sensitivity (Q10) of oxygen consumption in a cricket. *Journal of Experimental Biology* **206**, 4309-4315.

Newman, M. (2010). Networks: an introduction: Oxford University Press, Inc.

Nielsen, M., Elmes, G. and Kipyatkov, V. (1999). Respiratory Q10 varies between populations of two species of *Myrmica* ants according to the latitude of their sites. *Journal of Insect Physiology* **45**, 559-564.

Niswander, R. E. (1951). Life history and respiration of the milkweed bug *Oncopeltus fasciatus* (Dallas). *Ohio J. Sci* **51**, 27-33.

Niven, J. E. and Scharlemann, J. P. (2005). Do insect metabolic rates at rest and during flight scale with body mass? *Biology Letters* **1**, 346-349.

Noirot, C. and Darlington, J. (2000). Termite nests: architecture, regulation and defence. *Termites: Evolution, sociality, symbioses, ecology*. Dordrecht, Kluwer Academic Publishers, 121-139.

O'Connor, M. I., Bruno, J. F., Gaines, S. D., Halpern, B. S., Lester, S. E., Kinlan, B. P. and Weiss, J. M. (2007). Temperature control of larval dispersal and the implications for marine ecology, evolution, and conservation. *Proceedings of the National Academy of Sciences* **104**, 1266.

Oliver, D. (1971). Life history of the Chironomidae. *Annual Review of Entomology* **16**, 211-230.

Olsson, M., Wapstra, E. and Olofsson, C. (2002). Offspring size-number strategies: experimental manipulation of offspring size in a viviparous lizard (*Lacerta vivipara*). *Functional Ecology* **16**, 135-140.

Oster, G. F. and Wilson, E. O. (1978). Caste and ecology in the social insects. United States.

Packard, G. C. and Boardman, T. J. (2008). Model Selection and Logarithmic Transformation in Allometric Analysis. *Physiological And Biochemical Zoology* **81**, 496-507.

Penick, C. and Tschinkel, W. (2008). Thermoregulatory brood transport in the fire ant, *Solenopsis invicta*. *Insectes Sociaux* **55**, 176-182.

Peters, R. H. (1983). The Ecological Implications of Body Size. Cambridge: Cambridge University Press.

Petz, M., Stabentheiner, A. and Crailsheim, K. (2004). Respiration of individual honeybee larvae in relation to age and ambient temperature. *Journal of Comparative Physiology B: Biochemical, Systemic, and Environmental Physiology* **174**, 511-518.

Pinter-Wollman, N., Wollman, R., Guetz, A., Holmes, S. and Gordon, D. M. (2011). The effect of individual variation on the structure and function of interaction networks in harvester ants. *Journal of The Royal Society Interface*.

Porter, S. D. and Tschinkel, W. R. (1985). Fire Ant Polymorphism - the Ergonomics of Brood Production. *Behavioral Ecology and Sociobiology* **16**, 323-336.

Potts, S. G., Biesmeijer, J. C., Kremen, C., Neumann, P., Schweiger, O. and Kunin, W. E. (2010). Global pollinator declines: trends, impacts and drivers. *Trends in Ecology & Evolution* **25**, 345-353.

Quinlan, M. C. and Lighton, J. R. B. (1999). Respiratory physiology and water relations of three species of *Pogonomyrmex* harvester ants (Hymenoptera: Formicidae). *Physiological Entomology* **24**, 293-302.

R Development Core Team. (2011). R: A language and environment for statistical computing. . R Foundation for Statistical Computing, Vienna, Austria. URL http://www.R-project.org/.

Rasband, W. S. (1997-2012). ImageJ. U. S. National Institutes of Health, Bethesda, Maryland, USA*, http://imagej.nih.gov/ij/*.

Rascon, B. and Harrison, J. F. (2005). Oxygen partial pressure effects on metabolic rate and behavior of tethered flying locusts. *Journal of Insect Physiology* **51**, 1193-1199.

Reinhold, K. (1999). Energetically costly behaviour and the evolution of resting metabolic rate in insects. *Functional Ecology* **13**, 217-224.

Ricklefs, R. E. (2003). Is rate of ontogenetic growth constrained by resource supply or tissue growth potential? A comment on West et al.'s model. *Functional Ecology* **17**, 384-393.

Roberts, S. P., Harrison, J. F. and Dudley, R. (2004). Allometry of kinematics and energetics in carpenter bees (*Xylocopa varipuncta*) hovering in variable-density gases. *Journal of Experimental Biology* **207**, 993-1004.

Roberts, S. P., Harrison, J. F. and Hadley, N. F. (1998). Mechanisms of thermal balance in flying *Centris pallida* (Hymenoptera: Anthophoridae). *Journal of Experimental Biology* **201**, 2321-2331.

Robinson, W. R., Peters, R. H. and Zimmermann, J. (1983). The effects of body size and temperature on metabolic rate of organisms. *Canadian Journal of Zoology* **61**, 281-288.

Roces, F. and Lighton, J. R. B. (1995). Larger bites of leaf-cutting ants. *Nature* **373**, 392-393.

Rueppell, O. and Kirkman, R. W. (2005). Extraordinary starvation resistance in *Temnothorax rugatulus* (Hymenoptera, Formicidae) colonies: Demography and adaptive behavior. *Insectes Sociaux* **52**, 282-290.

Ruf, C. and Fiedler, K. (2002). Tent-based thermoregulation in social caterpillars of *Eriogaster lanestris* (Lepidoptera : Lasiocampidae): behavioral mechanisms and physical features of the tent. *Journal of Thermal Biology* **27**, 493-501.

Salganik, M. J., Dodds, P. S. and Watts, D. J. (2006). Experimental study of inequality and unpredictability in an artificial cultural market. *Science* **311**, 854-856.

Salvucci, M. E. and Crafts-Brandner, S. J. (2000). Effects of temperature and dietary sucrose concentration on respiration in the silverleaf whitefly, *Bemisia argentifolii*. *Journal of Insect Physiology* **46**, 1461-1467.

Sasaki, T. and Pratt, S. C. (2011). Emergence of group rationality from irrational individuals. *Behavioral Ecology* **22**, 276-281.

Savage, V. M., Deeds, E. J. and Fontana, W. (2008). Sizing Up Allometric Scaling Theory. *PLoS Computational Biology* **4**, e1000171.

Savage, V. M., Gillooly, J. F., Woodruff, W. H., West, G. B., Allen, A. P., Enquist, B. J. and Brown, J. H. (2004). The predominance of quarter-power scaling in biology. *Functional Ecology* **18**, 257-282.

Schmickl, T. and Crailsheim, K. (2001). Cannibalism and early capping: strategy of honeybee colonies in times of experimental pollen shortages. *Journal of Comparative Physiology A: Neuroethology, Sensory, Neural, and Behavioral Physiology* **187**, 541-547.

Schmidt-Nielsen. (1995). Scaling: why is animal size so important? Cambridge: Cambridge University Press.

Schmolz, E., Hoffmeister, D. and Lamprecht, I. (2002). Calorimetric investigations on metabolic rates and thermoregulation of sleeping honeybees (*Apis mellifera carnica*). *Thermochimica Acta* **382**, 221-227.

Schneiderman, H. A. and Williams, C. M. (1953). The physiology of insect diapause. VII. The respiratory metabolism of the *Cecropia* silkworm during diapause and development. *The Biological Bulletin* **105**, 320.

Schultz, T. D., Quinlan, M. C. and Hadley, N. F. (1992). Preferred body temperature, metabolic physiology, and water balance of adult *Cicindela*

longilabris: a comparison of populations from boreal habitats and climatic refugia. *Physiological Zoology* **65**, 226-242.

Secor, S. (2009). Specific dynamic action: a review of the postprandial metabolic response. *Journal of Comparative Physiology B: Biochemical, Systemic, and Environmental Physiology* **179**, 1-56.

Secor, S. and Diamond, J. (1998). A vertebrate model of extreme physiological regulation. *Nature* **395**, 659-662.

Seibel, B. A. and Drazen, J. C. (2007). The rate of metabolism in marine animals: environmental constraints, ecological demands and energetic opportunities. *Philosophical Transactions of the Royal Society B: Biological Sciences* **362**, 2061-2078.

Sendova-Franks, A. B., Hayward, R. K., Wulf, B., Klimek, T., James, R., PlanquÈ, R., Britton, N. F. and Franks, N. R. (2010). Emergency networking: famine relief in ant colonies. *Animal Behaviour* **79**, 473-485.

Shen-Orr, S., Milo, R., Mangan, S. and Alon, U. (2002). Network motifs in the transcriptional regulation network of Escherichia coli. *Nature genetics* **31**, 64-68.

Shik, J. (2010). The metabolic costs of building ant colonies from variably sized subunits. *Behavioral Ecology and Sociobiology*, 1-10.

Shik, J. Z. (2008). Ant colony size and the scaling of reproductive effort. *Functional Ecology* **22**, 674-681.

Sinervo, B. and Huey, R. B. (1990). Allometric engineering: an experimental test of the causes of interpopulational differences in performance. *Science* **248**, 1106-1109.

Sinervo, B., Zamudio, K., Doughty, P. and Huey, R. (1992). Allometric engineering: a causal analysis of natural selection on offspring size. *Science* **258**, 1927.

Socha, J. J., Förster, T. D. and Greenlee, K. J. (2010). Issues of convection in insect respiration: Insights from synchrotron X-ray imaging and beyond. *Respiratory Physiology & Neurobiology* **173**, S65-S73.

Socha, J. J., Lee, W.-K., Harrison, J. F., Waters, J. S., Fezzaa, K. and Westneat, M. W. (2008). Correlated patterns of tracheal compression and convective gas exchange in a carabid beetle. *Journal of Experimental Biology* **211**, 3409-3420.

Socha, J. J., Westneat, M. W., Harrison, J. F., Waters, J. S. and Lee, W. K. (2007). Real-time phase-contrast x-ray imaging: a new technique for the study of animal form and function. *Bmc Biology* **5**, -.

Sorensen, A. A., Busch, T. M. and Vinson, S. B. (1983). Factors affecting brood cannibalism in laboratory colonies of the imported fire ant, Solenopsis invicta Buren (Hymenoptera: Formicidae). *Journal of the Kansas Entomological Society* **56**, 140-150.

Sorensen, A. A., Busch, T. M. and Vinson, S. B. (1985). Control of food influx by temporal subcastes in the fire ant, <i>Solenopsis invicta</i>. *Behavioral Ecology and Sociobiology* **17**, 191-198.

Southwick, E. E. (1982). Metabolic energy of intact honey bee colonies. *Comp Biochem Physiol* **71A**, 277-281.

Southwick, E. E. (1985). Allometric relations, metabolism and heat conductance in clusters of honeybees at cool temperatures. *Journal of Comparative Physiology* **156**, 143-149.

Southwick, E. E. (1987). Cooperative Metabolism In Honey-Bees - An Alternative To Antifreeze And Hibernation. *Journal of Thermal Biology* **12**, 155-158.

Southwick, E. E., Roubik, D. W. and Williams, J. M. (1990). Comparative energy balance in groups of Africanized and European honey bees: ecological implications. *Comp. Biochem. Physiol.* **97A**, 1-7.

Stevens, E. D. and Josephson, R. K. (1977). Metabolic Rate and Body Temperature in Singing Katydids. *Physiological Zoology* **50**, 31-42.

Stoks, R., Block, M. D. and McPeek, M. A. (2006). Physiological Costs of Compensatory Growth in a Damselfly. *ECOLOGY* **87**, 1566-1574.

Strogatz, S. H. (2001). Exploring complex networks. *Nature* **410**, 268-276.

Terblanche, J. S. and Chown, S. L. (2007). The effects of temperature, body mass and feeding on metabolic rate in the tsetse fly *Glossina morsitans centralis*. *Physiological Entomology* **32**, 175-180.

Tschinkel, W. R. (1988). Social control of egg-laying rate in queens of the fire ant, *Solenopsis invicta*. *Physiological Entomology* **13**, 327-350.

Tschinkel, W. R. (1993). Sociometry and Sociogenesis of Colonies of the Fire Ant *Solenopsis invicta* During One Annual Cycle. *Ecological Monographs* **63**, 425-457.

Tschinkel, W. R. (1999). Sociometry and sociogenesis of colonies of the harvester ant, *Pogonomyrmex badius*: distribution of workers, brood and seeds within the nest in relation to colony size and season. *Ecological Entomology* **24**, 222-237.

van der Meer, J. (2006). Metabolic theories in ecology. *Trends in Ecology & Evolution* **21**, 136-140.

Van Voorhies, W. A. (2009). Metabolic function in *Drosophila melanogaster* in response to hypoxia and pure oxygen. *Journal of Experimental Biology* **212**, 3132-3141.

Van Voorhies, W. A., Khazaeli, A. A. and Curtsinger, J. W. (2004). Lack of correlation between body mass and metabolic rate in *Drosophila melanogaster*. *Journal of Insect Physiology* **50**, 445-453.

Van Zyl, A., Van Der Linde, T. and Grimbeek, R. (1997). Metabolic rates of pitbuilding and non-pitbuilding antlion larvae (Neuroptera: Myrmeleontidae) from southern Africa. *Journal of Arid Environments* **37**, 355-365.

Vogt, J. T. and Appel, A. G. (1999). Standard metabolic rate of the fire ant, *Solenopsis invicta* Buren: effects of temperature, mass, and caste. *Journal of Insect Physiology* **45**, 655-666.

Vollmer, S. V. and Edmunds, P. J. (2000). Allometric scaling in small colonies of the scleractinian coral Siderastrea siderea (Ellis and Solander). *Biological Bulletin* **199**, 21-28.

Walker, J. A. (2001). QuickImage: a modification of NIH Image with enhanced digitizing tools.

Wasserthal, L. (2001). Flight-motor-driven respiritory air flow in the hawkmoth *Manduca sexta*. *Journal of Experimental Biology* **204**, 2209-2220.

Wasserthal, L. T. (1996). Interaction of circulation and tracheal ventilation in holometabolous insects. *Advances In Insect Physiology* **26**, 297-351.

Waters, J. S. and Fewell, J. H. (2012). Information Processing in Social Insect Networks. *PLoS ONE* **7**, e40337.

Waters, J. S. and Harrison, J. F. (2012). Insect Metabolic Rates. In *Metabolic Ecology: A Scaling Approach*, eds. R. M. Sibly J. H. Brown and A. Kodric-Brown), pp. 198-211: Wiley-Blackwell.

Waters, J. S., Holbrook, C. T., Fewell, J. H. and Harrison, J. F. (2010). Allometric Scaling of Metabolism, Growth, and Activity in Whole Colonies of the Seed-Harvester Ant *Pogonomyrmex californicus*. *The American Naturalist* **176**, 501-510.

Weier, J., Feener, D. and Lighton, J. (1995). Inter-individual variation in energy cost of running and loading in the seed-harvester ant, *Pogonomyrmex maricopa*. *Journal of Insect Physiology* **41**, 321-327.

Weis-Fogh, T. (1967). Respiration and tracheal ventilation in locusts and other flying insects. *Journal of Experimental Biology* **47**, 561-587.

Went, F. W. (1968). The size of man. *American Scientist* **56**, 400-413.

Wernicke, S. and Rasche, F. (2006). FANMOD: a tool for fast network motif detection. *Bioinformatics* **22**, 1152.

West, G. B., Brown, J. H. and Enquist, B. J. (1997). A general model for the origin of allometric scaling laws in biology. *Science* **276**, 122-126.

West, G. B., Brown, J. H. and Enquist, B. J. (2001). A general model for ontogenetic growth. *Nature* **413**, 628-631.

Wey, T., Blumstein, D. T., Shen, W. and Jordan, F. (2008). Social network analysis of animal behaviour: a promising tool for the study of sociality. *Animal Behaviour* **75**, 333-344.

Wheeler, W. M. (1911). The ant-colony as an organism. *Journal of Morphology* **22**, 307-325.

White, C. R., Kearney, M. R., Matthews, P. G. D., Kooijman, S. A. L. M. and

Marshall, D. J. (2011). A Manipulative Test of Competing Theories for Metabolic Scaling. *The American Naturalist* **178**, 746-754.

White, C. R. and Seymour, R. S. (2004). Does Basal Metabolic Rate Contain a Useful Signal? Mammalian BMR Allometry and Correlations with a Selection of Physiological, Ecological, and Life-History Variables. *Physiological And Biochemical Zoology* **77**, 929-941.

Wickham, H. (2009). ggplot2: elegant graphics for data analysis. New York: Springer.

Wilson, E. and Hölldobler, B. (1988). Dense heterarchies and mass communication as the basis of organization in ant colonies. *Trends in Ecology & Evolution* **3**, 65-68.

Wilson, E. O. (1971). The Insect Societies. Cambridge, Massachussets: Harvard University Press.

Wilson, E. O. (1980). Caste and division of labor in leaf-cutter ants (Hymenoptera: Formicidae: Atta). II. The ergonomics optimization of leaf-cutting. *Behavioral Ecology and Sociobiology* **7**, 157-165.

Wilson, E. O. (1985). The Biological Diversity Crisis. *BioScience* **35**, 700-706.

Xiao, X., White, E. P., Hooten, M. B. and Durham, S. L. (2011). On the use of log-transformation vs. nonlinear regression for analyzing biological power laws. *Ecology* **92**, 1887-1894.

Zanotto, F., Gouveia, S., Simpson, S. and Calder, D. (1997). Nutritional homeostasis in locusts: is there a mechanism for increased energy expenditure during carbohydrate overfeeding? *The Journal of Experimental Biology* **200**, 2437.

Zhou, S., Criddle, R. and Mitcham, E. (2000). Metabolic response of *Platynota stultana* pupae to controlled atmospheres and its relation to insect mortality response. *Journal of Insect Physiology* **46**, 1375-1385.

APPENDIX A

PERMISSION TO USE PUBLISHED ARTICLES

Chapters 1-3 of this dissertation are reformatted versions of papers that have already been published. As I am not the sole author for any of these publications, I would like to acknowledge the support and contributions of my co-authors by identifying the full citations for these chapters here. All co-authors have granted permission to use these articles in this dissertation.

Chapter 1 was previously published as:

Waters, J. S. and Harrison, J. F. (2012). Insect Metabolic Rates. In *Metabolic Ecology: A Scaling Approach*, eds. R. M. Sibly J. H. Brown and A. Kodric-Brown, pp. 198-211: Wiley-Blackwell.

Chapter 2 was previously published as:

Waters, J. S., Holbrook, C. T., Fewell, J. H. and Harrison, J. F. (2010). Allometric Scaling of Metabolism, Growth, and Activity in Whole Colonies of the Seed-Harvester Ant *Pogonomyrmex californicus*. *The American Naturalist* **176**, 501-510.

Chapter 3 was previously published as:

Waters, J. S. and Fewell, J. H. (2012). Information Processing in Social Insect Colonies. *PLoS One* **7**, e40337.

BIOGRAPHICAL SKETCH

James Stephen Waters was born to Linette S. and Stephen E. Waters on April 26, 1983 on Long Island in New York in the United States of America. Along with his siblings, Cindy, John, and Amanda, he attended the Mayflower Public School 191 and Hillside Junior High School 172 in Queens, NY. Both James and his brother John earned the rank of Eagle Scout in Troop 405. From 1997-2001, he attended The Bronx High School of Science in New York City. From 2001-2005 he studied liberal arts at The University of Chicago and concentrated in Mathematics. While at Chicago, his interest in biology was sparked by a course on Animal Locomotion for non-majors taught by Jake Socha and a course on the Biomechanics of Organisms taught by Michael LaBarbera. Following graduation (A.B., 2005), he worked as a research technician at The Field Museum with Mark Westneat, Wah-Keat Lee, and Melina Hale using synchrotron x-ray imaging to study insect respiratory dynamics. He was a graduate student at Arizona State University and a member of the Social Insect Research Group from 2006-2012. While at Arizona State, he was a member of the Harrison Lab for Ecological & Evolutionary Physiology, conducted dissertation research into the metabolic and behavioral integration in social insect colonies, developed a successful "Bug Theater" outreach program through the Maricopa County Parks & Recreation Department, and pursued a number of collaborations with colleagues investigating the physiology and behavior of social insect colonies. On December 29, 2011, he proposed to Catherine A. Nichols in Rayville, Louisiana; she accepted and they plan to marry.